Alma Mater Studiorum · Università di Bologna

Scuola di Scienze
Dipartimento di Fisica e Astronomia
Corso di Laurea Magistrale in Fisica

Cosmological effects of the Galileon term in scalar-tensor theories

Relatore:
Prof. Lauro Moscardini

Presentata da:
Angelo Giuseppe Ferrari

Correlatori:
Dott. Fabio Finelli
Dott.ssa Daniela Paoletti

Anno Accademico 2019/2020

Contents

Abstract

In questa tesi studiamo un'estensione con un termine di interazione cubica, $(g^{\mu\nu}\partial_\mu\sigma\partial_\nu\sigma)\Box\sigma$, della lagrangiana dei più semplici modelli scalari-tensoriali, come gravitá indotta (IG) e il modello Jordan-Brans-Dicke esteso con un potenziale(eJBD). Ne analizziamo gli effetti cosmologici sia a livello di background che di perturbazioni lineari. Il lavoro si suddivide in una parte analitica ed una numerica: nella parte analitica vengono ricavate le equazioni del moto del modello sia a livello omogeneo che per le perturbazioni lineari e si ottiene una classe di soluzioni analitiche in assenza di materia. La parte numerica, che ha richiesto l'implementazione delle equazioni della teoria in un codice Einstein-Boltzmann dedicato, ci ha permesso di studiare più nel dettaglio l'evoluzione della cosmologia omogenea e fare predizioni sulle anisotropie dello spettro di potenza angolare della radiazione cosmica di fondo (CMB) e dello spettro di potenza della materia, confrontando tali risultati con quelli ottenuti in IG e nel modello cosmologico standard ΛCDM.

Introduction

The cosmological concordance model is the so called ΛCDM model. This model has established itself in the last thirty years or so, and provides a good fit to many cosmological observations [1]. It assumes the cosmological principle (homogeneity and isotropy on large scales) and its basic ingredients are: Einstein's theory of General Relativity as theory of gravity, standard particles as photons, baryons and neutrinos, a cosmological constant to explain the recent acceleration of the expansion of the Universe and a cold dark matter (CDM) component. The nature of Dark Energy and Dark Matter is still unknown and must lie outside the standard model of particle physics. The study of different possibilities and alternatives for these dark components is one of the most active field of cosmology and particle physics. Dark matter does not interact (or does it very weakly) electromagnetically and its existence had been postulated on the basis of observational evidences [2] and is still supported by both astrophysical probes, as galaxy rotational curves and cluster mergers, and cosmological probes such as the cosmic microwave background. The prefix "cold" means that such matter was non-relativistic when, in the early Universe, it decoupled from radiation (as opposed to the "hot" dark matter) and current observations of structure formation suggest that the great majority of dark matter has to be "cold". The cosmological constant, as already anticipated, provides an explanation to the recent acceleration of the expansion of the Universe in the ΛCDM model and it is described as a perfect fluid with negative pressure; this new component is called Dark Energy. Beyond this simple model, also on the basis of a discrepancy between observations and theoretical predictions for the vacuum energy, many alternatives have been proposed, for instance quintessence, in which a scalar field drives the expansion solving some of the cosmological constant fine tuning problems.

Another interesting alternative to explain the recent acceleration of the Universe is modified gravity: in many scenarios of modified gravity, the the acceleration of the expansion is the result of a modification of the the gravitational sector of the theory and not the addition of a new fluid to the budget content of the Universe. This path is particularly alluring since it would result in a unification of two of the ingredients of the

standard cosmological model: the theory of gravity with dark energy. The repercussions of modified gravity on cosmology, which were merely speculations until few years ago, are already constrained by current cosmological observations such as CMB [3] and recently the detection of neutron star merger GW170817 [4, 5] and thanks to upcoming surveys which will lead us further on in the era of precision cosmology. Therefore, these models represent a valid class of alternatives to ΛCDM.

A subclass of these theories is that of scalar tensor theories, in which, beside the metric tensor field, a scalar degree of freedom, that modulates the strength of the gravitational interaction of matter with the metric, is present. In short, the scalar field changes the way in which matter generates the gravitational potentials.

The simplest scalar-tensor models of gravity are constrained by various cosmological and astrophysical observations as well as by ground laboratory experiments. For example, in the case of extended Jordan-Brans-Dicke (eJBD) the most recent cosmological constraints from Planck 2018 data and a combination of Baryonic Acoustic Oscillation (BAO) data from different galaxy surveys is $\gamma < 5.5 \times 10^{-4}$ at 95 %CL [6]. These cosmological constraints depend weakly on the potential, but could be relaxed when the coupling to the Ricci scalar is extended from the quadratic form of the eJBD case to more complicated forms which also turn on the second post-Newtonian parameter $\beta_{\rm PN}$. When screening mechanism are absent, the tightest constraints come however within the Solar System: $\gamma_{\rm PN} - 1 = (2.1 \pm 2.3) \times 10^{-5}$ at 68% CL [7] and $\beta_{\rm PN} - 1 = (4.1 \pm 7.8) \times 10^{-5}$ at 68% CL [8].

Considering this observational scenario, in this thesis we plan to study an extension of these models that includes a Galileon-like cubic interaction term, $(g^{\mu\nu}\partial_\mu\sigma\partial_\nu\sigma)\Box\sigma$, in the lagrangian of Induced Gravity and eJBD. This term is particularly interesting because it can give rise to the so called Vainsthein screening [9, 10], which allows to recover General Relativity nearby localized sources of matter and could therefore help relax the solar system constraints for the other parameters of the theory. Since, in order to have cosmological constraints at the level of those from the Solar System, it is sufficient to consider models with a non minimal coupling to the Ricci scalar of the form $F(\sigma) = N_{pl}^2 + \xi\sigma^2$ [11, 12], we restrict ourselves to the eJBD case $F(\sigma) = \gamma\sigma^2$, for which, instead, the Solar System limits are the tightest.

Thus, after implementing the Galileon interaction we study the model both analytically and numerically, at the level of background and linear perturbations theory. To perform the numerical analysis we extend Einstein-Boltzmann code CLASSig [13, 14].

The thesis is structured as follows:

(i) In the first chapter we introduce the basic concepts of Einstein's General Relativity

and the current cosmological concordance model. We also introduce an alternative to the cosmological constant: quintessence, in which the accelerated expansion of the Universe is driven by a scalar field and dark energy varies with time.

(ii) In chapter two we describe the relativistic theory of cosmological perturbations and CMB anisotropies. We present in this chapter the perturbed Einstein and the Boltzmann equations in the synchronous gauge.

(iii) Chapter three is a general overview of Horndeski theories: the most general scalar tensor theories with second order equations of motion. Particular emphasis is given to the models which predicts a propagation of the tensor degrees of freedom at the speed of light. Within this class of models there are the extended Jordan-Brans-Dicke theory (eJBD) and Induced Gravity (IGG), which are the models we will extend with a cubic interaction term. We conclude the chapter with a review of the screening mechanism in scalar tensor theories.

(iv) In the fourth chapter we present the extension with a Galileon-like interaction term of the type $\tilde{G}_3(\sigma)X\Box\sigma$ for both the eJBD theory and Induced gravity, we show that, due to the non-equivalence of the cubic interaction term under field redefinition, the two theories are not equivalent anymore after this extension. We derive the equations of motion for both models and we then present some special, analytical solutions obtained in absence of matter. Finally, we show the numerical evolution of the background cosmology, comparing it with the evolution in IG and ΛCDM.

(v) In the fifth chapter we present the results, obtained from the extended CLASSig code, for the CMB anisotropies, linear matter power spectrum, metric and scalar field perturbations. As for the background all these results are shown compared to IG and the ΛCDM concordance model.

In this thesis we will use the signature $(-,+,+,+)$ and natural units: $c = \hbar = 1$ unless otherwise specified. An overdot denotes a derivative with respect to cosmic time while a prime stands for derivative with respect to conformal time. The convention for tensor indices is the following: greek letters for space-time indices ($\mu, \nu, ... = 0, 1, 2, 3$), and latin letters for spatial indices ($i, j, ... = 1, 2, 3$).

Chapter 1

The standard cosmological model

Recent cosmological observations show a nearly isotropic Universe, at least on large scales, scales larger than 300 Mpc. Assuming that we are not in a special place in the universe, we can infer that the Universe appears homogeneous and isotropic for all comoving observers, i.e. a family of "typical" freely falling observers which move with the average velocity of galaxies in their respective neighborhoods. This is the starting point of modern cosmology, the so called "cosmological principle". The cosmological principle reflects the assumption that we aren't special observers, that is known as "Copernican principle".

Beside homogeneity, isotropy and the Copernican principle, the other pillar of modern cosmology is the theory of general Relativity. With these assumptions, Friedmann in 1922 [15], Lemaître in 1927 [16], and Robertson [17][18] and Walker [19] more than a decade later, derived the so called Friedmann-Lemaître-Robertson-Walker (FLRW) metric, that describes an homogenous and isotropic Universe and is used in the standard cosmological model. Other facts of key importance for cosmology that confirmed the Big Bang theory are: the discovery of the expansion of the universe by Hubble [20] at the beginning of the past century, the theory of Big Bang Nucleosynthesis (BBN) [21], the discovery of the Cosmic Microwave Background radiation (CMB) by Penzias and Wilson in 1964 [22], whose existence was theoretically predicted by Gamow and his collaborators in a series of articles in the late forties [23–30][1]. In 1998 two independent teams discovered that the Universe is accelerating by studying distant SNIa [31, 32].

[1] Working on primordial Nucleosynthesis they needed radiation permeating the universe in order to have a consistent theory. Now we know that their ideas on nucleosynthesis were not correct, but still the prediction was confirmed.

1.1 General Relativity

In the standard cosmological model gravity is the dominant force on the cosmological scales, therefore, the theory of gravity represents the starting point of every cosmological model.

The best candidate we have so far is the Theory of General Relativity, proposed by Einstein in the beginning of the XX century [33] and corroborated by many experiments and observations since then [8], among which the recent observations of gravitational waves [5, 34]. General Relativity is based on the Principle of the Equivalence of Gravitation and Inertia. The Equivalence Principle says that in a sufficiently small neighborhood of any space-time point in an arbitrary gravitational field there always exists a "locally inertial" coordinate system in which the effects of gravity are absent.

To describe any physical process we need to specify its spatial and temporal coordinates. It is useful to combine these four real numbers – one to denote the time of occurrence of the event and the other three for its location in space – into a single entity $x^\mu = (x^0, x^1, x^2, x^3)$. We can think of an event as a point in a four-dimensional space with coordinates x^μ. The collection of all the events is called space-time. In Special Relativity, the invariant interval between two events at coordinates x^μ and $x^\mu + dx^\mu$ is

$$ds^2 = \eta_{\mu\nu} dx^\mu dx^\nu \,, \tag{1.1}$$

where η is the metric of flat or Minkowskian space-time, in cartesian coordinates $\eta_{\mu\nu} = diag(1, -1, -1, -1)$ and the invariant interval is

$$ds^2 = -dt^2 + dx^2 + dy^2 + dz^2 \,. \tag{1.2}$$

The essence of General Relativity is to transform gravity from a simple force into a property of space-time; in Einstein's theory, the space-time is not necessarily flat like in Minkowski but it is influenced, curved, by the matter living in it, whose motion in turn is described in the curved space-time. In General Relativity test particles move along geodesics that describe the analogous of flat-geometry straight lines in the curved space-time. The geodesic is defined as such that the integral $\int ds$ is stationary under infinitesimal variations of the path that leave the endpoint fixed. For massless particles as photons the path is simply given by $ds^2 = 0$. In a general space-time the invariant interval is

$$ds^2 = g_{\mu\nu} dx^\mu dx^\nu \,, \tag{1.3}$$

where $g_{\mu\nu} = g_{\mu\nu}(t, \mathbf{x})$ is the metric of curved space-time, and differently from Minkowski's

metric, it depends on time and space; indeed it is this dependence that incorporates the effects of gravity. As mentioned above, a particle moves in such a way that the integral along its path is stationary:

$$\delta \int_{path} ds = 0, \tag{1.4}$$

where the gravitational effects are contained in the metric $g_{\mu\nu}$. Performing the variation (1.4) we obtain the so called geodesic equation for the path $x^\mu(\lambda)$ [35]:

$$\frac{d^2x^\mu}{d\lambda^2} + \Gamma^\mu_{\rho\sigma}\frac{dx^\rho}{d\lambda}\frac{dx^\sigma}{d\lambda} = 0 \tag{1.5}$$

where the $\Gamma^\mu_{\rho\sigma}$ are the Christoffel symbols:

$$\Gamma^\rho_{\mu\nu} = \frac{1}{2}g^{\rho\sigma}\left(\frac{\partial g_{\nu\sigma}}{\partial x^\mu} + \frac{\partial g_{\mu\sigma}}{\partial x^\nu} - \frac{\partial g_{\mu\nu}}{\partial x^\sigma}\right), \tag{1.6}$$

and λ is a parameter which increases monotonically with time. In the following, in order to lighten the notation, standard derivatives will be written using a comma: for example, $g_{\mu\nu,\rho} \equiv \partial_\rho g_{\mu\nu}$. It is useful to introduce the the energy-momentum vector $P^\mu = (E, \mathbf{P})$:

$$P^\mu = \frac{dx^\mu}{d\lambda}; \tag{1.7}$$

in this way the geodesic equation (1.5) becomes

$$\frac{dP^\mu}{d\lambda} + \Gamma^\mu_{\rho\sigma}P^\rho P^\sigma = 0. \tag{1.8}$$

As we emphasized earlier, in General Relativity gravity is not anymore an external force acting on matter but it becomes a property of space-time, to say it in the words of John Archibald Wheeler [36]: "space-time tells matter how to move; matter tells space-time how to curve". This is encoded in Einstein's field equations which relate the geometry of space-time with its matter content:[2]

$$G_{\mu\nu} \equiv R_{\mu\nu} - \frac{1}{2}g_{\mu\nu}R = 8\pi G T_{\mu\nu}. \tag{1.9}$$

$G_{\mu\nu}$ is called the Einstein tensor, $R_{\mu\nu}$ is the Ricci tensor which depends on the metric and its derivatives, $R = g^{\mu\nu}R_{\mu\nu}$ is the Ricci scalar, G is Newton's Constant and $T_{\mu\nu}$ is the energy-momentum tensor. As anticipated this equation puts in relation the geometry of

[2]With *matter content* of the universe we usually refer to its total energy content.

space-time with the matter content of the universe: on the left hand side we have the the first, the space-time geometry of the Universe and on the right hand side we have the second, its total energy-momentum tensor.

The energy-momentum tensor of a perfect fluid with energy density ρ, pressure p and $4-$velocity u^μ is

$$T_{\mu\nu} = p\, g_{\mu\nu} + (\rho + p)\, u_\mu u_\nu \,, \tag{1.10}$$

this is the form of the energy momentum tensor used in the standard cosmological model to describe matter at the cosmological scales. We shall describe the reasons for this choice and its consequences in the next sections.

The Riemann Tensor is defined as follows

$$R^\lambda_{\ \mu\rho\nu} = \Gamma^\lambda_{\mu\nu,\rho} - \Gamma^\lambda_{\mu\rho,\nu} + \Gamma^\lambda_{\alpha\rho}\Gamma^\alpha_{\mu\nu} - \Gamma^\lambda_{\alpha\nu}\Gamma^\alpha_{\mu\rho}\,; \tag{1.11}$$

and since the Ricci tensor is a contraction of the Riemann tensor: $R_{\mu\nu} = R^\lambda_{\ \mu\lambda\nu}$, we can express it in terms of the Christoffel symbols:

$$R_{\mu\nu} = \Gamma^\lambda_{\mu\nu,\lambda} - \Gamma^\lambda_{\mu\lambda,\nu} + \Gamma^\lambda_{\alpha\lambda}\Gamma^\alpha_{\mu\nu} - \Gamma^\lambda_{\alpha\nu}\Gamma^\alpha_{\mu\lambda}\,. \tag{1.12}$$

By construction the Riemann tensor satisfies the Bianchi identity:

$$\nabla_\sigma R_{\mu\nu\lambda\rho} + \nabla_\rho R_{\mu\nu\sigma\lambda} + \nabla_\lambda R_{\mu\nu\rho\sigma} = 0\,, \tag{1.13}$$

where the covariant derivative has been introduced. It is common to write the covariant derivative as a semicolon, for example $\nabla_\rho\, g_{\mu\nu} \equiv g_{\mu\nu;\,\rho}$. An important consequence of the Bianchi identity is that the covariant derivative of the Einstein tensor is null

$$\nabla_\nu G^{\mu\nu} = 0\,, \tag{1.14}$$

from this and the Einstein field equation (1.9) we obtain the conservation law for the energy momentum tensor

$$\nabla_\nu\, T^{\mu\nu} = 0. \tag{1.15}$$

1.1.1 Einstein gravitational Action

We will now briefly introduce the Lagrangian for General Relativity and then show in the following chapters some of its major extensions.

If we have a physical system described by an action functional in flat space-time, the effect of gravity on such a system can be incorporated directly in the action by changing

the volume element d^4x to $\sqrt{-g}\,d^4x$, where $g = det[g_{\mu\nu}]$, replacing partial derivatives with covariant derivatives and $\eta_{\mu\nu}$ with $g_{\mu\nu}$. Therefore if the action of the system in Minkowski space has the form

$$S_{matter} = \int d^4x \mathcal{L}_{matter}\,, \tag{1.16}$$

then, in presence of gravity, i.e. in curved spacetime it will be

$$S_{matter} = \int d^4x \sqrt{-g}\,\mathcal{L}_{matter}\,. \tag{1.17}$$

This is known as principle of minimal gravitational coupling [37] [38].

The Lagrangian that describes the dynamics of the gravitational field itself is

$$S_g = \int d^4x \sqrt{-g}\,\mathcal{L}_g \;=\; \frac{1}{16\pi G}\int \sqrt{-g}\,d^4x\,R\,; \tag{1.18}$$

and to obtain the total action we have to add $\mathcal{L}_g$ to the matter Lagrangian:

$$S = \int d^4x \sqrt{-g}\left[\frac{R}{16\pi G} + \mathcal{L}_{matter}\right]. \tag{1.19}$$

In (1.19) matter is minimally coupled to gravity, we will show some examples of how this assumption is relaxed in many theories of modified gravity.

1.2 Friedmann-Lemaître-Robertson-Walker metric

Solving (1.9) is not an easy task, and one has to take advantage of the symmetries of the system in order to do it, especially in our case where we have to solve it for the entire matter distribution of the universe. The cosmological principle states the isotropy and homogeneity of the universe, providing rotational and translational invariances that greatly simplify the task of solving Einstein's equation and finding a metric describing the Universe. As we already mentioned the assumption of homogeneity and isotropy of the 3-space selects a preferred class of observers, the comoving ones, namely those observers for whom the universe appears isotropic. Then, we use a comoving coordinate system (t, x^i) associated with these observers.

$$ds^2 = g_{00}\,dt^2 + 2\,g_{0i}\,dtdx^i + \gamma_{ij}dx^i dx^j, \tag{1.20}$$

where γ_{ij} is the purely spatial metric. Now, we choose as time coordinate the proper time of the comoving observers, which implies $g_{00} = -1$; moreover, stationarity constrains the

components g_{0i} to be zero, giving us

$$ds^2 = -dt^2 + \gamma_{ij}dx^i dx^j \equiv -dt^2 + d\ell^2. \tag{1.21}$$

By writing the space interval $d\ell^2$ in spherical coordinates we have

$$d\ell^2 = a^2(t)\left[\lambda^2(r)dr^2 + r^2\left(d\theta^2 + sin^2\theta d\varphi^2\right)\right], \tag{1.22}$$

the scalar curvature is then

$${}^3R = \frac{3}{2a^2r^3}\frac{d}{dr}\left[r^2\left(1 - \frac{1}{\lambda^2(r)}\right)\right]. \tag{1.23}$$

Thanks to the assumed homogeneity, geometrical properties are independent on r, this means that ${}^3R$ is a constant, therefore, integrating, one obtains [37]

$$\lambda^2(r) = \frac{1}{1 - kr^2}. \tag{1.24}$$

We can always rescale r to make $k = \pm 1$, obtaining the usual form of the space-time metric of a homogeneous and isotropic universe, called the Friedmann-Lemaître-Robertson-Walker (FLRW) metric:

$$ds^2 = -dt^2 + a^2(t)\left[\frac{dr^2}{1 - kr^2} + r^2(d\theta^2 + sin^2\theta d\varphi^2)\right]. \tag{1.25}$$

The possible values for k are $k = 0, +1, -1$ which correspond respectively to flat, spherical and hyperbolic spatial hypersurfaces. Once k is fixed, the evolution of the metric is uniquely determined by the so called scale factor $a(t)$. It is worth noticing that the metric (1.25) has been obtained by just using symmetry arguments, i.e. without any reference to the source of gravity $T_{\mu\nu}$. To go further and determine the value of k and the functional form of $a(t)$ we have to specify the matter distribution and use the Einstein's equation.

It is useful to introduce the concept of conformal time $d\tau = a^{-1}(t)dt$ which allows, by writing the differential solid angle as $d\Omega$, to express the FLRW metric as:

$$ds^2 = a^2(\tau)\left[-d\tau^2 + \frac{dr^2}{1 - kr^2} + r^2 d\Omega^2\right]. \tag{1.26}$$

In this thesis an overdot will denote derivatives with respect to cosmic time while a prime

will denote a derivative with respect to conformal time.

Another useful representation of the FLRW metric (1.25) uses the coordinate redefinition $d\chi \equiv dr/(1-kr^2)$:

$$ds^2 = -dt^2 + a^2(t)\Big[d\chi^2 + S_k^2(\chi)d\Omega^2\Big]\,, \tag{1.27}$$

where

$$S_k^2(\chi) \equiv \frac{1}{\sqrt{|k|}}\begin{cases} sinh(\sqrt{|k|}\,\chi) & k<0 \\ \sqrt{k}\chi & k=0 \\ sin(\sqrt{|k}\,\chi) & k>0. \end{cases} \tag{1.28}$$

Expressed in conformal time it is

$$ds^2 = ds^2 = a^2(\tau)\Big[-d\tau^2 d\chi^2 + S_k^2(\chi)d\Omega^2\Big]. \tag{1.29}$$

1.3 Kinematics of the Friedmann models

1.3.1 Redshift and Hubble law

Due to the expansion of the Universe, the wavelength of light gets stretched out in its journey before reaching our detectors: light emitted at a certain time t_1 with wavelength λ_1 will be observed today at t_0[3] with wavelength

$$\lambda_0 = \frac{a(t_0)}{a(t_1)}\,\lambda_1\,. \tag{1.30}$$

The discovery of the expansion of the Universe by Hubble in 1929 [20] implies $a(t_0) > a(t_1)$ which means that the wavelength of light will increase, i.e. it will be redshifted. We can actually define the redshift z as

$$1+z = \frac{\lambda_0}{\lambda_1} = \frac{a(t_0)}{a(t_1)}\,, \tag{1.31}$$

For nearby sources we can expand $a(t_1)$ around t_0

$$a(t_1) = a(t_0)[\,1 + (t_1 - t_0)H_0 + ...\,]\,, \tag{1.32}$$

[3]The subscript 0 means today unless otherwise specified

where H_0 is the Hubble parameter today, often called the Hubble constant:

$$H_0 \equiv \frac{\dot{a}(t_0)}{a(t_0)}. \tag{1.33}$$

For close objects, $t_0 - t_1$ is the physical distance d ($c = 1$). Therefore, from the above equations we find that the redshift increases linearly with distance

$$z \simeq H_0 d. \tag{1.34}$$

This is the so called Hubble law, first introduced by Hubble [20], together with the constant that takes his name, in the form

$$v_{gal} = H d\,, \tag{1.35}$$

where v_{gal} is the recessional velocity of a galaxy at a physical distance d. The Hubble constant H_0 measures the expansion rate of the Universe and it's usually written in the following way

$$H_0 = 100\,h\ \ \mathrm{km\,s^{-1}Mpc^{-1}}. \tag{1.36}$$

Nowadays the Hubble constant is measured through a variety of both local and cosmological probes, from supernovae to the CMB and gravitational waves, with precision increasing with time. The two main probes are within complementary frameworks: the CMB, that provides an indirect measurement, the most precise to date but also dependent on the cosmology assumed, and the direct distance ladder constructed with Supernovae Ia dependent on short scale calibration with cefeids. Currently, the latest measurements of the two probes are the ΛCDM value inferred from Planck 2018 data which is $h = 0.674 \pm 0.005$ [3], whereas, at the moment of the writing, the direct measurement gives $h = 0.735 \pm 0.014$ resulting in a 4.4σ tension [39]

1.3.2 Distances

There are various way of defining the distance concept in cosmology. Consider the metric (1.27)

$$ds^2 = -dt^2 + a^2(t)\Big[d\chi^2 + S_k^2(\chi)d\Omega^2\Big], \tag{1.37}$$

the distance multiplying the solid angle $d\Omega^2$ is called *metric distance*:

$$d_m \equiv S_k(\chi). \tag{1.38}$$

The *comoving distance* between us and a galaxy at redshift z is

$$\chi(z) = \int_{t_1}^{t_0} \frac{dt}{a(t)} = \int_0^z \frac{dz}{H(z)}, \tag{1.39}$$

it coincides with the metric distance in the case of a flat universe ($k = 0$). The *physical distance*, also called proper distance is obtained multiplying the comoving distance by the scale factor: $d_{pr} = a(t)\chi$ and as we expected the physical distance increases (decreases) with the expansion (compression) of the universe. There are other distances of interest in cosmology: the *angular diameter distance* d_A and the *luminosity distance* d_L. The first measures the distance between us and an object of known physical size D with observed angular size $\delta\theta$ on the sky:

$$d_A = \frac{D}{\delta\theta}\ , \tag{1.40}$$

and its relation with the metric distance is

$$d_A = \frac{d_m}{1+z}; \tag{1.41}$$

for a flat Unverse

$$d_A = \frac{\chi}{1+z}. \tag{1.42}$$

The luminosity distance d_L of an object located at a fixed comoving distance χ and redshift z is given by the ratio between the observed flux F and the intrinsic luminosity L of the object:

$$F = \frac{L}{4\pi d_m^2 (1+z)^2} \equiv \frac{L}{4\pi d_L^2}\ , \tag{1.43}$$

which gives

$$d_L = d_m\,(1+z)\,. \tag{1.44}$$

Therefore, the relation between the luminosity distance and the angular distance is:

$$d_A = \frac{d_L}{(1+z)^2}\,. \tag{1.45}$$

1.3.3 Horizons

The definition of horizon in cosmology is not unique, in particular we can identify two different point of view at its base: an horizon can either define the size at which past events can be observed or the one at which future events will be observed. In particular, the particle horizon χ_p (also known as comoving horizon or cosmological horizon) is the maximum comoving distance travelled by a photon since the Big Bang, i.e. it represents

the comoving size of the visible universe:

$$\chi_p \equiv \tau_i - \tau_0 = \int_{t_i}^{t_0} \frac{dt}{a(t)} = \int_{\ln a_i}^{\ln a} (aH)^{-1} d \ln a, \tag{1.46}$$

where $(aH)^{-1}$ is called Hubble radius. In standard cosmologies $\chi_p \sim (aH)^{-1}$, therefore, the Hubble radius is often called the horizon even though it is conceptually different from the particle horizon. In fact, the particle horizon is the maximum distance a photon can travel since the Big Bang, whereas the Hubble radius is the distance over which photons can travel in an Hubble time H^{-1}.

The event horizon is is the largest comoving distance from which light emitted now can ever reach the observer in the future.

$$\chi_e \equiv \int_{t_0}^{t_f} \frac{dt}{a(t)} = \int_{a_0}^{a_f} \frac{da}{H(a)a^2} \tag{1.47}$$

where t_f is the the last moment of the universe, if the expansion goes on forever or if it reaches a steady state it will be $t_f \to \infty$.

1.4 Dynamics of the Friedmann models

As anticipated in section 1.2, in order to obtain the functional form of the scale factor $a(t)$ we need to specify an energy-momentum tensor and solve Einsein's equations (1.9) where the left hand side is uniquely specified by the FLRW metric. On large scales, matter can be approximated as a perfect fluid characterized by energy density ρ, pressure p and 4-velocity u^μ, its energy–momentum tensor is then

$$T_{\mu\nu} = p\, g_{\mu\nu} + (\rho + p)\, u_\mu u_\nu. \tag{1.48}$$

The equation of state $p = p(\rho)$ has the form $p = \omega\rho$, where ω is a constant. Simplifying the Einstein equations for the FLRW metric (1.25) and perfect fluid matter source we obtain that the only non null components of the Einstein tensor are the $0-0$ and the $i-i$. These components give the Friedmann Equations that describe the evolution and acceleration of the scale factor:

$$\left(\frac{\dot{a}}{a}\right)^2 \equiv H^2 = \frac{8\pi G}{3}\rho - \frac{k^2}{a} \tag{1.49}$$

$$\ddot{a} = -\frac{4\pi G}{3}(\rho + 3p)a. \tag{1.50}$$

For ordinary forms of matter and radiation we have $\rho + 3p \geq 0$, that implies $\ddot{a} \leq 0$.

A decelerated expansion is in contrast with cosmological observations pointing towards an accelerated expansion of the Universe. Accelerated expansion can be obtained from (1.50) only if the dominant component of the universe satisfies $\rho + 3p < 0$. The standard cosmological model ΛCDM assume the existence of a dark energy component in the form of a cosmological constant to solve this issue.

The Hubble law tells us that $\dot{a}_0 > 0$ and equation (1.49) shows that $\dot{a} > 0$ at all times, unless the right-hand side vanishes. Therefore going towards decreasing times, $a(t)$ decreases until it reaches $a(t) = 0$, a moment in which density and a pressure are infinite: a singularity, called the Big-Bang. This simple argument illustrates the inevitability of the Big-Bang in the Friedmann models.

We can define the critical density today as the current density of the Universe in order for it to be flat:

$$\rho_{crit,0} \equiv \frac{3H_0^2}{8\pi G}, \tag{1.51}$$

and it is useful to define dimensionless density parameters:

$$\Omega_{i,0} \equiv \frac{\rho_{i,0}}{\rho_{crit,0}}; \tag{1.52}$$

here i identifies different component of the universe: $i = r, m, \Lambda$, which stand, respectively, for radiation, non-relativistic matter and vacuum energy. Non-relativistic matter is usually divided in two species: cold dark matter which takes the subscript c and ordinary matter which takes the subscript b. The sum of the density parameters of each component $\Omega_{tot} = \sum_i \Omega_i i$ can either be larger than unity, leading to a closed universe, smaller than 1, leading to an open universe, or exactly 1, which corresponds to a flat one.

With these definitions, equation (1.49) can be rewritten in the following way:

$$H^2 = H_0^2 \left[\Omega_{r,0} \left(\frac{a_0}{a} \right)^4 + \Omega_{m,0} \left(\frac{a_0}{a} \right)^3 + \Omega_{k,0} \left(\frac{a_0}{a} \right)^2 + \Omega_{\Lambda,0} \right], \tag{1.53}$$

where $\Omega_{k,0} \equiv -k/(a_0 H_0)^2$ is the spatial curvature density parameter. For simplicity we drop the subscript 0 in the density parameters and we follow the convention $a_0 = 1$. We can simplify equation (1.53):

$$\frac{H^2}{H_0^2} = \Omega_r a^{-4} + \Omega_m a^{-3} + \Omega_k a^{-2} + \Omega_\Lambda \,. \tag{1.54}$$

It's also useful to rewrite the Friedmann equations using the conformal time τ:

$$\mathcal{H}^2 = \frac{8\pi G}{3} a^2 \rho - k \,, \tag{1.55}$$

$$\mathcal{H}' = -\frac{4\pi G}{3}(\rho + 3p) a^2 \,, \tag{1.56}$$

where

$$\mathcal{H} = \frac{a'}{a} = aH \,, \tag{1.57}$$

is the Hubble parameter in conformal time.

The two Friedmann equations are not independent if we take into account the $0-$th component of the conservation law of the energy-momentum tensor (1.15), which gives the continuity equation [40]:

$$\dot{\rho} + 3H(\rho + p) = 0 \,, \tag{1.58}$$

or, in conformal time

$$\rho' + 3\mathcal{H}(\rho + p) = 0. \tag{1.59}$$

As anticipated earlier the equation of state for the various components of the Universe is

$$p_i = \omega_i \rho_i \tag{1.60}$$

where ω_i is usually a constant and takes the values $\omega = 0$ for non-relativistic matter, $\omega = 1/3$ for radiation and $\omega = -1$ for the cosmological constant. Integrating (1.59) making use of (1.60) we obtain a relation between the density and the scale factor:

$$\rho_i(t) = \rho_{0,i}(t) \left(\frac{a}{a_0} \right)^{-3(1+\omega_i)} . \tag{1.61}$$

If the Universe is dominated by matter ($\omega = 0$) $\rho_m \propto a^{-3}$, whereas for radiation ($\omega = 1/3$) we have $\rho_r = a^{-4}$. We deduce that going back in time radiation was dominating up to a point called equivalence when matter overcame radiation. For the cosmological constant ($\omega = -1$) the density $\rho_\Lambda \propto a^0$, which means that its energy density is constant, this component is often interpreted as the energy of vacuum but the disagreement between theoretical predictions and the observed value has lead to the quest for alternative models.

1.4.1 ΛCDM Model

Observations show that the density parameters Ω_i of the different constituents of the Universe sum up to $\Omega_{tot} \simeq 1$, i.e. spatial curvature is consistent with a flat universe:

$\Omega_{\rm k} = 0.001 \pm 0.002$ [3] and

$$\Omega_m = \Omega_c + \Omega_b = 0.3153 \pm 0.0073, \quad \Omega_\Lambda = 0.6847 \pm 0.0073. \tag{1.62}$$

The matter density parameter can be split in the cold dark matter contribution $\Omega_c \simeq 0.26$ and the contribution coming from ordinary baryonic matter $\Omega_b \simeq 0.0049$. If ordinary matter is well know, we have only indirect information on the dark matter component, whose nature and properties can be studied only through its cosmological and astrophysical effects. The search for its constituents is one of the most active field in both astrophysics and particle physics. The radiation contribution is $\Omega_r \simeq 9.4 \times 10^{-5}$ and comes from CMB and the cosmic neutrinos background. The observed value $\Omega_\Lambda \simeq 0.68$ implies that the energy density of the Universe is dominated by a component with equation of state $\omega \simeq -1$, which makes it very similar to a cosmological constant. Indeed, the cosmological constant is the simplest and most effective way we have to parametrize this component, called *dark energy*. Dark energy is responsible for the recent accelerated expansion of the Universe. The Universe described in terms of these components is known as the ΛCDM model, when the cosmic inflation is added in the game we obtain an amazing fit to a variety of cosmological data of the so-called “concordance" model”.

1.5 Thermal evolution

We have already seen that the early Universe was dominated by relativistic degrees of freedom until the *matter-radiation equivalence* $z \simeq 3.4 \times 10^3$ [3] where matter starts dominating, until recent times where dark energy took over $z \simeq 0.3$. During the radiation era we can identify different stages:

- Quark era: $T > T_{QH} \simeq 200 - 300\,\text{MeV}$, in this phase we have free quarks in a quark gluon plasma. Temperature is too high to allow hadronization. At the end of this epoch, quarks and antiquarks bind together forming hadrons.

- Hadron era: $T_{QH} > T > T_\pi \simeq 130\,\text{MeV}$, hadrons dominate until pions and antipions annihilate at $T = T_\pi$.

- Lepton era: $T_\pi > T > T_e \simeq 0.5\,\text{MeV}$, leptons dominate Universe until we reach T_e, temperature at which positrons and electrons annihilate. In this era primordial nucleosynthesis occurs. Towards the end of this epoch neutrino decouples from the cosmological fluid at $T \sim 1\,\text{Mev}$.

- Plasma era: $T_e > T > T_{eq} \simeq 1$eV, the Universe is composed by photons, matter (protons, electrons and helium nuclei) and neutrino which are decoupled from the photon-baryon fluid since the beginning of the lepton epoch.

At around 1 eV it starts the process of recombination when neutral hydrogen is formed, around $z \simeq 1400-1100$. Recombination leads to a drop in free electrons either increasing the Thompson scattering rate beyond the Hubble time and decoupling baryons and photons. The ideal surface of the last photon interaction is called the *last scattering surface* and it happens at $z \simeq 1100$. The photons propagating since then constitute the cosmic microwave background (CMB).

1.6 Successes and problems of the hot Big-Bang model

Among the greatest successes of the hot Big Bang model we find three key predictions:

- the expansion of the Universe,
- the abundances of light elements produced in the Big-Bang Nucleosynthesis (BBN) during the initial phases of the Universe [41],
- the existence of the Cosmic Microwave Background (CMB),

that have all been verified by observations. Nonetheless the original hot Big Bang theory is unable to address some conceptual problems which we will discuss in the following. The most elegant solution to the problem is cosmic inflation, which postulates an accelerated stage in a cold and quantum era which occurred before the thermal one of the standard Big Bang cosmology.

Flatness problem

Observations are consistent with a flat universe: $\Omega_\kappa = -0.011^{+0.013}_{-0.012}$ [42].
The evolution of the spatial curvature parameter is $\Omega_\kappa = -k/(aH)^2 = -k/\dot{a}^2$. On considering an evolution for the scale factor as $a \propto t^{2/3} \propto T^{-1}$, this leads to an increase $\Omega_k \sim T^{-1}$ during the matter era, at the time of the equivalence the curvature parameter had to necessarily be less than 10^{-4}. If we extend the same logic further in the past into the radiation epoch, in which $\Omega_k \propto T^{-2}$, we obtain that at the time of electron-positron annihilation, which happened at $T \simeq 10^{10}K$, the curvature parameter was at most of the order of 10^{-16}. Using the same logic we expect it to be of the order $\sim 10^{-60}$ at initial

times. This means that, in order to justify what we observe today, the Universe had to be close to flatness to a very high level initially, giving rise to a fine tuning problem. A period of exponential expansion, called cosmic inflation, before the radiation dominated era would solve this problem. In fact, during inflation, the Hubble parameter H would have been more or less constant, in such a way that $|\Omega_k| \propto a^{-2}$ and the extremely small curvature at the beginning of the radiation dominated era would be justified.

More quantitatively, during inflation the scale factor increased by a factor $e^{\mathcal{N}}$. If, when inflation begins $|\Omega_t extsck| = \mathcal{O}(1)$, then at the end it would be of order $e^{-2\mathcal{N}}$. Therefore if inflation lasts long enough, which means $\mathcal{N}$ is large enough, we have solved the flatness problem. One obtains that the number of e-foldings of $\mathcal{N}$ necessary to solve the flatness problem is [43]

$$\mathcal{N} > 62. \tag{1.63}$$

Horizon problem:

The observed high degree of isotropy of the CMB poses a problem: the angular dimension of $1/H$ regions at the time of decoupling is approximately $\theta_{hor} \simeq 1.6°$ [43], which is only a small fraction of the sky. The CMB monopole is instead homogeneous on all the sky, i.e. scales much larger than the Hubble radius at the time when the CMB was formed; indeed, without inflation, the CMB pattern should be composed of about 10^6 causally disconnected patches [44]. If there were not enough time for these regions to communicate, no physical influence could have smoothed out initial inhomogeneities and brought regions separated by several degrees in the sky to the same temperature. This is known as the Horizon problem.

A period of exponential expansion would solve this problem as well: inflation would have stretched tiny causally connected patches to cosmic sizes, providing enough time to homogeneize our observable Universe. More quantitatively, the proper horizon, which is the scale factor times the particle horizon, at the time of last scattering t_L is

$$d_H(t_L) \equiv a(t_L) \int_{t_*}^{t_L} \frac{dt}{a(t)} \tag{1.64}$$

where t_* is the time of the beginning of inflation. Now suppose that, being t_I the time of the end of inflation, the scale factor increases exponentially at a rate H_I:

$$a(t) = a(t_*)e^{H_I(t-t_*)} = a_I e^{-H_I(t_I-t)}. \tag{1.65}$$

The number of e-foldings is then $\mathcal{N} = H_I(t_I - t)$ and the above equations give

$$d_H(t_L) = \frac{a(t_L)}{a_I H_I}\left(e^{\mathcal{N}} - 1\right). \tag{1.66}$$

We can drop the -1 in (1.66) because to solve the horizon problem we need $e^{\mathcal{N}} \gg 1$. Imposing now the proper horizon at the time of last scattering to be larger than the angular-diameter distance of the surface of last scattering: $d_I(t_L) > d_A(t_L)$ we obtain

$$\mathcal{N} > 62, \tag{1.67}$$

which is the same condition required to solve the flatness problem.

Monopole problem

In grand unified theories (GUT) the local symmetry group is spontaneously broken at an energy of the order $\sim 10^{16}$ GeV to the gauge symmetry of the Standard Model. All these theories predict the production of magnetic monopoles and their densities today should be much higher than that of matter [45], but so far we have not found any trace of magnetic monopoles.

To solve this problem, one needs inflation to dilute the magnetic monopoles, its duration, given in number of e-foldings, should be $\mathcal{N} > 23$ [43]. We see that the number of e-foldings necessary to solve the flatness and horizon problem automatically solves the monopoles problem.

The most serious of the three problems presented above is the flatness problem, because there are possible alternative solutions to the monopole and horizon problems that do not rely on inflation. A solution to the monopole problem may be that GUT theories are not the correct physical theories to describe the early stage of the universe and therefore the prediction of magnetic monopoles would be meaningless. As far as regards the horizon problem, early Universe models which have a suitable contraction rather than a nearly exponential expansion can offer a solution to the horizon problem which is alternative to inflation.

1.6.1 Slow-roll inflation

Inflation has been proposed first by Starobinski [46] [47], Kazanas [48] and Sato [49] and then developed by Guth [50], Linde [51] [52], and Albrecht and Steinhardt [53].

The simplest way to achieve inflation is by considering a fluid with negative pressure and we do this by means of a scalar field $\phi(t)$ called the *inflaton*. All we need to assume is that the inflaton at some early time takes a value such that the potential $V(\phi)$ is very

large but quite flat. At first the scalar field rolls very slowly down this potential, in this way the Hubble parameter decreases slowly, and the universe experiences a nearly exponential inflation before the field configuration changes very much. The action of a scalar field in curved spacetime is

$$S = \int d^4x\sqrt{-g}\Big(-\frac{1}{2}g^{\mu\nu}\partial_\mu\phi\,\partial_\nu\phi - V(\phi)\Big), \tag{1.68}$$

and its energy momentum tensor is [54]

$$T^{\phi}_{\mu\nu} = \partial_\mu\phi\,\partial_\nu\phi - g_{\mu\nu}\left[\frac{1}{2}g^{\rho\lambda}\,\partial_\rho\phi\,\partial_\lambda\phi - V(\phi)\right]; \tag{1.69}$$

from which, comparing it with (1.48) we can define the density and the pressure of the scalar field as follows:

$$\rho_\phi = \frac{1}{2}\dot{\phi}^2 + V(\phi); \tag{1.70}$$

$$p_\phi = \frac{1}{2}\dot{\phi}^2 - V(\phi)\,. \tag{1.71}$$

The Klein-Gordon equation, obtained from the variation of the action (1.68) with respect to ϕ, or alternatively from the conservation of $T^{\mu\nu}_{\phi}$, is

$$\ddot{\phi} + 3H\dot{\phi} + V_{,\phi} = 0\,, \tag{1.72}$$

while the first Friedmann equation (1.49) becomes

$$H^2 = \frac{8\pi G}{3}\big(\rho_\phi + \rho\big) - \frac{k}{a^2}\,, \tag{1.73}$$

the expansion rapidly causes ρ and k/a^2 to become negligible with respect to the density of the inflaton field, which is varying slowly. Equation (1.73) is then

$$H = \sqrt{\frac{8\pi G}{3}\rho_\phi} = \sqrt{\frac{8\pi G}{3}\left(\frac{1}{2}\dot{\phi}^2 + V(\phi)\right)}\,. \tag{1.74}$$

Taking the derivative of the square of equation (1.74) and combining it with (1.72) we obtain:

$$\dot{H} = -4\pi G\dot{\phi}^2\,. \tag{1.75}$$

For a nearly exponential expansion we require

$$|\dot{H}| \ll H^2, \tag{1.76}$$

which, thanks to (1.74) (1.75), it's equivalent

$$\dot{\phi}^2 \ll |V(\phi)|, \tag{1.77}$$

i.e. the kinetic term is negligible with respect to the potential and (1.74) becomes

$$H \simeq \sqrt{\frac{8\pi G\, V(\phi)}{3}}. \tag{1.78}$$

Another usual assumption which allows us to drop the inertial term from equation (1.72) is

$$|\ddot{\phi}| \ll H|\dot{\phi}|, \tag{1.79}$$

therefore we have

$$\dot{\phi} = -\frac{V_{,\phi}}{3H} = -\frac{V_{,\phi}}{\sqrt{24\pi G V}}. \tag{1.80}$$

This means that

$$\epsilon \equiv \frac{|\dot{H}|}{H^2} = \frac{1}{16\pi G}\left(\frac{V_{,\phi}}{V}\right)^2, \tag{1.81}$$

then inflation will last long enough if $\epsilon \ll 1$. Moreover, deriving equation (1.80) with respect to ϕ leads us to the condition for $|\ddot{\phi}|$ to be much less than $|V_{,\phi}|$:

$$\left|\frac{V_{,\phi,\phi}}{V}\right| \ll 24\pi G. \tag{1.82}$$

To summarize, the slow-roll conditions necessary to obtain inflation are:

$$\epsilon \equiv \frac{|\dot{H}|}{H^2} = \frac{1}{16\pi G}\left(\frac{V_{,\phi}}{V}\right)^2 \ll 1\,, \tag{1.83}$$

$$\eta \equiv \frac{1}{8\pi G}\left|\frac{V_{,\phi,\phi}}{V}\right| \ll 1. \tag{1.84}$$

Using these parameters we can determine, just from the shape of the potential, if inflation occurs.

At the end of inflation there is a period which goes under the name of *preheating* in which the inflaton is oscillating in the minimum of the potential and decays in other

particles. Preheating is the first stage of reheating which connects the cold and quantum inflation phase to the thermal hot Big Bang cosmology.

1.7 Dark matter

Studies of individual galaxies and clusters of galaxies led to the surprising outcome that these celestial objects contain way more mass than what is visible and would be estimated from the amount of stars and gas. In particular, only $10 - 20\%$ of their mass consists of visible matter, while most of the mass is invisible, i.e. it interacts only via gravitational effects. For this reason it is called *dark matter*. We only know of its presence through its gravitational effects: rotation curves in spiral galaxies, velocity dispersions in elliptic ones and in galaxy clusters, and gravitational lensing are the most known evidences of its existence. The first observation of dark matter was done in 1933 by Zwicky [55], who, studying the Coma cluster found that the velocity dispersion of the galaxies was so high that, to keep the system stable, the average mass density of the Coma system would have to be much more than that deduced from visible matter. Many other observations later proved without any doubt the existence of dark matter (for a detailed history of dark matter see the reviews [2] [56]). There are also cosmological evidences for the existence of dark matter and its greater abundance with respect to ordinary matter: from CMB anisotropies the Planck data lead to an estimate of $\Omega_c h^2 = 0.1200 \pm 0.0012$ [3]. A comparison with the baryonic fraction $\Omega_b h^2 = 0.02237 \pm 0.00015$ [3] shows that there is about five times more dark matter than ordinary matter.

Types of dark matter: Hot (HDM) and cold (CDM)

Many possibilities to classify different models of dark matter exist, for example thermal vs non-termal, or hot vs cold, etc. In particular, the HDM vs CDM categorization is especially relevant in cosmology and is related to the typical kinetic energy of the dark matter particles when they decouples from radiation. If dark matter was relativistic at the time of decoupling it's called hot dark matter (HDM), if it wasn't relativistic it takes the name of cold dark matter (CDM). This discrimination between HDM and CDM is of great importance in cosmology because they give rise to two different scenarios of structures formation: if the prevalent form of dark matter was the hot one this would lead to a top-down structure formation in which the most massive structures are formed first and through fragmentation smaller substructures like galaxies and stars are formed. CDM privileges instead a bottom up scenario, in which globular clusters are the first objects to collapse. In this situation larger structures are formed by subsequent merging of smaller ones. Galaxies has been observed to be present less than a billion years after the Big-Bang [57] and therefore the bottom-up scenario, and consequently the fact that

dark matter is mostly composed by CDM is favoured by observations.

Dark matter candidates

The first candidates for dark matter were baryonic, since in astrophysics there are various types of objects that are not visible, they are called Massive Astrophysical Compact Objects (MACHOs). With MACHOs we then refer to a variety of objects, the most important ones are red and brown dwarfs, neutron stars and stellar black holes. Unfortunately statistical analysis shows that there are not enough MACHOS to explain all the dark matter mass. Another class of MACHOS are primordial black holes whose existance has been proposed by Hawking in 1971 [58]. The possibility for primordial black holes to represent a significative fraction of the DM observed is a very interesting issue largery explored. Unfortunately currently results seem to point to a maximum of 10% of DM in the form of primordial black holes

The most promising candidates for dark matter, though, are non-baryonic and come from extension of the Standard model of Particle Physics, which per se does not contain any particle compatible with dark matter. The first candidate were massive neutrinos that represent one of the basic extension to the standard model whose existence has been verified experimentally. However, since massive neutrinos are HDM they can only minimally contribute to the DM amount, although the possibility of sterile neutrinos is still under investigation. Going beyond the standard model, new candidates have to satisfy a couple of criteria: being cold enough and not to interact much with the standard model particles. The two main hypotesis for the particle nature of dark matter which respect these conditions are:

- WIMPs (Weakly Interacting Massive Particles): these are very massive particles with masses of the order $m_{\text{WIMP}} \sim 10 - 10^3\,\text{GeV}$. Thanks to this large mass they are non-relativistic and since their mediator bosons have very large masses as well, their interactions are very short range causing interactions with standard model particles to be extremely rare. However a large mass causes some problems, as it makes WIMPs susceptible to decaying into standard model particles, therefore this instability on cosmological time scales would not help explaining the observed abudances of dark matter. One then needs to come up with some clever ideas to ensure the stability of WIMPs, such as symmetries that preserves their numbers [59].

- Axions: They are very light and stable particles. In quantum field theory language axions are pseudo Nambu-Goldstone bosons arising from the spontaeous breaking

of global chiral symmetries. They were first introduced to solve the charge-parity (CP) problem in 1977 [60]. Even if they have a small mass, axions can account for dark matter thanks to their high density. It is remarkable that axions produce a rich phenomenology in astroparticle physics and cosmology.

1.8 Dark energy

As already mentioned, the way to achieve accelerated expansion is to have a fluid with negative pressure that dominates the energy content of the Universe. To describe dark energy and the current accelerated expansion of the universe we need therefore such a fluid, the simplest way in which we can achieve this is by means of the *cosmological constant*. There's also alternatives to the cosmological constant which is called *quintessence* and which we will describe briefly.

1.8.1 Cosmological constant

The cosmological constant was first introduced by Einstein [61] in his field equation

$$G_{\mu\nu} = 8\pi G T_{\mu\nu} + \Lambda g_{\mu\nu}\,, \tag{1.85}$$

to satisfy a personal philosophical taste: the staticity of the Universe. After Hubble's discovery of the expansion of the Universe, the cosmological constant was abandoned, but in the early nineties it was proposed again as ΛCDM in alternative to the CDM model. Following the discovery that the expansion of the Universe is actually accelerated it became the the simplest candidate to describe dark energy.

The most common interpretation for the nature of the cosmological constant is the vacuum energy density of quantum fields [62] [63] [64]. Although we measure only differences of energy, since gravity couples with the total amount of energy density, the vacuum energy should enter the Einstein field equation giving a nonzero contribution. The strong disagreement between the theoretical prediction and the value from observational data has sparkled the search for alternative solutions to Λ.

1.8.2 Quintessence

An interesting alternative to a cosmological constant is an evolving dark energy component with a time dependent $\omega_{\rm DE} = p_{\rm DE}/\rho_{\rm DE}$, as in *quintessence* models [43] [65] [66] [67]. In quintessence models, just like in inflation, the expansion is driven by a scalar field φ. However we should assume a slow evolution of ρ_φ, in a way to obtain a cosmological constant behaviour at low redshift $z \simeq 0.3$ and have a small impact in the past epochs, already constrained by data. The field theory of the scalar field is exactly the

same we've seen in the case of inflation in section 1.6.1. In order to avoid fine tunings, the potential should allow for a wide range of initial values to produce the same scalar field behaviour today. The simplest example of such a potential is [65] [68]:

$$V(\varphi) = M^{4+\alpha}\varphi^{-\alpha} \tag{1.86}$$

with $\alpha > 0$ and arbitrary, and M is a constant having the dimension of a mass in natural units ($\hbar = c = 1$). The Klein-Gordon equation (1.72) can be rewritten as follows

$$\ddot{\varphi} + \frac{2}{(1+\omega)t}\dot{\varphi} - \alpha M^{4+\alpha}\varphi^{-\alpha-1} = 0. \tag{1.87}$$

In order to not spoil the Big Bang Nucleosynthesis we require $\rho_\varphi \ll \rho_R$ at the BBN epoch, leading to $H = 1/(2t)$. Therefore, a solution of Eq. (1.87) in the radiation era ($\omega = 1/3$) is

$$\varphi = \left[\frac{\alpha(2+\alpha)^2 M^{4+\alpha} t^2}{6+\alpha}\right]^{\frac{1}{2+\alpha}}, \tag{1.88}$$

from which we can see that both $\dot{\varphi}$ and $V(\varphi)$ go as $t^{-2\alpha/(2+\alpha)}$, providing a ρ_φ subdominant at early times with respect to the radiation density, $\rho_\mathrm{r} \propto t^{-2}$. This solution is an attractor, meaning that any solution coming close will approach it as t increases in a given cosmological era. To see this, one can perturb the Klein-Gordon equation:

$$\delta\ddot{\varphi} + \frac{3}{2t}\delta\dot{\varphi} + \frac{(6+\alpha)(1+\alpha)}{(2+\alpha)^2 t^2}\delta\varphi\,, \tag{1.89}$$

whose solutions are:

$$\delta\varphi \propto t^\gamma\,, \qquad \gamma = -\frac{1}{4} \pm \sqrt{\frac{1}{16} - \frac{(6+\alpha)(1+\alpha)}{(2+\alpha)^2}}\,. \tag{1.90}$$

Both solutions decay with time. This proves that the solution (1.88) is an attractor, or tracker solution.

When non-relativistic matter starts to dominate ($\omega = 0$), nothing changes: the tracker solution still grows as $t^{2/(2+\alpha)}$ and the density still goes as $t^{-2\alpha/(2+\alpha)}$, while matter and radiation densities decrease faster, in particular $\rho_\mathrm{m} \propto t^{-2}$ and $\rho_\mathrm{r} \propto t^{-8/3}$, which ensures that ρ_φ will eventually dominate. The time t_c when this happens is the time at wich $\rho_\varphi = \rho_\mathrm{m}$ and it is of order

$$t_c \sim M^{-(4+\alpha)/2}\, G^{-(2+\alpha)/4}, \tag{1.91}$$

which gives

$$\varphi(t_c) \sim G^{-1/2}. \tag{1.92}$$

After this "quintessence-matter equivalence", the Klein-Gordon equation becomes

$$\ddot{\varphi} + \sqrt{24\pi G\rho_\varphi}\dot{\varphi} - \alpha M^{4+\alpha}\varphi^{-\alpha-1} = 0. \tag{1.93}$$

The damping term proportional to $\dot{\varphi}$ will slow the growth of φ in such a way that $\dot{\varphi}^2$ will be less than $V(\varphi)$, also the the inertial term $\ddot{\varphi}$ will become negligible with respect to damping and potential terms (these are the same slow roll conditions we applied in sec. 1.6.1 on inflation). The equation of motion then becomes

$$\sqrt{24\pi G\rho_\varphi}\dot{\varphi} = \alpha M^{4+\alpha}\varphi^{-\alpha-1}, \tag{1.94}$$

whose solution is

$$\varphi = M\left(\frac{\alpha(2+\alpha/2)t}{\sqrt{24\pi G}}\right)^{1/(2+\alpha/2)}. \tag{1.95}$$

With the help of (1.95) one can perform a sanity check showing that the slowroll approximation was justified. Numerical calculations show that this solution is the asymptotic form approached for $t \to \infty$ by the tracker solution, we have then, at late time when ρ_φ dominates

$$\ln a \propto t^{2/(2+\alpha/2)}. \tag{1.96}$$

This behaviour is very similar to the evolution of the scale factor $a(t)$ that a cosmological constant would produce, which is $\ln a \propto t$, and they are exactly the same for $\alpha = 0$, as expected. In general the scale factor grows less rapidly in quintessence models with respect to the cosmological constant model.

Chapter 2

Theory of cosmological perturbations and CMB anisotropies

The cosmological principle, stating isotropy and homogeneity of the Universe, may hold only on very large scales (of the order of hundreds of Mpc) as is evidenced by the presence of gravitational bound structures as galaxies and clusters that are clearly local deviations from homogeneity and isotropy. The key idea is that small fluctuations in the energy density generated in the early Universe are amplified by gravitational instability leading to the formation of such structures. Observations of the CMB show temperature anisotropies of the order of $\Delta T/T \sim 10^{-5}$ that reflect the primordial fluctuations at the last scattering ($z \simeq 10^3$). The small amplitude of the fluctuations allows to use the linear perturbation theory to make predictions about the state of the Universe at that redshift and to study the CMB anisotropies.

For this reason, in this chapter we will introduce first order perturbation theory. Density perturbations are treated as a random Gaussian field in such a way that their Fourier modes are decoupled. The notation for the Fourier transform is:

$$A(\tau, \mathbf{x}) = \int \frac{d\mathbf{k}}{(2\pi)^3} A(\tau, \mathbf{k}) e^{i\mathbf{k}\cdot\mathbf{x}} \,. \tag{2.1}$$

Then, the power spectrum of a function A is

$$\langle A(k) A(k') \rangle = (2\pi)^3 \mathcal{P}(k) \delta^{(3)}(k - k') \,. \tag{2.2}$$

In this chapter we will mainly follow the notation and conventions of [69] and use the flat ($k = 0$) FLRW metric (1.26) in conformal time.

2.1 Metric perturbations

We start by perturbing at first order the FLRW metric:

$$g_{\mu\nu}(\tau, \mathbf{x}) = \bar{g}_{\mu\nu}(\tau) + \delta g_{\mu\nu}(\tau, \mathbf{x}), \tag{2.3}$$

where $\bar{g}_{\mu\nu}(\tau)$ is the unperturbed background metric. We write the general perturbed space-time interval in the following way [40]

$$ds^2 = a^2(\tau)\big[-(1+2A)d\tau^2 + 2B_i\, dx^i d\tau + (\delta_{ij} + h_{ij})\big], \tag{2.4}$$

where A, B_i and h_{ij} are functions of space-time and spatial indices are raised and lowered with the Kronecker delta. The metric perturbations can be decomposed into 3 categories according to their spin with respect to a local rotation of the spatial coordinates on hypersurfaces of constant time:

- **scalar perturbations** which have spin 0 and are induced by energy density inhomogeneities. They exhibit gravitational instability and lead to the formation of structure in the Universe;
- **vector perturbations** are spin 1 modes called also vorticity modes because they arise from the rotational motion of the fluid. In standard cosmology they decay very quickly;
- **tensor perturbations** are spin 2 modes, gravitational waves, and are supported also in vacuum.

This characterization is called scalar-vector-tensor (SVT) decomposition. We can procede further: thanks to Helmoltz decomposition theorem any 3-vector can be splitted into the gradient of a scalar field and a vector field with zero divergence:

$$B_i = \partial_i B + \hat{B}_i\,, \tag{2.5}$$

with $\partial^i \hat{B}_i = 0$. In a similar way we can decompose the perturbation δg_{ij} as follows:

$$h_{ij} = 2C\delta_{ij} + 2\partial_{\langle i}\partial_{j\rangle}E + 2\partial_{(i}\hat{E}_{j)} + 2\hat{E}_{ij}\,; \tag{2.6}$$

with

$$\partial_{\langle i}\partial_{j\rangle}E \equiv \Big(\partial_i\partial_j - \frac{1}{3}\delta_{ij}\nabla^2\Big)E, \tag{2.7}$$

$$\partial_{(i}\hat{E}_{j)} \equiv \frac{1}{2}\Big(\partial_i \hat{E}_j + \partial_j \hat{E}_i\Big). \tag{2.8}$$

The objects with an hat are divergenceless: $\partial^i \hat{E}_i = 0 = \partial^i \hat{E}_{ij}$; moreover $\hat{E}_{ij}$ is also traceless. In (2.6) we decomposed h_{ij} in a scalar part which correspond to the first two terms on the right hand side, a vector part which is the third term, and a tensor part corresponding to the fourth term. We have basically separated the 10 degrees of freedom of the metric in 4+4+2 SVT degrees of freedom, 4 of which are scalar ones.

At linear order, the scalar, vector and tensor perturbations are decoupled, i.e. they evolve independently [70]. Considering the subject of this work from now on we will focus only on scalar perturbations.

2.1.1 Gauge transformation

Consider a coordinate transformation from a coordinate system x^μ to another $\tilde{x}^\mu$

$$x^\mu \to \tilde{x}^\mu = x^\mu + d^\mu(x^\nu)\,, \tag{2.9}$$

with

$$d^0 = \alpha(\tau, \mathbf{x})\,, \tag{2.10}$$

$$d^i = \partial^i \beta(\tau, \mathbf{x}) + \epsilon^i(\tau, \mathbf{x})\,; \tag{2.11}$$

where the spatial part d^i has been decomposed into a longitudinal component $\partial^i\beta$ ($\varepsilon_{ijk}\partial^i\partial^j\beta = 0$) and a transverse component ϵ^i ($\partial_i\epsilon^i = 0$).
Under a coordinate transformation the metric transform as:

$$\tilde{g}_{\mu\nu}(\tilde{x}) = \frac{\partial x^\alpha}{\partial \tilde{x}^\mu}\frac{\partial x^\beta}{\partial \tilde{x}^\nu} g_{\alpha\beta}(x)\,, \tag{2.12}$$

assuming d^μ to be of the same order of the metric perturbation, keeping only first order terms in the right hand side of eq. (2.12) and writing $\tilde{g}_{\mu\nu}$ as

$$\tilde{g}_{\mu\nu}(\tilde{x}) = \bar{g}_{\mu\nu}(\tilde{x}) + \delta\tilde{g}_{\mu\nu}(\tilde{x})\,; \tag{2.13}$$

we can infer the following gauge transformation law

$$\delta g_{\mu\nu} \to \delta\tilde{g}_{\mu\nu} = \delta g_{\mu\nu} - d^\rho\,\partial_\rho\,\bar{g}_{\mu\nu} - \bar{g}_{\mu\rho}\,\partial_\nu d^\rho - \bar{g}_{\rho\nu}\,\partial_\mu d^\rho\,; \tag{2.14}$$

with the right and left hand side considered at the same coordinate value. Thanks to this we can now write the gauge transformation law of the scalar degrees of freedom:

$$A \to \tilde{A} = A - \alpha' - \mathcal{H}\alpha\,, \tag{2.15}$$

$$B \to \tilde{B} = B + \alpha - \beta'\,, \tag{2.16}$$

$$C \to \tilde{C} = C - \mathcal{H}\alpha - \frac{1}{3}\nabla^2\beta\,, \tag{2.17}$$

$$E \to \tilde{E} = E - \beta\,. \tag{2.18}$$

One way to deal with gauge problems is to define combinations of the metric perturbations that are invariant under the change of coordinates (2.9). The simplest variables of this kind have been introduced by Bardeen [71] and are therefore called Bardeen variables, they are

$$\Psi_B \equiv A + \mathcal{H}(B - E') + (B - E')'\,, \tag{2.19}$$

$$\Phi_B \equiv -C - \mathcal{H}(B - E') + \frac{1}{3}\nabla^2 E\,. \tag{2.20}$$

Using these variables is then straightforward to see whether a perturbation is physical or not: if Ψ_B and Φ_B vanish in a coordinate system, then they are null in every chart, this means that the metric perturbations are fictitious and can be removed by a coordinate transformation. For this reason the Bardeen variables can be thought as the "real" space-time perturbations.

2.1.2 Gauge fixing

Different topics may take advantage from different gauge choices, fixing the gauge corresponds to fixing the coordinate system. There are different possible gauge choices, hereafter we will work in the so called *synchronous gauge*. This gauge is widely used for the simple form of the equations and the stability for numerical implementation, i.e. in the Einstein-Boltzmann codes. The synchronous gauge is defined by

$$A = B_i = 0\,. \tag{2.21}$$

Under such a condition the metric (2.4) becomes

$$ds^2 = a^2(\tau)\big[-d\tau^2 + (\delta_{ij} + h_{ij})\big]. \tag{2.22}$$

To connect the notation presented so far with the one in [69] one simply needs to define $2C \equiv h/3$, $2E \equiv \mu$, $\hat{E}_i \equiv A_i$ and $2\hat{E}_{ij} \equiv h^T_{ij}$. Following [69] it is useful write the

scalar mode of of h_{ij} as a Fourier intgral

$$h_{ij}(\tau,\mathbf{x}) = \int \frac{d\mathbf{k}}{(2\pi)^3} e^{i\mathbf{k}\cdot\mathbf{x}} \left[\hat{k}_i\hat{k}_j\, h(\tau,\mathbf{k}) + \left(\hat{k}_i\hat{k}_j - \frac{1}{3}\delta_{ij}\right) 6\eta(\tau,\mathbf{k}) \right], \quad \mathbf{k} = k\hat{k}. \tag{2.23}$$

It is important to note that the synchronous gauge conditions do not fix all the gauge degrees of freedom since the choice of the initial hypersurface and its coordinate assignments are arbitrary. Such residual gauge freedom is manifested in the fictitious gauge modes in the solutions of the Einstein equations. To avoid the disturbance of the gauge modes it is customary to work in the CDM rest frame.

2.2 Linearized Einstein equations

We now study the Einstein equations at linear order in Fourier space. Within our conventions we substitute spatial derivatives ∂_i with ik_i. Splitting the energy-momentum tensor and the Einstein tensor into a background and a perturbed part we can write the perturbed Einstein equations as

$$\delta G^{\mu}{}_{\nu} = 8\pi G \delta T^{\mu}{}_{\nu}\,. \tag{2.24}$$

The first step is to obtain the perturbations to the energy-momentum tensor of a perfect fluid (1.48). Calling $\delta\rho$ and δp the density and pressure perturbations and considering the coordinate velocity $v^i = dx^i/d\tau$ of the same order of $\delta\rho$ and δp, the components of the perturbed energy-momentum tensor are

$$T^0{}_0 = -(\bar{\rho} + \delta\rho)\,, \tag{2.25}$$

$$T^0{}_i = (\bar{\rho} + \bar{p})v_i = -T^i{}_0\,, \tag{2.26}$$

$$T^i{}_j = (\bar{p} + \delta p)\delta^i_j + \Sigma^i{}_j\,, \tag{2.27}$$

with $\Sigma^i{}_j = T^i{}_j - \delta^i_j\, T^k{}_k/3$. We define new useful variables θ and σ related to the pertubations of the energy-momentum tensor:

$$\theta \equiv ik^j v_j\,, \tag{2.28}$$

$$(\bar{\rho} + \bar{p})\sigma \equiv -\left(\hat{k}_i\hat{k}_j - \frac{1}{3}\delta_{ij}\right)\Sigma^i{}_j\,. \tag{2.29}$$

The left hand side of eq. (2.24), the perturbed Einstein tensor, is derived computing the perturbed Christoffel symbols that provide the perturbed Ricci tensor and the perturbed Ricci scalar. In particular, in the synchronous gauge, the time-time, longitudinal

time-space, trace space-space and traceless space-space parts of the Einstein equations are, at linear order [69]

$$k^2\eta - \frac{1}{2}\mathcal{H}h' = -4\pi G a^2 \sum_i \delta\rho_i \,, \tag{2.30}$$

$$k^2\eta' = 4\pi G a^2 \sum_i (\bar{\rho} + \bar{p})\theta_i \,, \tag{2.31}$$

$$h'' + 2\mathcal{H}h' - 2k^2\eta = -24\pi G a^2 \sum_i \delta p_i \,, \tag{2.32}$$

$$h'' + 6\eta'' + 2\mathcal{H}(h' + 6\eta') - 2k^2\eta = -24\pi G a^2 \sum_i (\bar{p} + \bar{p_i})\sigma_i \,, \tag{2.33}$$

where, as usual, the index i runs over all the species contributing to the content of the Universe. At this point the only thing left to derive is the conservation equation of the perturbed energy-momentum tensor. The conservation equation (1.15) is still valid at linear level for single fluids, and for a fluid with equation of state $p = \omega\rho$ it leads to

$$\delta' = -(1+\omega)\left(\theta + \frac{h'}{2}\right) - 3\mathcal{H}\left(\frac{\delta p}{\delta\rho} - \omega\right)\delta \,, \tag{2.34}$$

$$\theta' = -\mathcal{H}(1 - 3\omega)\theta - \frac{\omega'}{1+\omega}\,\theta + \frac{\delta p}{\delta\rho}\,\frac{k^2\delta}{1+\omega} - k^2\sigma \,, \tag{2.35}$$

where $\delta = \delta\rho/\rho$ is the density contrast.

When two or more fluids are in interactions additional terms appears, we will go through the single components specific equations in the next section.

2.3 Boltzmann equations

We derive in this section the perturbed Boltzmann equations for photons, massless neutrinos, CDM and baryons. These equations coupled with the Einstein's ones completely describe the evolution of cosmological perturbations. We use the synchronous gauge as for the Einstein equations.

We work in the phase space described by three positions x_i and their conjugate momenta P_i. The conjugate momentum is simply the spatial part of the 4-momentum with lower indices and in the synchronous gauge it is related with the proper momentum $p^i = p_i$ (measured by an observer at a fixed spatial coordinate) by

$$P_i = a(\delta_{ij} + \frac{1}{2}h_{ij})p^j. \tag{2.36}$$

The phase space distribution $f = f(x^i, P_j, \tau)$ gives the number of particles in a differential volume $dx^1 dx^2 dx^3 dP_1 dP_2 dP_3$ of the phase space:

$$dN = f(x^i, P_j, \tau) dx^1 dx^2 dx^3 dP_1 dP_2 dP_3 \,. \tag{2.37}$$

It evolves according to the Boltzmann equation:

$$\frac{df}{dt} = C[f] \,, \tag{2.38}$$

where the term on the right hand side is the collision term which accounts for all possible interactions. The zeroth-order phase space distribution is the Fermi-Dirac distribution for fermions ($-$ sign) and the Bose-Einstein distribution for bosons ($+$ sign):

$$f_0 = f_0(\epsilon) = \frac{g_s}{e^{\,\epsilon/(aT)} \pm 1}, \tag{2.39}$$

where g_s is the number of spin degrees of freedom and $\epsilon = a(p^2 + m^2)^{1/2} = (P^2 + a^2 m^2)^{1/2}$ is related to the zeroth component of the 4-momentum by $P_0 = -\epsilon$. We have used units such that the Planck and the Boltzmann constant are equal to one.

Following [72], it is convenient to replace P_j with $q_j \equiv a p_j$ in order to eliminate the metric perturbations from the definition of the momenta. We write it as a function of its magnitude q and direction n_j as $q_j = q n_j$, with $n_i n^i = 1$. In this way we change our phase space variables replacing $f(x^i, P_j, \tau)$ with $f(x^i, q, n_j, \tau)$, and also ϵ becomes $\epsilon = (q^2 + a^2 m^2)^{1/2}$.

Now, writing the perturbed phase-space distribution as an expansion around its zeroth-order

$$f(x^i, P_j, \tau) = f_0(q)\big[1 + \Psi(x^i, q, n_j, \tau)\big] \,, \tag{2.40}$$

we can express, in terms of the perturbation Ψ the components of the energy-momentum tensor, whose general form is

$$T_{\mu\nu} = \int \sqrt{-g}\, dP_1 dP_2 dP_3 \frac{P_\mu P_\nu}{P^0} f(x^i, P_j, \tau) \,, \tag{2.41}$$

finding

$$T^0{}_0 = -a^{-4} \int q^2\, dq\, d\Omega\, \sqrt{q^2 + a^2 m^2}\, f_0(q)(1+\Psi)\,, \tag{2.42}$$

$$T^0{}_i = a^{-4} \int q^2\, dq\, d\Omega\, q\, n_i\, f_0(q)\, \Psi\,, \tag{2.43}$$

$$T^i{}_j = a^{-4} \int q^2\, dq\, d\Omega\, \frac{q^2 n_i n_j}{\sqrt{q^2 + a^2 m^2}}\, f_0(q)(1+\Psi)\,, \tag{2.44}$$

where $d\Omega$ is the solid angle. Now, we can expand the Boltzmann equation (2.38) as

$$\frac{df}{d\tau} = \frac{\partial f}{\partial \tau} + \frac{dx^i}{d\tau}\frac{\partial f}{\partial x^i} + \frac{dq}{d\tau}\frac{\partial f}{\partial q} + \frac{dn_i}{d\tau}\frac{\partial f}{\partial n_i} = C[f] = \left(\frac{\partial f}{\partial \tau}\right)_C\,, \tag{2.45}$$

and, using of the geodesic equation (1.8) to obtain an expression for $dq/d\tau$ we can write the Boltzmann equation in k-space in the following way

$$\frac{\partial \Psi}{\partial \tau} + i\frac{q}{\epsilon}(\mathbf{k}\cdot\hat{n})\Psi + \frac{d\,\ln f_0}{d\,\ln q}\left[\eta' - \frac{h' + 6\eta'}{2}(\hat{k}\cdot\hat{n})^2\right] = \frac{1}{f_0}\left(\frac{\partial f}{\partial \tau}\right)_C\,. \tag{2.46}$$

where $\hat{n} = \mathbf{q}/|\mathbf{q}|$. We will now detail the Boltzmann equation for each species in the cosmological fluid.

Cold dark matter

CDM interacts with other species only through gravity and can be treated as a pressure-less perfect fluid, $\omega = \omega' = 0$ and zero anisotropic pressure $\sigma_c = 0$. The collisional term is zero and we remind that in the synchronous gauge we set in the rest frame of CDM $\theta_c = 0$. Therefore, from eq. (2.34) and (2.35) we just get

$$\delta_c' = -\frac{1}{2}h'\,. \tag{2.47}$$

Neutrinos

In general for massless particles we have $q = \epsilon$. In addition, for massless neutrinos we can neglect the collisional term. In order to reduce the number of variables we integrate out the q-dependence in the neutrino distribution function and expand the angular dependence of the perturbation Ψ in a series of Legendre polynomials $P_l(\hat{k}\cdot\hat{n})$:

$$F_\nu(\mathbf{k},\hat{n},\tau) \equiv \frac{\int q^2\, dq\, q\, f_0(q)\Psi}{\int q^2\, dq\, q\, f_0(q)} \equiv \sum_{l=0}^{\infty}(-i)^l(2l+1)F_{\nu l}(\mathbf{k},\tau)P_l(\hat{k}\cdot\hat{n})\,. \tag{2.48}$$

In terms of the new variable F_ν, the perturbations δ_ν, θ_ν and σ_ν take the form

$$\delta_\nu = \frac{1}{4\pi}\int d\Omega\, F_\nu(\mathbf{k},\hat{n},\tau) = F_{\nu\,0}\,, \tag{2.49}$$

$$\theta_\nu = \frac{3i}{16\pi}\int d\Omega\,(\hat{k}\cdot\hat{n})\,F_\nu(\mathbf{k},\hat{n},\tau) = \frac{3}{4}\,k\,F_{\nu 1}\,, \tag{2.50}$$

$$\sigma_\nu = -\frac{-3}{16\pi}\int d\Omega\left[(\hat{k}\cdot\hat{n})^2 - \frac{1}{3}\right]F_\nu(\mathbf{k},\hat{n},\tau) = \frac{1}{2}F_{\nu 2}\,. \tag{2.51}$$

Then, integrating equation (2.46) over $q^2\,dq\,q\,f_0(q)$ and dividing it by $\int q^2\,dq\,q\,f_0(q)$, the Boltzmann equation becomes

$$\frac{\partial F_\nu}{\partial\tau} + ik\mu F_\nu = -\frac{2}{3}h' - \frac{4}{3}(h'+6\eta')P_2(\mu)\,, \tag{2.52}$$

where $\mu = \hat{k}\cdot\hat{n}$. Thus, making use of the Legendre expansion (2.48), we obtain:

$$\delta'_\nu = -\frac{4}{3}\theta_\nu - \frac{2}{3}h'\,, \tag{2.53}$$

$$\theta_\nu = k^2\left(\frac{1}{4}\delta_\nu - \sigma_\nu\right), \tag{2.54}$$

$$F'_{\nu\,2} = 2\sigma'_\nu = \frac{8}{15}\theta_\nu - \frac{3}{5}kF_{\nu\,3} + \frac{4}{15}(h'+6\eta')\,, \tag{2.55}$$

$$F'_{\nu\,l} = \frac{k}{2l+1}\left[lF_{\nu\,(l-1)} - (l+1)F_{\nu\,(l+1)}\right], \quad l\geq 3\,. \tag{2.56}$$

From the Boltzmann equation we have then obtained an infinite hierarchy of equations. The hierarchy is truncated at some maximum multipole order $l_{\max}$, in the standard case the terms higher than $F_{\nu\,3}$ are negligible, therefore, it is used to truncate the hierarchy at $l = 3$.

Photons

Photons can be treated similarly to massless neutrinos, with the difference that we cannot neglect the collisional terms.

Before recombination photons interact via Thomson scattering with baryons, in the so-called tight coupling; after recombination photons start to free-stream with some residual energy and momentum transfer due to residuals Thomson interactions. In addition, photons are linearly polarized in the plane perpendicular to their propagation direction $\hat{n}$ due to scattering of electron density perturbations with wavevector $\mathbf{k}$. We denote the sum (total intensity) of phase space densities in the the two polarization states for each k and $\hat{n}$ by $F_\gamma(\mathbf{k},\hat{n},\tau)$, defined as in equation (2.48), and the difference by $G_\gamma(\mathbf{k},\hat{n},\tau)$. Their explicit expressions and the collision factor can be found in [69],

while the Boltzmann equations are:

$$\delta'_\gamma = -\frac{4}{3}\theta_\gamma - \frac{2}{3}h' \,, \tag{2.57}$$

$$\theta'_\gamma = k^2\left(\frac{1}{4}\delta_\gamma - \sigma_\gamma\right) + a\, n_e\, \sigma_T(\theta_b - \theta_\gamma) \,, \tag{2.58}$$

$$\sigma'_\gamma = \frac{4}{15}\theta_\gamma - \frac{3k}{10}F_{\gamma\,3} + \frac{2}{15}(h' + 6\eta') - \frac{a\, n_e}{20}\sigma_T(18\sigma_\gamma - G_{\gamma\,0} - G_{\gamma\,2}) \,, \tag{2.59}$$

$$F'_{\gamma\,l} = \frac{k}{2l+1}\left[lF_{\gamma\,(l-1)} - (l+1)F_{\gamma\,(l+1)}\right] - a\, n_e\, \sigma_T F_{\gamma\,l}, \quad l \geq 3 \,, \tag{2.60}$$

where $\sigma_T = 0.6652 \times 10^{-24}\,\mathrm{cm}^{-2}$ is the Thomson cross-section and n_e is the proper mean density of the electrons.

Baryons

Baryons behave like a perfect pressureless non-relativistic fluid. Anyway, differently from CDM, for baryons we need to account for the interaction with photons that produces a transfer of momentum and energy between the two components, represented by the term $a\, n_e\, \sigma_T\, (\theta_b - \theta_\gamma)$. Moreover we need also to consider the evolution of the momentum. In particular, the momentum density is related to θ by $ik_j\delta T^j_0 = (\bar\rho + \bar p)\theta$. The conservation of momentum then implies that we add a term $4\bar\rho_\gamma/(3\bar\rho_b)\, a\, n_e\, \sigma_T(\theta_\gamma - \theta_b)$ to the equation for θ'_b; thus, the Boltzman equations for Baryons are

$$\delta'_b = -\theta_b - \frac{1}{2}h' \,, \tag{2.61}$$

$$\theta'_b = -\mathcal{H}\theta_b + c_s^2 k^2 \delta_b + \frac{4\bar\rho_\gamma}{3\bar\rho_b} a\, n_e\, \sigma_T(\theta_\gamma - \theta_b) \,, \tag{2.62}$$

in which $c_s^2 = \delta p/\delta\rho$ is the squared baryon sound speed.

2.3.1 Tight coupling approximation

At early times, the characteristic time scale for the photon-baryon interaction $t_{b\,\gamma} \simeq (n_e\, \sigma_T)^{-1}$ is smaller than the the Hubble time $t_H \simeq a\,\tau$, therefore any deviations from zero of $\theta_\gamma - \theta_b$ rapidly decays. This can be seen subtracting eq. (2.58) and (2.62) and considering $\mathcal{H}\theta_b + \frac{1}{3}k^2\delta_\gamma$ as a forcing term. In the limit $\sigma_T \to \infty$ one obtains $\theta_b = \theta_\gamma$, i.e. a tight coupling between baryons and photons. Therefore, at early times we can assume $\theta_b = \theta_\gamma = \theta_{\gamma b}$ and combining (2.58) and (2.62) in such a way that the scattering terms cancel we get [73]:

$$\left(\frac{4}{3}\Omega_\gamma - \Omega_b\right)\theta'_{\gamma b} = -\Omega_b\mathcal{H}\theta_{\gamma b} + \frac{1}{3}\Omega_\gamma k^2\delta_\gamma \,, \tag{2.63}$$

while the baryons and photons density contrasts evolve as

$$\delta_b' = -\theta_{\gamma b} - \frac{1}{2}h' \,, \tag{2.64}$$

$$\delta_\gamma' = -\frac{4}{3}\theta_{\gamma b} - \frac{2}{3}h' \,. \tag{2.65}$$

2.4 Initial conditions for the cosmological perturbations

In order to solve the Einstein-Boltzmann system of differential equations we have to set the initial conditions. These initial values for the perturbative quantities are usually set deep in the radiation era but after the decoupling of neutrinos. This simplifies the computation since the density is dominated by photons and neutrinos, i.e. $\rho_{tot} \simeq \rho_\gamma + \rho_\nu$. In the radiation era $a \sim \tau$ and $\mathcal{H} \sim \tau^{-1}$ and we consider scales which are outside the horizon $k\tau \ll 1$.[1]

A natural mechanism for the origin of the initial perturbations is provided by inflation. The simplest inflationary models predict the initial perturbations to be adiabatic [74], an hypothesis supported also by the limited amount of isocurvatures allowed by CMB data [42], we will therefore focus on them.

2.4.1 Adiabatic fluctuations

Consider a matter and radiation plasma before the equivalence: the entropy per matter particle is given by $\Gamma = T^3/n_m$ with n_m the number density of matter particles. Thus, defining the entropy perturbation $\mathcal{S}$ as $\mathcal{S} = \delta\Gamma/\Gamma$ we have, since $\rho_r \propto T^4$,

$$\mathcal{S} = 3\frac{\delta T}{T} - \delta_m = \frac{3}{4}\delta_r - \delta_m \,. \tag{2.66}$$

Then, if we impose a vanishing entropy perturbations we obtain the following conditions:

$$\delta_\gamma \simeq \delta_\nu \simeq \frac{4}{3}\delta_c \simeq \frac{4}{3}\delta_b \,. \tag{2.67}$$

Perturbations satisfying the above equations are said to be adiabatic or iso-entropic.

Alternatively one could define the entropy perturbation in a gauge invariant way:

$$\mathcal{S} = \mathcal{H}\left(\frac{\delta p}{p'} - \frac{\delta\rho}{\rho'}\right) , \tag{2.68}$$

[1] k is a superhorzon scale if $k\tau < 1$ while it is a subhorizon mode when $k\tau > 1$.

and obtain that, for two barotropic fluids with constant $\omega_i = p_i/\rho_i$, the relative entropy perturbation is given by

$$\mathcal{S}_{ij} = \frac{\delta_i}{1+\omega_i} - \frac{\delta_j}{1+\omega_j}\,, \tag{2.69}$$

from which it is evident that iso-entropic perturbations satisfy (2.67).

Adiabatic perturbations are characterized by the fact that there are equal fractional perturbations in number density for both radiation and non-relativistic matter, this leads to a global perturbation to the total energy density and, through the Einstein equations, to a perturbation to the local geometry of the Universe. It is however possible to perturb the matter components without perturbing the geometry: this is the case of isocurvature perturbations, which give a non-vanishing entropy perturbation but do not contribute to the curvature perturbation at the leading order.

Following [69] we derive now the initial conditions for adiabatic perturbations. From (2.30) and (2.32), remembering that deep in the radiation era $\rho_{tot} = \rho_\gamma + \rho_\nu$ and $\mathcal{H} \sim \tau^{-1}$ we obtain:

$$\tau^2 h'' + \tau h' + 6\big[(1-R_\nu)\delta_\gamma + R_\nu \delta_\nu\big] = 0 \tag{2.70}$$

where $R_\nu = \rho_\nu/(\rho_\nu+\rho_\gamma)$. Due to the tight coupling with baryons, photons do not develop anisotropic pressure, leading to negligible multipoles $l \geq 2$ in the hierarchy. Then, from the Boltzmann equations for the various components we have:

$$\begin{aligned}
&\delta'_\gamma + \frac{4}{3}\theta_\gamma + \frac{2}{3}h' = 0\,, \qquad \theta'_\gamma - \frac{1}{4}k^2\delta_\gamma = 0\,,\\
&\delta'_\nu + \frac{4}{3}\theta_\nu + \frac{2}{3}h' = 0\,, \qquad \theta'_\nu - \frac{1}{4}k^2(\delta_\gamma - 4\sigma_\nu) = 0\,,\\
&\sigma'_\nu - \frac{2}{15}(2\theta_\nu + h' + 6\eta') = 0\,.
\end{aligned} \tag{2.71}$$

Now, expanding the perturbations in power series of $k\tau$ and considering the growing mode, the initial conditions at leading order are [69][73]:

$$h = C(k\tau)^2\,, \qquad \eta = 2C - \frac{5+4R_\nu}{6(15+4R_\nu)}C(k\tau)^2\,, \tag{2.72}$$

$$\delta_\gamma = -\frac{2}{3}C(k\tau)^2\,, \qquad \delta_c = \delta_b = \frac{3}{4}\delta_\nu = \frac{3}{4}\delta_\gamma\,, \tag{2.73}$$

$$\theta_c = 0\,, \qquad \theta_\gamma = \theta_b = -\frac{1}{18}C(k^4\tau^3)\,, \qquad \theta_\nu = \frac{23+4R_\nu}{15+4R_\nu}\theta_\gamma\,, \tag{2.74}$$

$$\sigma_\nu = \frac{4C}{3(15+4R_\nu)}(k\tau)^2\,, \tag{2.75}$$

where C represents the primordial power spectrum of fluctuations.

2.4.2 The curvature perturbation

We now define the curvature perturbation in terms of the metric perturbations introduced in section 2.1 as

$$\mathcal{R} \equiv -C + \frac{\nabla^2 E}{3} - \mathcal{H}\left(B - \frac{\theta}{k^2}\right). \tag{2.76}$$

This quantity is also gauge invariant, in fact, it is related to the Bardeen potentials by [75]:

$$\mathcal{R} = -\Psi_B - \frac{2}{3(1+\omega)\mathcal{H}}(\Psi_B' + \mathcal{H}\Phi_B). \tag{2.77}$$

Furthermore, it obeys the following evolution equation [75]:

$$\mathcal{R}' = \frac{2}{3(1+\omega)\mathcal{H}}\,k^2\left[c_s^2\Psi_B + \frac{1}{3}(\Psi_B - \Phi_B)\right] + 3\mathcal{H}\,c_s^2\,\mathcal{S}\,, \tag{2.78}$$

from which we see that for adiabatic fluctuations and on large scales (neglecting therefore terms proportional to k) the curvature perturbation remains constant outside the horizon. For this reason adiabatic perturbations are often called curvature perturbations and in fact they can be characterized by $\mathcal{R}$.

2.5 Anisotropies of CMB

At sufficiently early times the frequent collisions between free electrons and photons maintained the thermal equilibrium between matter and radiation. The radiation then follows a black-body spectrum:

$$n_T(\nu)d\nu = \frac{8\pi\nu^2 d\nu}{e^{h\nu/(k_B T)} - 1}\,. \tag{2.79}$$

As time passed, the universe expanded and cooled down to the temperature allowing neutral atoms to form, the so-called recombination, at $z_{rec} \simeq 1100$. The recombination decouples matter and radiation and the latter becomes free to propagate. This radiation is called the *Cosmic Microwave Background* (CMB) and today has a temperature of $T_{\rm CMB} = 2.72548 \pm 0.00057$ [76]. It is also isotropic on the sky, in fact we only observe

small temperature anisotropies of the order $\Theta \equiv \delta T/T \sim 10^{-5}$. These anisotropies are the imprints of primordial fluctuations generated by inflation and can be divided in two groups: primary and secondary anisotropies. The primary anisotropies are those already present at the time of the decoupling while the secondary ones originated after recombination, during the journey of the photons from the last scattering surface to us.

Primary anisotropies are the result of different processes at different scales. We can identify three main categories: superhorizon, subhorizon and very small scales. On superhorizon scales the photons are only subject to the gravitational interaction. Inhomogeneities in the gravitational potential cause photons that originate in regions of higher density to climb out of a potential well, loosing energy for gravitational redshift. For the same reason a photon rolling down a potential hill will gain energy being blueshifted. This mechanism causes a variation in the Temperature contrast $\Theta = \Phi$, where Φ is the gravitational potential. This effect is partly compensated by a gravitational time delay: a photon originating in an overdense region will be scattered at a slightly earlier time and thus at an higher temperature compared to a photon from a region of average or below average density. This gives a contribution $\Theta = -2\Phi/3$. The resulting net effect is then $\Theta = \Phi/3$, which is known as *Sachs-Wolfe effect* [77]. Since on large scales $2\Phi = -\delta$, the hot spots in the CMB corresponds to underdense regions while overdense regions will be identified by cold spots. On subhorizon scales we have the acoustic oscillations due to the density and velocity fluctuations of the coupled photon-baryon fluid. Qualitatively these oscillations are due to the fact that the baryon-photon fluid falls in the potential wells created by the dark matter perturbations and gets compressed in the process, this leads to an increase in the radiation pressure which counteracts the compression, resulting in an oscillating behaviour of the fluid. In the density peaks of these sound waves, the baryon-photon fluid is adiabatically compressed and thus hotter than the average, viceversa for the bottoms. Both contribute to the CMB power spectrum because it is quadratic in the perturbations and therefore we expect peaks corresponding to the scales that were in the extrema of their oscillations at z_{dec}, even peaks for rarefaction and odd peaks for compression.

At even smaller scales the dominating process is the so called *Silk damping*. Owing to the finite mean free path of photons, the perfect fluid approximation for the photon-baryon fluid is not valid at the smallest scales, and the two components are effectively decoupled. This implies that under a certain characteristic size λ_S called the Silk scale, the temperature fluctuations can be washed out by the diffusion of photons. Because of this process, primary CMB anisotropies are strongly damped on the smallest angular scales (less than few arcmins).

Secondary anisotropies, being generated during the propagation from the last scattering surface, provide important information about structure formations. They consists of different effects, the most relevant are:

- Integrated Sachs-Wolfe effect (ISW): Photons propagating towards us are traversing a Universe in which structure formation takes place, i.e. the gravitational potential is varying with time. If it was time-independent, photons would enter and leave a potential well with their frequency being unaffected: the blueshift of the fall being balanced by the redshift of the climb; this is no longer true if the potential changes over time. This process can be divided in early ISW that happens right after decoupling when the radiation density has still important gravitational effects, and late ISW arising in the dark energy dominated era due to the decay of gravitational potentials in accelerated expansion.

- Gravitational lensing: photons that reach us encounter in their journey various gravitational fields which deflect them, for this reason we observe them coming from a slightly different direction with respect to the original one. This effect affects the primary anisotropies by smoothing out the acoustic peaks and generating a non-zero B-mode polarization on small angular scales. At the same time the lensing presence induces a non-zero four point correlation function which is used to reconstruct the lensing potential and the underlying dark matter distribution.

- The Thermal Sunyaev–Zeldovich effect: CMB photons passing through clusters of galaxies or other regions of dense and hot gas are Inverse Compton scattered by the hot electrons causing a localized spectral distortion of the black body with an analytical frequency shape. The TSZ effect can be clearly identified in detected galaxy clusters thanks to the current multifrequency observations covering both frequencies below and over 217 GHz which represents the zero point. Undetected SZ together with the Kynetic Sunyaev Zeldovich effect, caused by peculiar motions, are considered an additional source of noise in CMB dedicated experiments.

2.5.1 Angular power spectrum

In order to perform a statistical analysis of the CMB anisotropies we compress the data from maps to the angular power spectrum. The spherical harmonics are the eigenfunctions of the Laplace operator on the sphere and form a complete basis

for scalar functions on the sky, therefore we can expand the temperature anisotropy $\Theta(\theta,\varphi) = \delta T(\theta,\varphi)/T$ in terms of spherical harmonics:

$$\Theta(\theta,\varphi) = \sum_{\ell=1}^{\infty} \sum_{m=-\ell}^{\ell} a_{\ell m} Y_{\ell m}(\theta,\varphi)\,, \tag{2.80}$$

where the index ℓ represents the multipole and is related to a characteristic angular scale $\theta \sim 2\pi/\ell$, while the index m describes the angular orientation. For statistically isotropic fluctuations, the ensemble average of the temperature fluctuations is described by the power spectrum

$$\langle a^*_{\ell' m'} a_{\ell m} \rangle = \delta_{\ell\ell'}\delta_{mm'} C_\ell\,, \tag{2.81}$$

furthermore, for Gaussian fluctuations all the statistical information are encoded in the power spectrum. Of course, we cannot average over an ensemble of different realizations of the sky: we are limited to only one sky and what is actually observed is a quantity averaged over m:

$$C_\ell^{obs} = \frac{1}{2\ell+1} \sum_{m=-\ell}^{m=\ell} |a_{\ell m}|^2\,. \tag{2.82}$$

This gives rise to a limitation on how accurately the CMB angular power spectrum can be known. This uncertainty is known as *cosmic variance* and it's due to the fact that for each mode ℓ we can only average over a finite number $(2\ell+1)$ of independent modes. The error on the C_ℓ's is given by

$$\Delta C_\ell = \sqrt{\frac{2}{2\ell+1}} C_\ell. \tag{2.83}$$

We briefly describe the observed temperature power spectrum: figure 2.1 shows the temperature anisotropies power spectrum and the best-fit obtained by Planck 2018 [3], the quantity D_ℓ in the y-axis is related to our notation by $D_\ell = T^2_{\rm CMB}\frac{\ell(\ell+1)}{2\pi}C_\ell$. On large angular scales (small ℓ) the spectrum is dominated by the Sachs wolfe effect which leads to a plateau in that region of the graph. Dark energy, which dominates the matter content of the Universe at recent times, enhances the spectrum on very small ℓ ($\ell < 10$) through ISW effects. At smaller scales we observe the characteristic acoustic peaks, the first peak at $\ell \simeq 220$ correspond to the angular scale of the horizon at recombination ($\theta \sim 1^\circ$), and it can give us an estimate of the total density parameter. Then we have a sequence of acoustic peaks which is damped for large values of ℓ ($\ell > 1000$) by the Silk damping.

The cosmological parameters constrained with the angular temperature power spec-

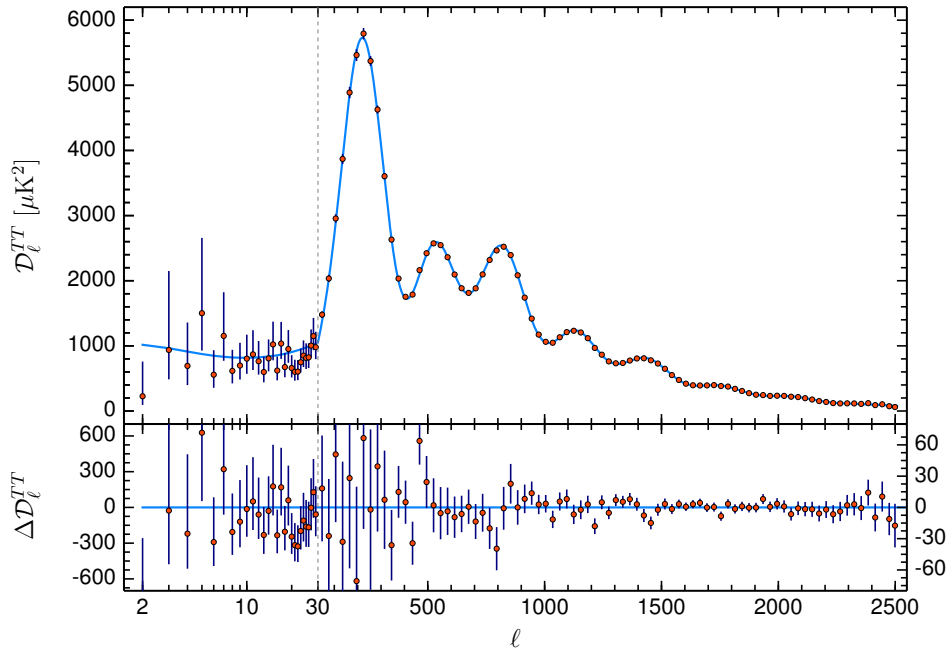

Figure 2.1: Temperature anisotropies power spectrum and best fit measured by Planck. $D_\ell^{TT} = T_{\rm CMB}^2\, \ell(\ell+1)C_\ell/(2\pi)$ in our notation. Figure taken from [3]

trum may be degenerate which means that for different choices of the parameters one may obtain the same power spectrum. To break the degeneracy it is convenient to take advantage of the polarization of the CMB.

2.5.2 CMB polarization anisotropies

The CMB is linearly polarized, in fact if a radiation field possesses a quadrupole, then Thomson scattering induces a linear polarization of the scattered radiation. Polarization anisotropies are much weaker than the ones in temperature: they are only 1% of the total temperature fluctuations on large angular scales and about 10% at small angular scales. A radiation fields is usually measured with the Stokes parameters I, Q and U, where the latter two are referred to polarization and the first to the total intensity. The parameter Q measures the difference in brightness between two orthogonal linear polarizations, while the U parameter measures the difference in brightness between two linear polarizations at 45° to those used to define Q. For CMB polarization is usual to combine the Q and U parameters into E (electric) and B (magnetic) modes. The advantage offered by E and B modes is that they are invariant under rotations. The electric modes are scalar functions describing the component of the polarization with even parity, they correlate with temperature fluctuations, which are also even. The B modes are odd under parity (hence the name magnetic) and represent the odd component

of the polarization; due to parity there is no correlation between the B modes and either Θ or E modes. Another important distinction is that E modes are related with density perturbations whereas primordial B modes are generated by tensor perturbations and are therefore signature of primordial gravitational waves generated during inflation.

Analogously to what has been done above for the temperature field we can expand the E and B modes in spherical harmonics and define the C_ℓ's for these quantities as

$$\langle E^*_{\ell' m'} E_{\ell m} \rangle = \delta_{\ell' m'} \delta_{\ell m} C_\ell^{EE} \,, \tag{2.84}$$

$$\langle a^*_{\ell' m'} E_{\ell m} \rangle = \delta_{\ell' m'} \delta_{\ell m} C_\ell^{TE} \,, \tag{2.85}$$

$$\langle B^*_{\ell' m'} B_{\ell m} \rangle = \delta_{\ell' m'} \delta_{\ell m} C_\ell^{BB} \,. \tag{2.86}$$

In figure 2.2 and 2.3 are shown, respectively, the EE and TE spectrum and best fit obtained by Planck [3]. The peaks in the EE spectrum is π out of phase with respect to those in the temperature spectrum, because the polarization is the result of Thomson scattering and its effect is therefore maximum when the fluid velocity is maximal. The polarization anisotropies are also affected by lensing, in particular lensing generates B modes from the E, with the consequence that it is possible to measure non-vanishing B signals even in absence of tensor perturbations. This is one of the main sources of noise in the detection of primordial B modes.

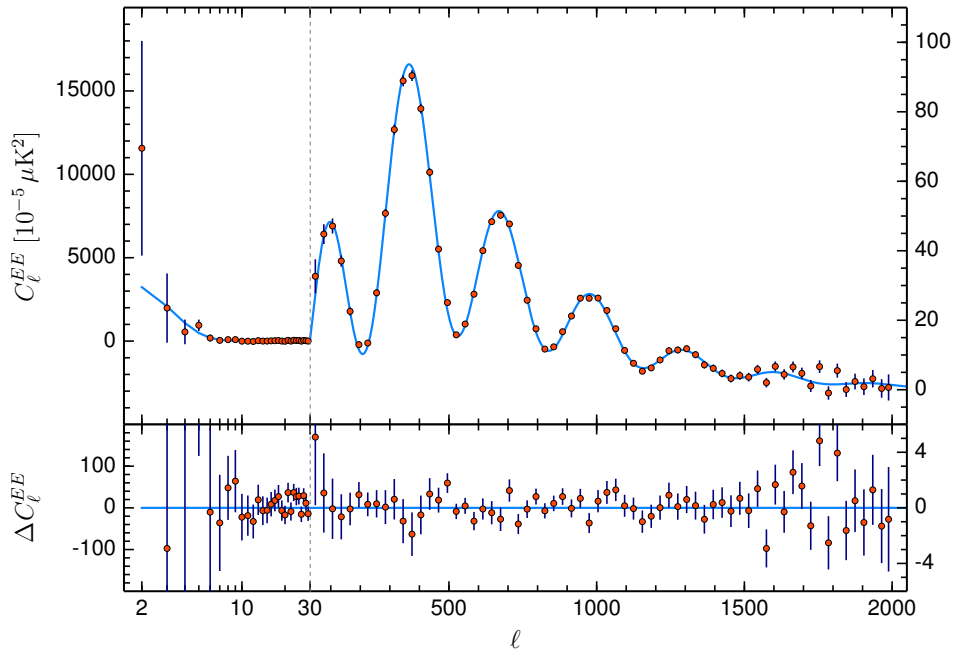

Figure 2.2: E-mode polarization power spectrum measured by Planck and best-fit. Figure taken from [3].

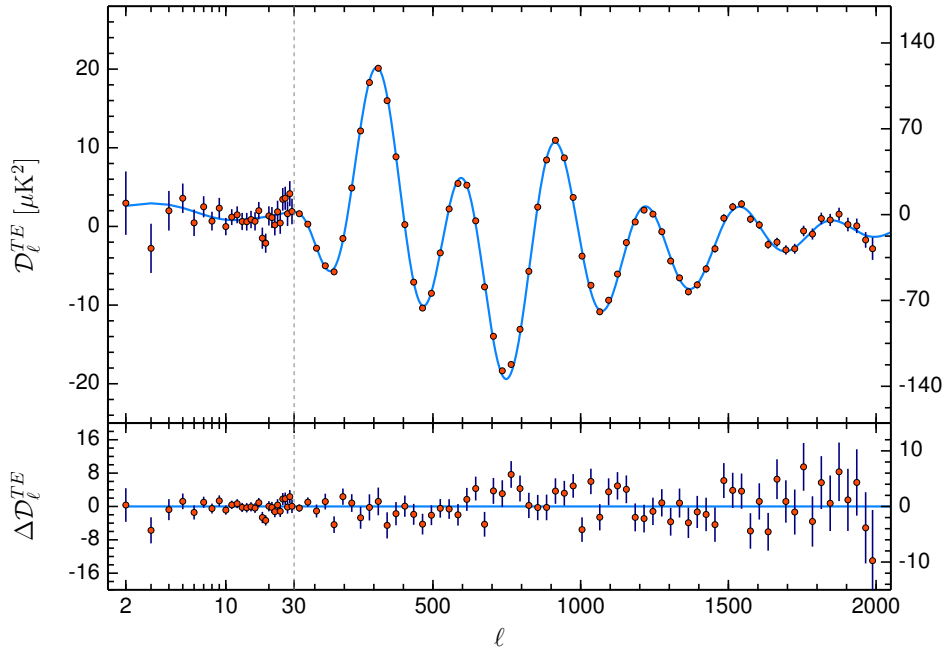

Figure 2.3: Temperature and E-mode polarization cross-correlation power spectrum measured by Planck and best-fit. Both figures taken from [3]

Chapter 3

Scalar tensor gravity: Horndeski theories

Einstein's theory of General Relativity is a geometrical theory of space-time, based on the equivalence principle and whose fundamental building block is the metric tensor. For this reason it can be called a "tensor" theory of gravity. Historically this theory was not the only attempt to generalize Newtonian gravity, in fact the most nautral path to do so was by building a so called "scalar theory": an example of such a theory is Nordstrom gravity [78] in which he promoted the Newtonian potential to be a Lorentz scalar. This theory though, could not predict the deflection of light caused by gravity and the prediction of Mercury's perihelion shift had the wrong sign with respect to observations. Therefore general relativity has since been accepted as the standard theory of gravitation. In spite of this fact many new proposal have advanced through the years, both for theoretical and experimental purposes and scalar tensor theories (STT) of gravity are one of these many proposals.

Even if they were first proposed in the 50s, scalar-tensor theories became more appealing, from the observational point of view, after the discovery of the accelerated expansion of the Universe, which posed an issue to the Standard Cosmological Model. In the framework of GR this has led to the introduction of an extra energy fluid: dark energy. This dark energy, as we've seen in Ch.1, might be described as a constant energy density (cosmological constant), or might be due to a varying component, such as a scalar field (quintessence). Scalar tensor theories, on the contrary, included automatically a candidate for dark energy, allowing for an alternative approach: instead of keeping general relativity and add new fluids to explain the observations, one can implement new theories of gravity that lead naturally to the observed acceleration and whose behaviour

is similar to that of GR on scales comparable to those of the solar system, while deviates from GR on large scales. So we briefly introduce scalar-tensor theories as an example of this alternative approach.

In scalar tensor models a scalar field is present and it is non minimally coupled to the Ricci scalar R, while it does not couple with matter at the lagrangian level. Consequently only the distribution of matter in the Universe determines the local value of the gravitational field. In this way scalar tensor theories naturally incorporate Mach's principle, which states that the global distribution of matter should determine local gravitation. This is a distinguishing feature of the theory: the cosmological distribution of matter affects local gravitational experiments and therefore the strong equivalence principle does not hold anymore [79]. The first scalar–tensor theory was originally conceived by Jordan [80] and later by Brans and Dicke [81], such theories incorporate the Dirac's argument that the gravitational constant should be time dependent [82]. This Jordan-Brans-Dicke model is the archetype of all the different scalar tensor theories developed in the later years. Today there is a plethora of scalar-tensor models, and within this framework there are Horndeski theories [83] which are the most general scalar-tensor theories with second-order equation of motion. In this thesis we will focus mainly on a particular subclass of Horndeski theories: the models that, consistently with observations [4], predict that gravitational waves travel at the speed of light.

In the present chapter we first present the entire Horndeski lagrangian and some of its special cases, with particular emphasis on the Jordan-Brans-Dicke theory and Induced gravity, which are the models that we are going to extend. Then we will briefly describe the conformal frame issue of Scalar-Tensor Theories and finally we will adrress the important topic of the recovery of general relativity at small scales, like the solar system. This is a necessary feature of a STT and one has to come up with some mechanisms that naturally do that, these mechanisms are called *screening mechanisms* and will deserve their own section.

3.1 Horndeski Action and its special cases

Theories containing a scalar field ϕ coupled to gravity are, in general, called scalar-tensor theories [79]. Horndeski theories [83] are the most general scalar-tensor theories with second-order equations of motion. This property implies the absence of the Ostrogradski instability [84] associated with an Hamiltonian unbounded from below. Horndeski theories are given by the action [85]

$$S_H = \int d^4x\sqrt{-g}\left(\mathcal{L}_H + \mathcal{L}_m\right), \tag{3.1}$$

where g is the determinant of the metric tensor and

$$\begin{aligned}\mathcal{L}_H =& G_2(\phi,X)+G_3(\phi,X)\Box\phi+G_4(\phi,X)R+G_{4,X}(\phi,X)\left[(\Box\phi)^2-(\nabla_\mu\nabla_\nu\phi)(\nabla^\mu\nabla^\nu\phi)\right]\\ &-\frac{1}{6}G_{5,X}(\phi,X)\left[(\Box\phi)^3-3(\Box\phi)\,(\nabla_\mu\nabla_\nu\phi)(\nabla^\mu\nabla^\nu\phi)+2(\nabla^\mu\nabla_\alpha\phi)(\nabla^\alpha\nabla_\beta\phi)(\nabla^\beta\nabla_\mu\phi)\right]\\ &+G_5(\phi,X)G_{\mu\nu}\nabla^\mu\nabla^\nu\phi\,.\end{aligned} \tag{3.2}$$

Here, $\Box\equiv\nabla^\mu\nabla_\mu$ is the covariant d'Alembert operator, R is the Ricci scalar, $G_{\mu\nu}$ is the Einstein tensor, and

$$X\equiv-\frac{1}{2}\nabla^\mu\phi\nabla_\mu\phi=-\frac{1}{2}\partial^\mu\phi\,\partial_\mu\phi=-\frac{1}{2}(\partial\phi)^2. \tag{3.3}$$

The functions $G_{2,3,4,5}$ depend on the field ϕ and on the kinetic term X, with $G_{i,\phi}\equiv\partial G_i/\partial\phi$ and $G_{i,X}\equiv\partial G_i/\partial X$. Originally, in Ref. [83], Horndeski presented the Lagrangian of scalar-tensor theories with second-order equations of motion in a form different from the one we presented in Eq. (3.2), but their equivalence was explicitly demonstrated in Ref. [85].

The action (3.1) encompasses many model, we list some of them below:

Quintessence and k-essence

K-essence [86–89] is characterized by the functions

$$G_2=G_2(\phi,X)\,,\qquad G_3=0\,,\qquad G_4=\frac{M_{\rm Pl}^2}{2}\,,\qquad G_5=0\,, \tag{3.4}$$

where $M_{Pl}=1/\sqrt{8\pi G}$ is the reduced Planck mass. Quintessence [65, 66] corresponds to the choice:

$$G_2=X-V(\phi)\,, \tag{3.5}$$

where $V(\phi)$ is the potential of ϕ.

Jordan-Brans-Dicke (JBD), Extended JBD (eJDB) theory and Induced Gravity

Jordan-Brans-Dicke theory [80, 81] is defined by

$$G_2=2\frac{\omega_{\rm BD}}{\phi}X\,,\qquad G_3=0\,,\qquad G_4=\phi\,,\qquad G_5=0\,, \tag{3.6}$$

or equivalently, by the following action:

$$S_{BD} = \int d^4x\sqrt{-g}\Big(\phi R - \frac{\omega_{\rm BD}}{\phi}(\partial\phi)^2 + \mathcal{L}_m\Big)\,. \tag{3.7}$$

General-Relativity is recovered in the limit $\omega_{\rm BD} \to \infty$ and the value of this parameter has been has been strongly constrained by the Cassini probe in 2003 to be $\omega_{\rm BD} > 40000$ [7]. Therefore Brans-Dicke theory with a free or light scalar field is viable in the limit of large ω_{bd}, but the large value required to satisfy the experimental bounds is fine-tuned and makes the model unappealing. However, this fine-tuning becomes unnecessary if the scalar has a sufficiently large mass and, therefore, a short range. This means that a self-interaction potential $V(\phi)$ has to be considered when discussing the possible value of $\omega_{\rm BD}$. The JBD theory with a potential is called extended Jordan-Brans-Dicke model (eJBD) and is given by the functions

$$G_2 = 2\frac{\omega_{\rm BD}}{\phi}X - V(\phi)\,, \qquad G_3 = 0\,, \qquad G_4 = \phi\,, \qquad G_5 = 0\,. \tag{3.8}$$

Thus, the action is

$$S_{BD} = \int d^4x\sqrt{-g}\Big(\phi R - \frac{\omega_{\rm BD}}{\phi}(\partial\phi)^2 - V(\phi) + \mathcal{L}_m\Big). \tag{3.9}$$

We note that there are also more general non-minimally coupled theories given by the couplings $G_2 = \omega(\phi)X - V(\phi)$, $G_3 = 0$, $G_4 = F(\phi)$, $G_5 = 0$, they've been studied for example in [90–96].

The extended Jordan-Brans-Dicke Theory is equivalent to Induced Gravity [97–99]: after a redefinition of the field $\phi = \gamma\sigma^2/2$, with $\gamma = (4\omega_{\rm BD})^{-1}$, we have that the action (3.9) becomes

$$S_{IG} = \int d^4x\sqrt{-g}\Big(\frac{1}{2}\gamma\sigma^2 R - \frac{1}{2}(\partial\sigma)^2 - V(\sigma) + \mathcal{L}_m\Big)\,. \tag{3.10}$$

In this model one recovers general relativity for $\gamma \to 0$ and the actual constraint on its value is $\gamma < 0.0017$ [100]. The cosmological implications of Induced gravity have been extensively studied in [14, 100–103].

Covariant Galileons gravity

In original Galileons [104], the field equations of motion are invariant under the shift $\partial_\mu\phi \to \partial_\mu\phi + b_\mu$ in Minkowski spacetime. In curved spacetime, the Lagrangian of covariant Galileons [105] keeps the equations of motion to second order by construction,

and the Galilean shift symmetry is recovered in the Minkowski limit. Covariant Galileons are given by the following G functions

$$G_2 = \beta_1 X - m^3\phi\,, \qquad G_3 = \beta_3 X\,, \qquad G_4 = \frac{M_{pl}^2}{2} + \beta_4 X^2\,, \qquad G_5 = \beta_5 X^2\,, \tag{3.11}$$

where $\beta_{1,3,4,5}$ and m are constants. In absence of the linear potential $V(\phi) = m^3\phi$, there exists a self-accelerating de Sitter solution satisfying $X = constant$ [106, 107].

Kinetic braidings and its extensions: BDG and IGG

We will see later that the theories given by the lagrangian

$$L = G_2(\phi, X) + G_3(\phi, X)\Box\phi + G_4(\phi)R\,, \tag{3.12}$$

are the most general Horndeski theories with the tensor propagation speed c_t equivalent to 1. The kinetic braiding scenario [108, 109] corresponds to the minimally coupled case, i.e., $G_4 = M_{pl}^2/2$. The cubic Galileon given by $\mathcal{L} = \beta_1 X - m^3\phi + \beta_3 X\Box\phi + (M_{pl}^2/2)R$ belongs to a subclass of kinetic braidings.

The Cubic Galileon model $\mathcal{L} = \beta_1 X - m^3\phi + \beta_3 X\Box\phi + (M_{pl}^2/2)R$ can be extended to a more general model of the form

$$G_2 = 2\frac{\omega_{BD}}{\phi}X + c\phi\,, \qquad G_3 = -2f(\phi)X = f(\phi)(\partial\sigma)^2\,, \qquad G_4 = \phi\,, \tag{3.13}$$

where a coupling of the field to the curvature R together with a function $f(\phi)$ modulating the intensity of cubic self-interaction $X\Box\phi$ have been added to the model. This theory and its cosmological effects has been first studied in [110] where it was shown that it admitted a self accelerating solution with $X =$ constant for $c = \rho = p = 0$.

This model can be further extended with the introduction of a generic potential $V(\sigma)$, and this extension, which, following [111], we call Brans-Dicke Galileon (BDG) will be one of the two models we will analyse in the thesis.

Another possibility is to also extend the Induced gravity model (3.10) with a cubic Galileon-like self interaction of the form $-2g(\sigma)\,\chi\Box\sigma$, where $\chi \equiv -(\partial\sigma)^2/2$. The extension of Induced gravity to Induced Gravity Galileon (IGG) is the main model we wish to study in the following chapters.

Horndeski theories contain many other models like $f(R)$ gravity, Gauss-Bonnet couplings, $f(\mathcal{G})$ gravity and others, for a complete review see [111] and [112].

3.2 Background Equations

Considering a flat FLRW spacetime:

$$ds^2 = -dt^2 + a^2(t)\delta_{ij}dx^i\,dx^j\,, \tag{3.14}$$

and matter described by a perfect fluid like in (1.48), from (3.1) and (3.2) the equations of motion are obtained using a variational principle [112]:

$$\begin{aligned}
&6G_4H^2 + G_2 - \dot\phi^2 G_{2,X} + \dot\phi^2\left(3H\dot\phi G_{3,X} - G_{3,\phi}\right) + 6H\dot\phi\left(G_{4,\phi} + \dot\phi^2 G_{4,X\phi} - 2H\dot\phi G_{4,X} - H\dot\phi^3 G_{4,XX}\right)\\
&+ H^2\dot\phi^2\left(9G_{5,\phi} + 3\dot\phi^2 G_{5,X\phi} - 5H\dot\phi G_{5,X} - H\dot\phi^3 G_{5,XX}\right) = \rho_m\,, \qquad (3.15)\\
&2q_t\dot H - D_6\ddot\phi + D_7\dot\phi = -\rho_m - P_m\,, \qquad (3.16)\\
&3D_6\dot H + 2D_1\ddot\phi + 3D_7H - D_5 = 0\,, \qquad (3.17)
\end{aligned}$$

where the quantity q_t is defined by

$$q_t = 2G_4 - 2\dot\phi^2 G_{4,X} + \dot\phi^2 G_{5,\phi} - H\dot\phi^3 G_{5,X}\,, \tag{3.18}$$

and the quantities $D_{1,5,6,7}$ are

$$\begin{aligned}
D_1 &= H^3\dot\phi\left(3G_{5,X} + \frac{7}{2}\dot\phi^2 G_{5,XX} + \frac{1}{2}\dot\phi^4 G_{5,XXX}\right) + 3H^2\left[G_{4,X} - G_{5,\phi} + \dot\phi^2\left(4G_{4,XX} - \frac{5}{2}G_{5,X\phi}\right)\right.\\
&\left.+\dot\phi^4\left(G_{4,XXX} - \frac{1}{2}G_{5,XX\phi}\right)\right] - 3H\dot\phi\left[G_{3,X} + 3G_{4,X\phi} + \dot\phi^2\left(\frac{1}{2}G_{3,XX} + G_{4,XX\phi}\right)\right]\\
&+ \frac{1}{2}\left[G_{2,X} + 2G_{3,\phi} + \dot\phi^2\left(G_{2,XX} + G_{3,X\phi}\right)\right]\,,
\end{aligned}$$

$$\begin{aligned}
D_5 &= -H^3\dot\phi^3(5G_{5,X\phi} + \dot\phi^2 G_{5,XX\phi}) + 3H^2\Big[2G_{4,\phi} - \dot\phi^2(4G_{4,X\phi} - 3G_{5,\phi\phi})\\
&- \dot\phi^4(2G_{4,XX\phi} - G_{5,X\phi\phi})\Big] + 3H\dot\phi\left[2G_{4,\phi\phi} + \dot\phi^2(G_{3,X\phi} + 2G_{4,X\phi\phi})\right] - \dot\phi^2(G_{2,X\phi} + G_{3,\phi\phi}) + G_{2,\phi}\,,
\end{aligned}$$

$$\begin{aligned}
D_6 &= H^2\dot\phi^2(3G_{5,X} + \dot\phi^2 G_{5,XX}) + 2H\dot\phi\left[2(G_{4,X} - G_{5,\phi}) + \dot\phi^2(2G_{4,XX} - G_{5,X\phi})\right]\\
&- \dot\phi^2(G_{3,X} + 2G_{4,X\phi}) - 2G_{4,\phi}\,,
\end{aligned}$$

$$D_7 = H^3\dot{\phi}^2(3G_{5,X} + \dot{\phi}^2 G_{5,XX}) + 2H^2\dot{\phi}\left[3(G_{4,X} - G_{5,\phi}) + \dot{\phi}^2(3G_{4,XX} - 2G_{5,X\phi})\right] - H\left[2G_{4,\phi} + \dot{\phi}^2(3G_{3,X} + 10G_{4,X\phi} - 2G_{5,\phi\phi})\right] + \dot{\phi}(G_{2,X} + 2G_{3,\phi} + 2G_{4,\phi\phi})\,.$$

The conservation of the energy momentum tensor still holds, and we have the continuity equation

$$\dot{\rho}_m + 3H\left(\rho_m + P_m\right) = 0\,. \tag{3.19}$$

We can express Eqs. (3.15) and (3.16) in the forms

$$3M_{\rm Pl}^2 H^2 = \rho_{\rm DE} + \rho_m\,, \tag{3.20}$$

$$2M_{\rm Pl}^2 \dot{H} = -\rho_{\rm DE} - P_{\rm DE} - \rho_m - P_m\,, \tag{3.21}$$

where the density $\rho_{\rm DE}$ and pressure $P_{\rm DE}$ of the "dark" component are

$$\rho_{\rm DE} = 3H^2\left(M_{Pl}^2 - 2G_4\right) - G_2 + \dot{\phi}^2 G_{2,X} - \dot{\phi}^2\left(3H\dot{\phi}G_{3,X} - G_{3,\phi}\right) - 6H\dot{\phi}\left(G_{4,\phi} + \dot{\phi}^2 G_{4,X\phi} - 2H\dot{\phi}G_{4,X} - H\dot{\phi}^3 G_{4,XX}\right) - H^2\dot{\phi}^2\left(9G_{5,\phi} + 3\dot{\phi}^2 G_{5,X\phi} - 5H\dot{\phi}G_{5,X} - H\dot{\phi}^3 G_{5,XX}\right)\,, \tag{3.22}$$

$$P_{\rm DE} = 2\left(q_t - M_{\rm Pl}^2\right)\dot{H} - D_6\ddot{\phi} + D_7\dot{\phi} - \rho_{\rm DE}\,. \tag{3.23}$$

We define the dark energy equation of state, as

$$w_{\rm DE} \equiv \frac{P_{\rm DE}}{\rho_{\rm DE}} = -1 + \frac{2(q_t - M_{pl}^2)\dot{H} - D_6\ddot{\phi} + D_7\dot{\phi}}{\rho_{\rm DE}}\,, \tag{3.24}$$

The necessary condition for the late time cosmic acceleration is $w_{\rm DE} < -1/3$. Observing equation (3.24) we see that even in models where we have $q_t = M_{Pl}^2$, like quintessence and k-essence, the time variation of ϕ leads to a deviation of $w_{\rm DE}$ from -1. In other theories presented in the previous section, the quantity q_t is, in general, different from M_{Pl}^2, so the term $2(q_t - M_{\rm Pl}^2)\dot{H}$ in (3.24) also contributes to the additional deviation of $w_{\rm DE}$ from -1. Therefore, the evolution of $w_{\rm DE}$ is different depending on dark energy models, and it is then possible to distinguish between them from the observations of SNIa, CMB, and BAO.

3.3 Speed of tensor perturbations in Horndeski theories

The detection of gravitational waves from the neutron star-neutron star merger GW170817 [4] and the simultaneous measurement of the gamma-ray burst GRB170817A

[113] has costrained the propagation speed of gravitational waves, c_t, to be [5]

$$-3\times10^{-15}\leq c_t-1\leq 7\times10^{-16}\,, \tag{3.25}$$

for redshifts $z<0.009$. Here we discuss the speed of propagation of tensor degrees of freedom in Horndeski theories. Following the approach of [114] it can be shown that such speed is given by [85, 111, 112]

$$c_t^2=\frac{1}{q_t}\left(2G_4-\dot\phi^2G_{5,\phi}-\dot\phi^2\ddot\phi G_{5,X}\right)=\frac{G_4-X\left(\ddot\phi G_{5,X}+G_{5,\phi}\right)}{G_4-2XG_{4,X}-X\left(H\dot\phi G_{5,X}-G_{5,\phi}\right)}\,, \tag{3.26}$$

if we now request that $c_t^2=1$ we arrive at the conditon

$$2G_{4,X}-2G_{5,\phi}+\left(H\dot\phi-\ddot\phi\right)G_{5,X}=0\,. \tag{3.27}$$

Then, unless we allow for some fine tuning of the functions, the dependence of G_4 on X is forbidden, as well as the dependence of G_5 on ϕ and X. Thus, as anticipated, the general Horndeski lagrangian (3.2) is constrained to be of the form (3.12):

$$L=G_2(\phi,X)+G_3(\phi,X)\Box\phi+G_4(\phi)R\,. \tag{3.28}$$

Therefore, models like the covariant Galileon can be discarded while the Galileon lagrangian up to the cubic interaction is allowed, as well as all the models that fall under the subclass of Extended Kinetic Braidings: notable examples of such models are the Jordan-Brans-Dicke (3.9) theory, the Brans-Dicke cubic Galileon and the Induced gravity theory with cubic interaction which are presented in the next chapter.

3.4 Conformal transformations

We shall now briefly describe one of the most longstanding issues in Scalar-Tensor theories: the conformal frame issue. A conformal transformation takes a metric $g_{\mu\nu}$ and transforms it into another metric $\tilde g_{\mu\nu}$ through:

$$\tilde g_{\mu\nu}=\Omega^2(x)g_{\mu\nu}\,, \tag{3.29}$$

where Ω is an arbitrary function of the coordinates. This transformation affects the quantities related to the metric in the following way [79]:

$$\begin{aligned} g^{\mu\nu} &= \Omega^2 \tilde{g}^{\mu\nu} \\ \sqrt{-g} &= \Omega^{-4}\sqrt{-\tilde{g}} \\ \Gamma^{\mu}_{\ \nu\rho} &= \tilde{\Gamma}^{\mu}_{\ \nu\rho} - (f_{,\nu}\delta^{\mu}_{\rho} - f_{,\rho}\delta^{\mu}_{\nu} - \tilde{g}^{\mu\lambda} f_{,\lambda}\tilde{g}_{\nu\rho}) \\ R &= \Omega^2(\tilde{R} - 6\tilde{\Box} f - 6\tilde{g}^{\mu\nu} f_{,\mu} f_{,\nu}) \,, \end{aligned} \tag{3.30}$$

where $f \equiv \ln\Omega$. The application of a conformal transformation is commonly referred to as moving from a conformal frame to another. Under such transformations of the metric a given Scalar-Tensor theory may be re-formulated in an infinite set of mathematically equivalent theories, each of them in a different conformal frame. The two most interesting ones are the Jordan and the Einstein frame. The former is the frame where the scalar field, while non-minimally coupled to gravity, is minimally coupled to matter at the lagrangian level; the latter is the frame where the theory has been recasted as an Einstein theory plus a scalar field non minimally coupled to the matter Lagrangian. We show how this works in one of the simplest of these theories: the Jordan-Brans-Dicke theory, whose action is given, in the Jordan frame, by (3.7)

$$S = \int d^4x\sqrt{-g}\Big(\phi R - \frac{\omega}{\phi}(\nabla\phi)^2 + \mathcal{L}_m\Big) \,. \tag{3.31}$$

This action can be recast, through a conformal transformation $g_{\mu\nu} \to \Omega^2 g_{\mu\nu}$, and with the choice $\phi = \Omega^2 = e^{-\alpha}$, into

$$S = \int \sqrt{-g}\left[R - \left(\omega + \frac{3}{2}\right)(\nabla\alpha)^2 + e^{-2\alpha}\mathcal{L}_{matter}\right] , \tag{3.32}$$

which is its Einstein frame form. This frame is very useful because the field equations have the the familiar form they have in General Relativity and thus one can obtain exact solutions of scalar tensor theories starting from the ones already known in GR. However, the issue of which of these two frames is the physical one and of the conditions under which they are physically equivalent is still open [115, 116]. We will consider the equations in the Jordan frame, because in this frame we can use the usual Boltzmann equations described in Sec. 2.3.

3.5 Screening mechanisms

A scalar-tensor theory as an alternative to GR is supposed to give rise to modification of gravity on cosmological scales, but the extra force mediated by the scalar degree of

freedom is strongly constrained on scales of the size of the Solar System where general relativity is very precisely tested. The two most popular screening mechanisms are the chameleon effect [117, 118] and the Vainshtein mechanism [9]. For this reason, in this section we will illustrate the basics of the Chameleon and the Vainshtein mechanism, the latter being relevant to Galileon theories and Galileon-like cubic interactions in general.

In the chameleon mechanism the scalar field is effectively massive in the vicinity of a source, the effective mass is so large that the contribution of the scalar field to gravity is short-ranged, leading to an effective screening within the Solar System.

The Vainshtein mechanism, instead, acts around local sources in the presence of non-linear scalar derivative interactions, these nonlinear interactions lead to the decoupling of the field from matter within a radius r_V commonly called the Vainshtein radius.

Other screening mechanisms worth mentioning, but are beyond the scopes of this thesis, are the symmetron [119, 120] and k-Mouflage models [121]; both effectively suppress the coupling to matter.

3.5.1 Chameleon mechanism

In the literature the *chameleon effect* is almost exclusively described in the Einstein frame [117, 118, 122], where the chameleon is minimally coupled to the Ricci curvature and non-minimally coupled to the matter sector. This means, as explained in the previous section, that, due to a fifth-force, particles paths deviate from the geodesics of the gravitational metric and the weak equivalence principle does not hold anymore. This leads to the non conservation of the matter energy-momentum tensor in this conformal frame. In the Jordan frame instead, matter interacts with the scalar field only gravitationally, this may lead to the idea that there is no need to look for a screening effect like the chameleon mechanism in this frame. This is not true, since the need to find a screening mechanism in this frame arises when trying to weaken the very stringent constraint on the free parameter of the JBD theory: The Cassini probe constrained the first post-Newtonian parameter $\gamma_{\rm ppn}$, related to $\omega_{\rm BD}$ by $\gamma_{\rm ppn} = (1+\omega_{\rm BD})/(2+\omega_{\rm BD})$, to be $\gamma_{\rm ppn} = 1 + (2.1 \pm 2.3) \times 10^{-5}$ [7]. This implies that the Brans-Dicke parameter has to be $\omega_{\rm BD} > 4 \times 10^4$, or, more relevant for this the thesis, the parameter γ in induced gravity (3.10) has to satisfy the costraint: $\gamma < 6.25 \times 10^{-6}$.

Here we will focus on the description of the chameleon effect in the Jordan frame of the Jordan-Brans-Dicke theory extended with a potential. Before working out the details, we describe the key concepts and the key features of how the mechanism works: considering for example the Brans-Dicke theory with a potential mentioned above, due to the chameleon effect, the effective mass of the scalar field m_ϕ, depends on the background

energy density of the environment: at large cosmological scales where the average energy density is approximately of the same order of the critical density $\rho_{crit} \sim 10^{-31}\,\mathrm{g\,cm^{-3}}$, the effective mass can then be very small, depending on the form of the potential it can even be of the order of $H_0 \sim 10^{-33}\,\mathrm{eV}$, in such a way that the scalar field affects the cosmological dynamics. However, at small scales like in the solar system, where the energy density of the environment is much larger than ρ_{crit}, the effective mass becomes large ($m_\phi^{\mathrm{eff}} > 10^{-3}\,\mathrm{eV}$), and in such a scenario the Yukawa–like contribution of the scalar field to gravity $\propto \exp(m_\phi r)/r$, is short-ranged, thus leading to an effective screening of the scalar field in the solar system.

We describe how this works using the paradigmatic example of the extended Jordan-Brans-Dicke theory: we consider therefore the following action

$$S_{BD} = \int d^4x\sqrt{-g}\Big(\phi R - \frac{\omega_{\mathrm{BD}}}{\phi}(\partial\phi)^2 - 2\,V(\phi) + 2\,\mathcal{L}_m\Big)\,, \tag{3.33}$$

the equations of motion are obtained from a variational principle: the variation of the action with respect to the metric and the scalar field yields, respectively

$$G_{\mu\nu} = \frac{1}{\phi}\,T^{(m)}_{\mu\nu} + \frac{\omega_{\mathrm{BD}}}{\phi^2}\left[\partial_\mu\phi\partial_\nu\phi - \frac{1}{2}g_{\mu\nu}\,(\partial\phi)^2\right] - g_{\mu\nu}\frac{V}{\phi} + \frac{1}{\phi}\left(\nabla_\mu\partial_\nu\phi - g_{\mu\nu}\Box\phi\right)\,, \tag{3.34}$$

$$\Box\phi = \frac{2}{3+2\omega_{\mathrm{BD}}}\left(\phi\partial_\phi V - 2V + \frac{1}{2}\,T^{(m)}\right)\,, \tag{3.35}$$

where

$$T^{(m)}_{\mu\nu} = -\frac{2}{\sqrt{-g}}\frac{\partial\left(\sqrt{-g}\,\mathcal{L}_m\right)}{\partial g^{\mu\nu}}, \tag{3.36}$$

is the conserved energy-momentum tensor of the matter, and $T^{(m)}$ is its trace.

Effective mass of the field

The key concept when discussing the chameleon effect is the mass of the field, and to give a proper, meaningful definition of this concept is not a trivial task, for a through analysis see [123]. We will follow that reference to define the mass here, highlighting the rationale behind the result without addressing all the subtleties presented there. First, we observe that the Klein-Gordon equation can be rewritten in the form

$$\Box\phi = \partial_\phi V_{\mathrm{eff}} + \frac{1}{3+2\omega_{\mathrm{BD}}}T^{(m)}\,, \tag{3.37}$$

with

$$\partial_\phi V_{\rm eff} = \frac{2}{3+2\omega_{\rm BD}}\left[\phi\,\partial_\phi V(\phi) - 2V(\phi)\right], \tag{3.38}$$

which, integrated, gives

$$V_{eff} = \frac{2}{3+2\omega_{\rm BD}}\left(\phi\,V(\phi) - 3\int d\phi\,V(\phi)\right). \tag{3.39}$$

Note that V and $V_{\rm eff}$ have different dimensions: while V has the dimensions of an energy density, $V_{\rm eff}$ has the dimensions of an energy density times a mass squared. Moreover, Eq. (3.39) shows that for a quadratic potential, which correspond to a quartic potential in the σ field in Induced Gravity, we have $V_{\rm eff} = 0$.

Now, with the example of the conventional Klein-Gordon equation in mind, it is natural to define the mass of the scalar field in the following way [123]:

$$m_\phi^2 \equiv \partial_\phi^2 V_{\rm eff} = \frac{2}{3+2\omega_{\rm BD}}\left[\phi\,\partial_\phi^2 V(\phi) - \partial_\phi V(\phi)\right]. \tag{3.40}$$

This mass is associated with a Yukawa-like term $\phi \sim \exp(-m_\phi r)/r$ in the weak field, slow-motion regime, under the assumption of spherical symmetry $\phi = \phi(r)$. We first show this in the vacuum $T_{\mu\nu} = 0$, for simplicity. Under all these assumptions the Klein-Gordon equation (3.35) becomes

$$\frac{1}{r^2}\frac{d}{dr}\left(r^2\frac{d\phi}{dr}\right) - \frac{dV_{eff}}{d\phi} = 0\,. \tag{3.41}$$

What is usually referred to as an effective mass, is a concept linked with the oscillations of the field around the minimum of the effective potential, which propagate in spacetime, assuming then that V_{eff} has a minimum at some ϕ_*, the effective mass is determined by expanding $\partial_\phi V_{eff}$ around the ϕ_*

$$\partial_\phi V_{eff}(\phi) \simeq \partial_\phi V_{eff}\Big|_{\phi_*} + \partial_\phi^2 V_{\rm eff}\Big|_{\phi_*}\delta\phi + ... = m_*^2\delta\phi\,, \tag{3.42}$$

where $m_*^2 \equiv \partial_\phi^2 V_{eff}\Big|_{\phi_*}$ is the effective mass of the scalar field perturbations. Then, equation (3.41) admits the usual Yukawa solution $\phi = \phi_* + \delta\phi \propto e^{-m_* r}/r$ with range m_* determined by the definition (3.40), and, since as we will show, the effective mass depends on the density, that is the parameter that decides the effective screening of the field, in different densities configurations

If the effective potential has no minimum, the meaning of effective mass is not clear:

the Yukawa-like solution, which is the manifestation of a massive propagator, might not arise. In this case the corresponding mass in Eq. (3.40) would just just be a useful field theoretical construction with the dimensions of mass. Nonetheless, following the most common point of view [111], here we will consider the parameter m_ϕ given by Eq. (3.40) to represent the mass of the field even away from the minimum of V_{eff}.

The presented argument was in the vacuum but in general the scalar field satisfies a Klein-Gordon equation with a source term S independent of ϕ:

$$\Box\phi = \partial_\phi V_{\rm eff} + S, \tag{3.43}$$

in such a scenario we define the chameleon potential as

$$V_{ch} = V_{eff} + \phi S\,, \tag{3.44}$$

which allows us to write the general coupled Klein-Gordon equation as

$$\Box\phi = \partial_\phi V_{ch}\,. \tag{3.45}$$

Now, focusing on Eq. (3.35) and using the definition (3.44) of the chameleon potential we have

$$V_{ch}(\phi) = V_{eff}(\phi) + \frac{T^{(m)}}{3+2\omega_{\rm BD}}\,\phi = \frac{2\,\phi\,V(\phi) - 6\int d\phi\,V(\phi) + \phi T^{(m)}}{3+2\omega_{\rm BD}}\,, \tag{3.46}$$

in such a way that

$$\Box\phi = \partial_\phi V_{ch} \;= \frac{2}{3+2\omega_{\rm BD}}\left(\,\phi\,\partial_\phi V \,-\, V + \frac{1}{2}T^{(m)}\right). \tag{3.47}$$

Now, following the procedure explained above we assume spherical symmetry and that the chameleon potential V_{ch} has a minimum at some ϕ_*, then in the weak-field and low-velocity limit we obtain

$$\frac{d^2\,\delta\phi}{dr^2} + \frac{2}{r}\frac{d\,\delta\phi}{dr} = m^2_{\phi_*}\,\delta\phi \tag{3.48}$$

where $m^2_{\phi_*} = \partial^2_\phi V_{ch}\Big|_{\phi_*}$ is the effective mass of the perturbations around the minimum of the chameleon potential V_{ch}.

Solving Eq. (3.48) we have for $\phi(r) = \phi_* + \delta\phi(r)$.

$$\phi(r) = \phi_* + C_1 \frac{e^{-m_{\phi_*} r}}{r} + C_2 \frac{e^{m_{\phi_*} r}}{r}, \tag{3.49}$$

in which C_1 and C_2 are integration constants to be determined using the boundary conditions. For example if we assume that $\phi(r) \xrightarrow[r\to\infty]{} \phi_\infty = constant$ then

$$\phi(r) = \phi_\infty + C_1 \frac{e^{-m\phi_* r}}{r}. \tag{3.50}$$

Once again, the effective mass m_{ϕ_*} determines the range of this Yukawa-like solution.

The most important thing here, which is the key fact of this section, is that the effective chameleon mass is a function of the surrounding density ρ, through the trace of the energy momentum tensor that enters the definition of the chameleon potential in Eq. (3.46). This property of the effective mass is what is called *the chameleon effect*.

Quartic potential example and estimates

Choosing a quartic potential $V(\phi) = \lambda\phi^4$ with $\lambda \geq 0$, we can see from Eq. (3.39) that $V_{eff} \propto \phi^5$ and therefore the effective potential does not admit a minimum. By contrast, assuming a pressureless dust background $T^{(m)} = -\rho$, the corresponding chameleon potential (3.46)

$$V_{ch}(\phi) = \frac{4}{3+2\omega_{\rm BD}} \left(\frac{\lambda}{5}\,\phi^5 + \frac{T^{(m)}}{4}\,\phi \right) = \frac{4}{3+2\omega_{\rm BD}} \left(\frac{\lambda}{5}\,\phi^5 + \frac{\rho}{4}\,\phi \right), \tag{3.51}$$

admits a minimum at $\phi_* = \left[\rho/(4\lambda)\right]^{1/4}$ if $\omega_{\rm BD} \geq -3/2$. We can then identify the effective mass of the field, as usual as, the second derivative of the chameleon potential:

$$m^2_{\phi_*} = \partial^2_\phi V_{ch}\Big|_{\phi_*} = \frac{16\lambda}{3+2\omega_{\rm BD}} \left(\frac{\rho}{4\,\lambda} \right)^{3/4}. \tag{3.52}$$

The density distribution ρ could be in principle arbitrarily complicated; let's choose, for simplicity, the following distribution: a spherical region of radius R, filled with a static fluid with isotropic and homogeneous density ρ_0 surrounded by a fluid with different homogeneous constant density ρ_∞:

$$\rho(r) = \begin{cases} \rho_0 & \text{for } r \leq R; \\ \rho_\infty & \text{for } r \gg R. \end{cases} \tag{3.53}$$

In this case the effective mass would have two values: one, $m_{\phi_0} = \sqrt{\partial^2_\phi V_{ch}\big|_{\phi_0}}$, for the modes propagating inside the spherical region, and another, $m_{\phi_\infty} = \sqrt{\partial^2_\phi V_{ch}\big|_{\phi_\infty}}$, for the ones that propagate far from it. For the quartic potential, they are,

$$m_{\phi_0} = \frac{2(4\lambda)^{1/8}\rho_0^{3/8}}{\sqrt{3+2\omega_{\rm BD}}}\,, \tag{3.54}$$

$$m_{\phi_\infty} = \frac{2(4\lambda)^{1/8}\rho_\infty^{3/8}}{\sqrt{3+2\omega_{\rm BD}}}\,. \tag{3.55}$$

Therefore, the mass the determines the range of the Yukawa-like correction depends on the density as $m_{\phi_*} \propto \rho^{3/8}$. Now, in order to make some estimates, following [124], we can rewrite the effective mass in units particularly useful to this scope [125][1]:

$$m_{\phi_*}[mm^{-1}] \simeq \frac{10^{-3}\lambda^{1/8}}{\sqrt{3+2\omega_{\rm BD}}}\Big(\rho[{\rm g/cm^3}]\Big)^{3/8}\,. \tag{3.56}$$

To plug in some numbers, we consider the scalar field immersed in the earth's atmosphere, which has an average density $\rho^{\rm atm} \simeq 10^{-3}\,{\rm g/cm^3}$; then, if we assume a millimiter range screening [124], $m_\phi{}^{\rm atm} \sim mm^{-1}$, and $\lambda \sim \mathcal{O}(1)$ it follows that $\omega_{\rm BD} \sim -3/2$, i.e., very close to the singular value of the Brans-Dicke coupling parameter. This entails that the JBD theory may describe the gravitational phenomena with a small, even negative coupling constant of order unity and, the chameleon potential (3.46) could screen the field from experiments that look for violation of the Newton's law, for distances above the millimeter. In the Solar System where the relevant matter background is the nearly homogeneous baryonic gas and dark matter, with density $\rho_{SS} \sim 10^{-24}\,{\rm g\,cm^{-3}}$ the interaction range is of the order of $m^{-1}_{\phi_*,\,\rm SS} \sim 100\,{\rm km}$.

In the literature, the discussion of the screening usually stops here, once has been proven that such an effect arises naturally and it is effective. But the next step, often overlooked, is as important as the previous one and it has the aim of answering the following question: can the above model be a good candidate for cosmology as well? To answer this let us compute the ratio of the mass of the field measured at large cosmological scales, to the one estimated in earth's atmosphere:

$$\frac{m^{\rm cosm}_{\phi_*}}{m^{\rm atm}_{\phi_*}} = \left(\frac{\rho^{\rm crit}}{\rho^{\rm atm}}\right)^{3/8} \approx 3\times 10^{-11}, \tag{3.57}$$

[1]The corresponding formula in [125] contains a typo, which we corrected here. Kindly confirmed by I. Quiros, author of Ref. [125], private communication.

where we have used the critical energy density of the Universe $\rho^{\rm crit} \simeq 10^{-31}\,{\rm g\,cm^{-3}}$. If we take as given the millimeter-range screening described above, $(m_{\phi_*}^{\rm atm})^{-1} \simeq 1\,{\rm mm}$, equivalent to $m_{\phi_*}^{\rm atm} \simeq 10^{-4}$ eV, then the estimated mass of the cosmological BD scalar field is

$$m_{\phi_*}^{\rm cosm} \simeq 3\times 10^{-11}\, m_{\phi_*}^{\rm atm} \simeq 3\times 10^{-15}\ {\rm eV}, \tag{3.58}$$

which is 18 orders of magnitude larger than the expected value $m_\phi^{\rm cosm} \sim H_0 \sim 10^{-33}\,{\rm eV}$. Hence, if assuming that the JBD field with a quartic potential is effectively screened from solar system experiments, the field would not have cosmological effects.

To reconcile cosmological and terrestrial constraints all at once, one needs power-law potentials which lead to a chameleon mass, $m_{\phi_*} \propto (\rho)^{k/2}$, with $k \approx 29/14 \simeq 2.071$, or higher [125]. Clearly, the reconciliation would be more natural if, for example, $m_{\phi_*} \propto \exp(\rho)$.

As a final note we want to point out that for some kind of potentials, like $V(\phi) \propto \phi^2$ there is no chameleon screening at all.

3.5.2 Vainshtein mechanism

We start highlighting the need for a screening mechanism in a simple model without cubic interaction, and then introduce the Vainshtein mechanism adding the cubic interaction to the simple model.

Consider a theory of the form

$$S = \int d^4x\sqrt{-g}\big[f(\phi)R + X\big] + S_m, \tag{3.59}$$

We examine perturbations around a Minkowski background with a constant scalar field ϕ,

$$g_{\mu\nu} = \eta_{\mu\nu} + M_{\rm Pl}^{-1}h_{\mu\nu}(t,\vec{x}), \quad \phi = \phi_0 + \varphi(t,\vec{x}), \tag{3.60}$$

caused by the energy-momentum tensor of matter $T_{\mu\nu}$ (the theory admits the background solution $g_{\mu\nu} = \eta_{\mu\nu}$ and $\phi = \phi_0 = {\rm const}$). We have defined the metric perturbations in such a way that $h_{\mu\nu}$ has the dimension of mass. We also take $f(\phi_0) = M_{pl}^2/2$. In order to obtain the effective Lagrangian for the description of weak gravitational fields we Expand (3.59) to second order in perturbations, this yields

$$\mathcal{L}_{eff} = -\frac{1}{4}h^{\mu\nu}\hat{\mathcal{E}}^{\alpha\beta}_{\mu\nu}h_{\alpha\beta} - \frac{1}{2}\partial_\mu\varphi\partial^\mu\varphi - \xi h^{\mu\nu}X^{(1)}_{\mu\nu} + \frac{1}{2M_{\rm Pl}}h^{\mu\nu}T_{\mu\nu}, \tag{3.61}$$

where $\xi := M_{\rm Pl}^{-1} df/d\phi|_{\phi=\phi_0}$,

$$X^{(1)}_{\mu\nu} \equiv \eta_{\mu\nu}\Box\varphi - \varphi_{\mu\nu}\,; \qquad \varphi_{\mu\nu} \equiv \nabla_\mu\nabla_\nu\varphi \tag{3.62}$$

and

$$\hat{\mathcal{E}}^{\alpha\beta}_{\mu\nu} h_{\alpha\beta} := -\frac{1}{2}\Box h_{\mu\nu} + \partial^\lambda\partial_{(\mu}h_{\nu)\lambda} + \frac{1}{2}\eta_{\mu\nu}\Box h - \frac{1}{2}\eta_{\mu\nu}\partial_\lambda\partial_\rho h^{\lambda\rho} - \frac{1}{2}\partial_\mu\partial_\nu h \tag{3.63}$$

is the linearized Einstein tensor divided by $M_{\rm Pl}$. Indices are raised and lowered making use of the Minkowski metric $\eta_{\mu\nu}$.

The third term in (3.61) reveals the mixing of the scalar degree of freedom with the metric perturbations. It can be disentangled thanks the following field redefinition

$$h_{\mu\nu} = \tilde{h}_{\mu\nu} - 2\xi\varphi\eta_{\mu\nu}, \tag{3.64}$$

which gives us

$$\mathcal{L}_{eff} = -\frac{1}{4}\tilde{h}^{\mu\nu}\hat{\mathcal{E}}^{\alpha\beta}_{\mu\nu}\tilde{h}_{\alpha\beta} - \frac{1+6\xi^2}{2}\partial_\mu\varphi\partial^\mu\varphi + \frac{1}{2M_{\rm Pl}}\tilde{h}^{\mu\nu}T_{\mu\nu} - \frac{\xi}{M_{\rm Pl}}\varphi T\,. \tag{3.65}$$

The transformation (3.64) is equivalent to the linear part of the conformal transformation to the Einstein frame, $\tilde{g}_{\mu\nu} = C(\phi)g_{\mu\nu}$ with $C = f(\phi)/f(\phi_0)$. In this new frame we a nonminimal coupling of the field with matter of the form φT, where T is the trace of the energy momentum tensor. The equations of motion in this frame are:

$$\hat{\mathcal{E}}^{\alpha\beta}_{\mu\nu}\tilde{h}_{\alpha\beta} = M_{\rm Pl}^{-1}T_{\mu\nu}, \tag{3.66}$$

$$(1+6\xi^2)\Box\varphi = M_{\rm Pl}^{-1}\xi T\,. \tag{3.67}$$

Thus, if the parameter ξ is of the order of unity, we expect a modification of gravity of the same order.

Considering now a spherical distribution of nonrelativistic matter, $T_{\mu\nu} = \rho(r)\delta^0_\mu\delta^0_\nu$, with $\tilde{h}_{00} = -2\tilde{\Phi}(r)$ and $\tilde{h}_{ij} = -2\tilde{\Psi}(r)\delta_{ij}$, the equations of motion become

$$\frac{1}{r^2}\partial_r\left(r^2\partial_r\tilde{\Psi}\right) = \frac{\rho}{2M_{\rm Pl}}, \tag{3.68}$$

$$\tilde{\Psi} - \tilde{\Phi} = 0, \tag{3.69}$$

$$\frac{1}{r^2}\partial_r\left(r^2\partial_r\varphi\right) = -\frac{\xi}{1+6\xi^2}\frac{\rho}{M_{\rm Pl}}\,. \tag{3.70}$$

Integrating these equations we obtain

$$\frac{1}{M_{\rm Pl}}\partial_r\tilde{\Phi} = M_{\rm Pl}^{-1}\tilde{\partial}_r\Psi = \frac{1}{8\pi M_{Pl}^2}\frac{\mathcal{M}(r)}{r^2}\,; \quad \frac{1}{M_{\rm Pl}}\partial_r\varphi = -\frac{2\xi}{1+6\xi^2}\cdot\frac{1}{8\pi M_{Pl}^2}\frac{\mathcal{M}(r)}{r^2}, \tag{3.71}$$

where $\mathcal{M}(r)$ is the mass enclosed up to a radius r: $\mathcal{M}(r) := 4\pi\int^r \rho(s)s^2ds$. From Eq. (3.64) it follows that metric perturbations in the original frame are $\Phi = \tilde{\Phi} - \xi\varphi$ and $\Psi = \tilde{\Psi} + \xi\varphi$. Then, outside the matter distribution, the metric potentials are

$$\Phi = -\frac{G_N\mathcal{M}}{r}, \quad \Psi = \gamma\Phi, \tag{3.72}$$

with

$$8\pi G_N := \frac{1+8\xi^2}{1+6\xi^2}\frac{1}{M_{\rm Pl}^2}, \quad \gamma - 1 = -\frac{4\xi^2}{1+8\xi^2}. \tag{3.73}$$

For ξ of the order of unity we have that $\gamma - 1 = \mathcal{O}(1)$, which contradicts solar-system constraints [8].

Now, adding a Galileon-like cubic interaction to (3.65) we have

$$\mathcal{L}_{eff} = -\frac{1}{4}\tilde{h}^{\mu\nu}\hat{\mathcal{E}}^{\alpha\beta}_{\mu\nu}\tilde{h}_{\alpha\beta} - \frac{1+6\xi^2}{2}(\partial\varphi)^2 - \frac{1}{2\Pi^3}(\partial\varphi)^2\Box\varphi + \frac{1}{2M_{\rm Pl}}\tilde{h}^{\mu\nu}T_{\mu\nu} - \frac{\xi}{M_{\rm Pl}}\varphi T. \tag{3.74}$$

In this case, the scalar-field equation of motion is given by

$$(1+6\xi^2)\Box\varphi + \frac{1}{\Pi^3}\left[(\Box\varphi)^2 - \varphi_{\mu\nu}\varphi^{\mu\nu}\right] = \frac{\xi}{M_{\rm Pl}}T, \tag{3.75}$$

which, for a spherical matter distribution, yields

$$(1+6\xi^2)r^2\partial_r\varphi + \frac{2}{\Pi^3}r(\partial_r\varphi)^2 = -\frac{\xi\mathcal{M}(r)}{4\pi M_{\rm Pl}}\,, \tag{3.76}$$

whose algebraic solution is

$$\partial_r\varphi = c\Pi^3 r\left[-1 + \sqrt{1 - \frac{\xi}{c^2}\left(\frac{r_V}{r}\right)^3}\right], \tag{3.77}$$

where $c := (1+6\xi^2)/4$ is an constant of the order of unity and we defined the so called *Vainshtein radius* as

$$r_V := \left(\frac{\mathcal{M}}{8\pi M_{\rm Pl}\Pi^3}\right)^{1/3}. \tag{3.78}$$

We also considered the exterior of the source, such that $\mathcal{M}$, now a constant is the mass of the star.

For $r \ll r_V$, we have

$$\partial_r \varphi \simeq (-\xi)^{1/2} \left(\frac{r}{r_V}\right)^{3/2} \partial_r \tilde{\Phi} \ll \partial_r \tilde{\Phi}\,, \tag{3.79}$$

which leads to

$$\frac{\Phi}{M_{\rm Pl}} \simeq \frac{\Psi}{M_{\rm Pl}} \simeq -\frac{G_N \mathcal{M}}{r}\,, \tag{3.80}$$

with $8\pi G_N \equiv \frac{1}{M_{\rm Pl}^2}$. Therefore the nonlinear interaction introduced in (3.74) helps to naturally recover standard gravity. The solar-system constraints can then be evaded if the Vainshtein raidus r_V, the radius within which general relativity is recovered, is large enough.

If the scalar degree of freedom is responsible for the present acceleration in the expansion of the Universe, Π is expected to be of the order [126]

$$\Pi \sim (M_{\rm Pl} H_0^2)^{1/3},\,. \tag{3.81}$$

If we consider a celestial body of a solar mass, $M \sim M_\odot$, from Eq. (3.78) with (3.81) we get

$$r_V \sim 100\,{\rm pc}, \tag{3.82}$$

which is much larger than the size of the solar system.

While this was a simple example to show how the Vainshtein mechanism works, one can apply the same philosophy to the entire Horndeski action and obtain a similar result [127–129]. If we consider the lagrangian (3.28), which is the most general scalar-tensor theory with a propagation speed of gravitational waves equal to 1, we obtain that for a celestial body of mass $\mathcal{M}$, an estimate for the Vainsthein radius in a cosmological background is [129]

$$r_V = \left(\frac{\mathcal{B}\mathcal{C}\mu}{H^2}\right)^{1/3}, \tag{3.83}$$

where the mass $\mathcal{M}$ enters (3.83) through $\mu = \mathcal{M}/(16\pi G_4)$ and $\mathcal{B}$ and $\mathcal{C}$ are complicated functions of the G_i's. Their complete expression can be found in [129]. If the product $\mathcal{B}\mathcal{C}$ if of the order of unity, the estimate for the Vainsthein radius according to Ref. [129],

using $G_4 = 1/(8\pi G_N)$, gives

$$r_V \simeq \left(\frac{\mu}{H^2}\right)^{1/3} \simeq 120\left(\frac{H_0}{H}\right)^{2/3}\left(\frac{\mathcal{M}}{M_\odot}\right)^{1/3}\mathrm{pc}\,, \tag{3.84}$$

if $H_0 = 70\mathrm{kms}^{-1}\mathrm{Mpc}^{-1}$. Thus for a star of the mass of the sun we have a $r_V \sim 120\,\mathrm{pc}$, while for a cluster of, say, $10^{15}M_\odot$ the estimate of the Vainsthein radius is 12 Mpc, large enough to encompass a cluster of said mass. Therefore the screening is effective when $\mathcal{BC} = \mathcal{O}(1)$.

Chapter 4

Induced Gravity Galileon and Brans-Dicke Galileon

As discussed in previous chapters, the most general Horndeski theories with the tensor propagation speed c_t equivalent to 1 are given by the action [112]

$$S = \int d^4x\sqrt{-g}\left[G_4(\phi,X)R + G_2(\phi,X) + G_3(\phi,X)\Box\phi + \mathcal{L}_{matter}\right]. \tag{4.1}$$

Since the term $G_3\Box\phi$ is in general not invariant under field redefinition we restrict ourselves to two relevant cases that fall among the class of theories (4.1). The first one, following the nomenclature of [111], is the Brans-Dicke Galileon (BDG), described by:

$$S^{(\phi)}_{BDG} = \int d^4x\sqrt{-g}\left[\phi R + \frac{\omega_{\text{BD}}}{\phi}X - V(\phi) + f(\phi)\,(g^{\mu\nu}\partial_\mu\phi\,\partial_\nu\phi)\Box\phi + \mathcal{L}_{matter}\right], \tag{4.2}$$

this lagrangian, after the field redefinition $\phi = \gamma\sigma^2/2$ with $\gamma = (4\,\omega_{\text{BD}})^{-1}$, becomes

$$S^{(\sigma)}_{BDG} = \int d^4x\sqrt{-g}\left[\frac{1}{2}\gamma\sigma^2 R - \frac{1}{2}(\partial\sigma)^2 - V(\sigma) + \zeta(\sigma)\,(\partial\sigma)^4 + g(\sigma)\,(\partial\sigma)^2\,\Box\sigma + \mathcal{L}_{matter}\right], \tag{4.3}$$

with $\zeta = \zeta(\sigma) = \sigma^2\gamma^3 f(\sigma)$ and $g = g(\sigma) = \sigma^3\gamma^3 f(\sigma)$.

The other theory we consider is what we call Induced Gravity Galileon (IGG), whose action is formally equivalent to (4.3) with $\zeta = 0$:

$$S^{(\sigma)}_{IGG} = \int d^4x\sqrt{-g}\left[\frac{1}{2}\gamma\sigma^2 R - \frac{1}{2}(\partial\sigma)^2 - V(\sigma) + g(\sigma)\,(\partial\sigma)^2\,\Box\sigma + \mathcal{L}_{matter}\right]. \tag{4.4}$$

It can be rewritten, using the Brans-Dicke field ϕ and the relation between $f(\sigma)$ and

$g(\sigma)$ given above, in the following way

$$S^{(\phi)}_{IGG} = \int d^4x\sqrt{-g}\left[\phi R - \frac{\omega_{\rm BD}}{\phi}(\partial\phi)^2 - V(\phi) + f(\phi)\,(\partial\phi)^2\Box\phi - \frac{1}{2\phi}f(\phi)\,(\partial\phi)^4 + \mathcal{L}_{matter}\right]. \tag{4.5}$$

In the next sections we will study the equations of motion of these theories and some special solutions of cosmological relevance. We will also present the results of numerical study of the background cosmology in these models.

4.1 Background equations

We start from an Action of the form

$$S = \int d^4x\sqrt{-g}\left[\frac{1}{2}F(\sigma)R - \frac{1}{2}(\partial\sigma)^2 - V(\sigma) + \zeta(\sigma)\,(\partial\sigma)^4 + g(\sigma)\,(\partial\sigma)^2\,\Box\sigma + \mathcal{L}_{matter}\right], \tag{4.6}$$

where, even though for most of the thesis we will stick to a coupling of the form $F(\sigma) = \gamma\sigma^2$, for more generality we keep an arbitrary non-minimal coupling term $F(\sigma)$, in such a way that any different choice of this term can be easily implemented directly in the equations of motion derived below. Moreover it's useful to keep this form to check that the equations derived here, reduce to the ones in [11], in the limit of $f(\sigma) = 0$

The action (4.6) encapsulates both the Jordan-Brans-Dicke and the Induced-Gravity Galileon. In fact for $F(\sigma) = \gamma\sigma^2$ it reduces to the model (4.3), while it reduces to (4.4) for $F(\sigma) = \gamma\sigma^2$ and $\zeta = 0$. To not give the wrong idea that the IGG model is just a special case of the BDG model when $\zeta = 0$, we stress their non equivalence: as described above, in the BDG model the functions ζ and g are not independent, therefore setting $\zeta = 0$ would mean setting $g = 0$ as well. Thus, the IGG theory should not be considered as a particular case of the BDG one but rather as a different, unequivalent model, whose equation can be formally obtained from the BDG ones by setting only $\zeta = 0$.

Below, the equations of motion for the general lagrangian (4.6) are derived and one can specialize them to a specific model using the choices just described.

Einstein's Equations

Variation of (4.6) with respect to the metric yields the Einstein equations:

$$G_{\mu\nu} = \frac{1}{F(\sigma)}\left[T^{(m)}_{\mu\nu} + T^{(g)}_{\mu\nu} + \partial_\mu\sigma\partial_\nu\sigma - \frac{1}{2}g_{\mu\nu}\partial^\rho\sigma\partial_\rho\sigma \quad - g_{\mu\nu}V(\sigma) + (\nabla_\mu\nabla_\nu - g_{\mu\nu}\Box)F(\sigma)\right], \tag{4.7}$$

where

$$T^{(g)}_{\mu\nu} = -2\Big\{ g(\sigma)\,\nabla_\mu\sigma\nabla_\nu\sigma\,\Box\sigma - \nabla_{(\mu}\,\sigma\,\nabla_{\nu)}\big[\,g(\sigma)(\partial\sigma)^2\,\big] + \frac{1}{2}g_{\mu\nu}\nabla_\alpha\,\sigma\nabla^\alpha\big[\,g(\sigma)(\partial\sigma)^2\,\big] - \frac{\zeta}{2}g_{\mu\nu}(\partial\sigma)^4 + 2\zeta\nabla_\mu\sigma\nabla_\nu\sigma\;(\partial\sigma)^2\,\Big\}; \tag{4.8}$$

with $\nabla_{(\mu}\,\sigma\,\nabla_{\nu)} = \frac{1}{2}\big(\nabla_\mu\,\sigma\,\nabla_\nu + \nabla_\nu\,\sigma\,\nabla_\mu\big)$. The explicit form of $T^{(g)}_{\mu\nu}$, using $f(\sigma)$ defined in the previous section is

$$T^{(g)}_{\mu\nu} = -2\Big\{ \gamma^3\sigma^3 f(\sigma)\,\nabla_\mu\sigma\nabla_\nu\sigma\,\Box\sigma - \gamma^3\sigma\nabla_{(\mu}\,\sigma\,\nabla_{\nu)}\big[\,\sigma^2 f(\sigma)(\partial\sigma)^2\,\big] + \frac{1}{2}g_{\mu\nu}\,\gamma^3\sigma\nabla_\alpha\sigma\nabla^\alpha\big[\,\sigma^2 f(\sigma)(\partial\sigma)^2\,\big] + \gamma^3\sigma^2 f(\sigma)\nabla_\mu\sigma\nabla_\nu\sigma\;(\partial\sigma)^2\,\Big\}, \tag{4.9}$$

from which we can see that Eq. (4.7) reduces to equation (3) of [11] for $f(\sigma) = 0$, as expected. For later convenience it's useful to write down the trace of the Einstein equation (4.7), which is

$$R = \frac{1}{F}\Big[\,-T^{(m)} - T^{(g)} + (\partial\sigma)^2 + 4V + 3\Box F(\sigma)\Big]; \tag{4.10}$$

with $T^{(g)}$ being the trace of the term coming from the cubic interaction:

$$T^{(g)} = -2\Big\{ g(\sigma)\,(\partial\sigma)^2\Box\sigma + \nabla_\mu\sigma\nabla^\mu\big[g(\sigma)\,(\partial\sigma)^2\big]\Big\}. \tag{4.11}$$

Note that the trace of this "Galileon Energy momentum tensor" does not contains $\zeta(\sigma)$. Like before, for $f(\sigma) = 0$, equation (4.10) reduces to equation (4) of [11].

Klein-Gordon Equation

The variation of (4.6) with respect to the Galileon field σ yields the Klein-Gordon equation:

$$\Box\sigma\Big[1 - 4\zeta\,(\partial\sigma)^2\Big] - 2g\Big\{(\Box\sigma)^2 - \nabla^\mu\nabla^\nu\sigma\nabla_\mu\nabla_\nu\sigma - \nabla^\mu\sigma\nabla^\nu\sigma\Big[R_{\mu\nu} + 2\frac{g_{,\sigma}}{g}\nabla_\mu\nabla_\nu\sigma\Big]\Big\} + \frac{1}{2}F_{,\sigma}R + g_{,\sigma,\sigma}(\partial\sigma)^4 - 3\zeta_{,\sigma}(\partial\sigma)^4 - 4\zeta(\sigma)\nabla_\mu\big[(\partial\sigma)^2\big]\nabla^\mu\sigma - V_{,\sigma} = 0. \tag{4.12}$$

As a sanity check one can obtain (4.7) and (4.12) varying directly the action in the form (4.2) (coupling a general $F(\phi)$ instead of ϕ to the Ricci scalar), and then applying the field redefinition at the very end. The variations of an action identical to (4.2) are

carried out almost step by step in the very pedagogical article [130] and the equations derived here are consistent with it.

4.1.1 Friedmann and Klein-Gordon equations in a flat FLRW Universe

We consider now a flat FLRW metric in cosmic time

$$ds^2 = -dt^2 + a(t)^2 dx_i\, dx^i\,, \tag{4.13}$$

using this metric the Friedmann equations are

$$3H^2F = \rho + \frac{\dot\sigma^2}{2} + V(\sigma) - 3H\dot F + \dot\sigma^2\left[(6\,g\,H - \dot g)\,\dot\sigma + 3\zeta\,\dot\sigma^2\right], \tag{4.14}$$

$$-2\dot H F = \rho + p + \dot\sigma^2 + \ddot F - H\dot F + \dot\sigma^2\left[2(3\,g\,H - \dot g)\,\dot\sigma + 4\,\zeta\,\dot\sigma^2 - 2\,g\,\ddot\sigma\right]. \tag{4.15}$$

They reduce to the equations (8) and (9) of [11] when $f(\sigma) = 0$, as expected.

Alternatively, we can express the Friedmann equations using the conformal time τ, as a function of which, the spacetime metric is $ds^2 = a^2(\tau)(-d\tau^2 + dx_i dx^i)$. As usual the prime will stand for derivative with respect to conformal time and $\mathcal{H} = a'/a$. We then have

$$3\mathcal{H}^2F = a^2(\rho + V) + \frac{1}{2}\sigma'^2 - 3\mathcal{H}F' + \frac{\sigma'^2}{a^2}\left[\big(6g\,\mathcal{H} - g'\big)\sigma' + 3\zeta\sigma'^2\right], \tag{4.16}$$

$$-2\mathcal{H}'F + 2\mathcal{H}^2F = a^2(p+\rho) + \sigma'^2 + F'' - 2\mathcal{H}F' + \frac{\sigma'^2}{a^2}\left[2\big(4g\,\mathcal{H} - g'\big)\sigma' + 4\zeta\sigma'^2 - 2g\,\sigma''\right]. \tag{4.17}$$

Using (4.16) we can rewrite (4.17) in the following form

$$-2\mathcal{H}'F = a^2\Big(\frac{1}{3}\rho + p - \frac{2}{3}V\Big) + \frac{2\sigma'^2}{3} + F'' + \frac{\sigma'^2}{a^2}\left[4\Big(g\mathcal{H} - \frac{1}{3}\,g'\Big)\sigma' + 2\zeta\,\sigma'^2 - 2g\,\sigma''\right]. \tag{4.18}$$

Using cosmic time, the Klein Gordon equation is:

$$\begin{aligned}\ddot{\sigma}\big(1+12\zeta\dot{\sigma}^2+12g\,H\dot{\sigma}-4g_{,\sigma}\dot{\sigma}^2\big)+3H\dot{\sigma}+\dot{\sigma}^2\Big(18g\,H^2+6g\,\dot{H}\Big)\\ +12H\zeta\dot{\sigma}^3+\dot{\sigma}^4(3\zeta_{,\sigma}-g_{,\sigma,\sigma})-\frac{1}{2}F_{,\sigma}R+V_{,\sigma}=0;\end{aligned} \tag{4.19}$$

which, expressed in conformal time takes the form

$$\begin{aligned}\frac{\sigma''}{a^2}\left(1+\frac{12\zeta}{a^2}\sigma'^2+\frac{12g\,\mathcal{H}}{a^2}\sigma'-\frac{4g_{,\sigma}}{a^2}\sigma'^2\right)+\frac{2\mathcal{H}}{a^2}\sigma'+\frac{6g\,\mathcal{H}'}{a^4}\sigma'^2+\frac{4g_{,\sigma}\mathcal{H}}{a^4}\sigma'^3\\ +\frac{1}{a^4}(3\zeta_{,\sigma}-g_{,\sigma,\sigma})\sigma'^4-\frac{1}{2}F_{,\sigma}R+V_{,\sigma}=0\,.\end{aligned} \tag{4.20}$$

The explicit form of the Ricci scalar which enters the Klein-Gordon equation is obtained from the Einstein trace equation (4.10):

$$\begin{aligned}R=6(\dot{H}+2H^2)=\frac{1}{F}\Big[\rho-3p-\dot{\sigma}^2+4V+3F_{,\sigma}\big(-\ddot{\sigma}-3H\dot{\sigma}\big)\\ -3F_{,\sigma,\sigma}\dot{\sigma}^2+2\dot{\eta}\dot{\sigma}^3+6\eta\dot{\sigma}^2\big(\ddot{\sigma}+H\dot{\sigma}\big)\Big]\end{aligned} \tag{4.21}$$

or, as a function of conformal time

$$\begin{aligned}R=\frac{6}{a^2}(\mathcal{H}'+\mathcal{H}^2)=\frac{1}{F}\left[\rho-3p-\frac{\sigma'^2}{a^2}+4V-\frac{3F_{,\sigma}}{a^2}\Big(\sigma''+2\mathcal{H}\sigma'\Big)\right.\\ \left.-3\frac{F_{,\sigma,\sigma}}{a^2}\sigma'^2+\frac{2\eta'\sigma'^3}{a^4}+\frac{6\eta\sigma'^2}{a^4}\sigma''\right].\end{aligned} \tag{4.22}$$

4.2 Special solutions of the background equations

Every model of dark energy has to be able to describe the accelerating expansion of the Universe at late times. In order to solve for the full theory is necessary to use numerical tools but, under some specific assumptions is it possible to find analytical solutions: e.g. it has been shown that the BDG model (4.2) with a null potential admits de Sitter solutions in absence of matter for $f(\phi)\propto\phi^{-2}$ [110]. Self accelerating solutions have later been obtained in [131] and [132], where they considered more general forms of $f(\phi)$ and recovered the solution found in [110] as a particular case.

We now consider the Induced Gravity Galileon (4.4) to see if it admits analytical solutions of the same kind. In this section we work using cosmic time and specialize the Friedmann and the Klein-Gordon equations of the previous section to the IGG model,

setting as usual $F = \gamma\sigma^2$ and $\zeta = 0$. The background equations then read

$$H^2 + 2H\frac{\dot\sigma}{\sigma} = \frac{\rho + V(\sigma)}{3\gamma\sigma^2} + \frac{\dot\sigma^2}{6\gamma\sigma^2} + \frac{\dot\sigma}{3\gamma}\frac{\dot\sigma^2}{\sigma^2}\Big(6Hg(\sigma) - \dot g(\sigma)\Big); \tag{4.23}$$

$$\begin{aligned}\ddot\sigma + 3H\dot\sigma + \frac{\dot\sigma^2}{\sigma} + \frac{1}{1+6\gamma}\Big[- \frac{\sum_i \rho_i - 3p_i}{\sigma} + \Big(V_{,\sigma} - \frac{4V}{\sigma}\Big) - 2\dot g\frac{\dot\sigma^3}{\sigma} - \dot\sigma^4 g_{,\sigma,\sigma} \\ + \ddot\sigma\Big(12Hg\dot\sigma - 4g_{,\sigma}\,\dot\sigma^2 - 6g\frac{\dot\sigma^2}{\sigma}\Big) + 6\,g\dot\sigma^2\Big(3H^2 + \dot H - H\frac{\dot\sigma}{\sigma}\Big)\Big] = 0\,.\end{aligned} \tag{4.24}$$

In order to mimic the late time cosmology where matter and radiation are far subdominant with respect to dark energy we assume: $T_{\mu\nu} = 0$.

We also choose a potential of the form $V(\sigma) = \lambda_n\sigma^n$ and a common choice of $g(\sigma)$ will be

$$g(\sigma) = \tilde\alpha\gamma^3\sigma^{k+3} = \alpha\sigma^{k+3}\,. \tag{4.25}$$

4.2.1 deSitter solutions

We found solutions where the scale factor $a(t)$ grows exponentially for two particular potentials: quartic and quadratic. For the quartic case it's exactly the same solution obtained in [133] since the $g(\sigma)$ does not contribute in this case. The solution derived for the quadratic potential instead reduces in a continuous way to the one found in IG for the same potential, when $g(\sigma) \to 0$, as we should expect. In the following we will describe these solutions in more detail.

n = 4 As anticipated, the model admits a de Sitter solution: $a(t) \propto e^{Ht}$ with $H > 0$ and constant, in fact the solution found in [100]: $\sigma = \text{constant} = \pm H\sqrt{3\gamma/\lambda_n}$, is still valid in our case, for every possible form of $g(\sigma)$, which does not contribute under the ansatz $\sigma = \text{constant}$.

n = 2 For the quadratic potential things are more complicated. For $g(\sigma) = \tilde\alpha\gamma^3\sigma^{-1}$, i.e. $k = -4$ in equation (4.25), there are solutions of the form $\sigma \propto \exp\{Ht\delta_1\}$, with $\delta_1 = \delta_1(\alpha, \gamma, H)$. Its explicit form is

$$\delta_1 = -1 \qquad \text{or} \qquad \delta_1 = \frac{-1 - 4\gamma \pm \sqrt{(1+4\gamma)^2 + 48\,\tilde\alpha\,\gamma^4 H^2}}{12\,\tilde\alpha\,\gamma^3 H^2}\,. \tag{4.26}$$

For $\alpha \to 0$ these solution reduces to the ones discussed in [133]:

$$\delta_1 = -1 \qquad \text{or} \qquad \delta_1 = \frac{2\gamma}{1+4\gamma}\,. \tag{4.27}$$

4.2.2 Scaling solutions

With the choice of $g(\sigma) = \tilde{\alpha}\,\gamma^3\sigma^{k+3}$ the system has power law solutions of the form $a(t) \propto t^p$ and $\sigma(t) = c_0\,t^q$ when $k = (2-4q)/q$ and $q = -2/(n-2)$. This means that n and k are related by

$$k = -(n+2)\,, \tag{4.28}$$

which implies that for a potential of the form $V(\sigma) = \lambda_n\sigma^n$ there are scaling solutions if $g(\sigma) = \tilde{\alpha}\,\gamma^3\,\sigma^{1-n}$, and vice versa. Note that also the de Sitter solution for $n = 2$ satisfies the relation (4.28). This seems to suggest a natural relationship between the form of the potential, the $g(\sigma)$ and accelerating late-time solutions, which led to us to implement numerically models satisfying (4.28).

Coming back to the power law solutions, the integration constant c_0 and the exponent $p = p(\gamma, n, \lambda, \tilde{\alpha})$ have very complicated forms and they are hard to handle, but we want to recover the values found in [100] and [133], when $\tilde{\alpha} \to 0$. To do this we perform the following: from the Klein-Gordon equation (or equivalently from the Friedmann one or the Lagrangian) we have that dimensionally, for $n \neq 2$

$$\left[\tilde{\alpha}\right] = \left[c_0^{n-2}\right]; \tag{4.29}$$

therefore we can reparameterize $\tilde{\alpha} = \tilde{\beta}c_0^{n-2}$, where $\tilde{\beta}$ is a dimensionless parameter; this simplifies the form of $p = p(n, \gamma, \tilde{\beta})$, which is:

$$p_\pm = \frac{4 + n(n-4) - 8\gamma + 2\gamma n(8 + n(n-5)) + 24\tilde{\beta}\gamma^3 \pm \sqrt{\tilde{f}(\gamma, n, \tilde{\beta})}}{\gamma(n-4)(n-2)^3 + 24\tilde{\beta}\gamma^3(n-2)}\,, \tag{4.30}$$

with

$$\tilde{f}(\gamma, n, \tilde{\beta}) = 192(7-2n)\tilde{\beta}^2\gamma^6 + (n-2)^4(1+6\gamma)^2 - (n-2)^2\,16\tilde{\beta}\gamma^3[3+\gamma(26+(n-6)n)]. \tag{4.31}$$

Now, one can easily see that for $\tilde{\beta} = 0$, $p_\pm$ from equation (4.30) reduce to the value obtained for the corresponding cosmological model studied in [100] and [133]:

$$p_-\Big|_{\tilde{\beta}=0} = \frac{2}{n-2} \tag{4.32}$$

and

$$p_+\Big|_{\tilde{\beta}=0} = 2\frac{1+(n-2)\gamma}{(n-2)(n-4)\gamma} \tag{4.33}$$

4.2.3 Curved Space

In case of curved space the first Friedmann equation simply becomes

$$H^2 + 2H\frac{\dot{\sigma}}{\sigma} + \frac{\kappa}{a^2} = \frac{\rho + V(\sigma)}{3\gamma\sigma^2} + \frac{\dot{\sigma}^2}{6\gamma\sigma^2} + \frac{\dot{\sigma}}{3\gamma}\frac{\dot{\sigma}^2}{\sigma^2}\Big(6Hg(\sigma) - \dot{g}(\sigma)\Big); \tag{4.34}$$

while the Klein-Gordon one keeps the same form.

Scaling solutions

The presence of the term $\frac{\kappa}{a^2}$ in (4.34) restricts the space of possible scaling solutions, in fact if we want $a(t) \propto t^p$, the piece proportional to a^{-2} forces $p = 1$. Therefore the only scaling solution is

$$\begin{cases} a(t) \propto t, \\ \sigma(t) \propto t^q, \quad \text{with} \quad q = -\frac{2}{n-2} \end{cases} \tag{4.35}$$

de Sitter solutions

With the ansatz $a(t) \propto e^{Ht}$ and $H = H_0 =$ constant the term $\frac{\kappa}{a^2}$, which corresponds to κe^{-2Ht}, does not allow for analytical de Sitter solutions for $n = 2$ and $n = 4$.

4.3 Numerical evolution for the Background

In this section we give a description of the numerical evolution for the background in IGG for some particular choices of the potential and the function $g(\sigma)$. We implemented an extension of the Einstein-Boltzmann code CLASSig developed in [13, 14] and validated against other codes in [134]; CLASSig is itself an extension for IG and JBD, which solves for both the perturbations and the background, of the CLASS code [135]. We implemented the modified Einstein and Klein-Gordon equations, both at the level of background and linear perturbation theory, for the IGG and the BDG models. In this section we focus our discussion mostly on the comparison of IGG and BDG with IG in their background evolution, while we study the perturbation theory of the two Galileon

Initialization parameters	
$H_0\,[\mathrm{km\,s^{-1}Mpc^{-1}}]$	67.31
$T_{\mathrm{CMB}}\,[\mathrm{K}]$	2.7255
$\Omega_{\mathrm{b},0}$	0.049
$\Omega_{\mathrm{cdm},0}$	0.264
n_s	0.9655
A_s	2.195×10^{-9}
τ_{reio}	0.078

Table 4.1: Set of the cosmological parameters used to initialize to code: the Hubble parameter today H_0, the CMB temperature T_{CMB}, baryon density parameter today $\Omega_{\mathrm{b},0}$, cold dark matter density parameter today $\Omega_{\mathrm{cdm},0}$, the spectral index n_S, the amplitude of the matter power spectrum A_s referred to curvature perturbations, and the reionization optical depth τ_{reio}

models together with their consequences on cosmological observables in the next chapter.

In table (4.1) we show the set of cosmological parameters used to initialize the extended code.

4.3.1 Choice of the potential and the function $g(\sigma)$

The evolution of the scalar field depends on the form of the potential and its choice is therefore of great importance; in the literature, there are various examples of potentials studied in the context of Induced Gravity (or equivalently extended Jordan-Brans-Dicke) theory [14, 95, 100, 136]. We consider quartic and quadratic power law potentials:

$$V(\sigma) = \frac{\lambda_4}{4}\sigma^4\,, \tag{4.36}$$

$$V(\sigma) = \frac{\lambda_2}{4}\sigma^2\,, \tag{4.37}$$

where λ_4 is a dimensionless parameter and λ_2 has the dimensions of a squared mass. We also consider and show some results for a constant potential. With the choice $V(\sigma) \propto \sigma^4$, all the terms containing the potential and its derivatives cancel out both in the Klein-Gordon and perturbed Klein-Gordon equations for the field and its fluctuations.

The function $g(\sigma)$ is, in principle, arbitrary, but the analytical study of the equations

of motion carried out in the previous section suggests as natural choice: a power law of the type

$$g(\sigma) = \alpha\, \sigma^{k+3} \tag{4.38}$$

with $k = -(n+2)$, and where n is the exponent of the field in the potential $V \propto \sigma^n$, to guarantee the presence of accelerating solutions at late times.[1] Notice that with respect to the expression given in Sec. (4.2) we incorporated the factor γ^3 into the parameter α. The $g(\sigma)$ is the only function that needs to be fixed since it automatically fixes the $\zeta(\sigma)$ in the BDG model. Therefore, with the choice of a quartic potential we have $g(\sigma) = \alpha\sigma^{-3}$; in such a scenario the parameter α is dimensionless, just like λ. A quadratic potential, corresponds instead, to $g(\sigma) = \alpha\sigma^{-1}$; in this case α has the dimensions of a squared length.

4.3.2 Evolution of the scalar field and the density parameters

We first show in figure 4.1, 4.2 and 4.3 the evolution of the scalar field, σ, and its derivative with respect to conformal time, σ', in IGG and compare it with IG, for the quartic, quadratic and constant potential respectively. The behaviour is qualitatively the same in all the cases: it can be seen in figure (4.1) that for values of α of the order of $10^{111} - 10^{109}$ the IGG field evolution is substantially different from the IG field especially at early times during the radiation era when we note a stronger dynamics. For smaller values of α the differences with IG are hard to notice since the lines are superimposed, but appreciable differences remain in the evolution of the field derivative σ' (right panel). As expected reducing α brings IGG towards IG. A similar behaviour is reported in fig. 4.2 for the quadratic potential and in fig. 4.3 for a constant potential. We note that switching the sign of the $g(\sigma)$ we obtain an instability much larger than the one displayed in these plots.

The different evolution of the scalar field and its derivative in IGG and BDG is shown in figure 4.4 and 4.5, respectively, for the quartic and quadratic potentials. As it can be seen, the difference between the BDG and IGG models is negligible for all the values of α analyzed. For this reason we will only compare the IGG model to ΛCDM in the rest of the section.

[1] We remind anyway that for $n = 4$ the de Sitter solution was always present regardless of the form of $g(\sigma)$

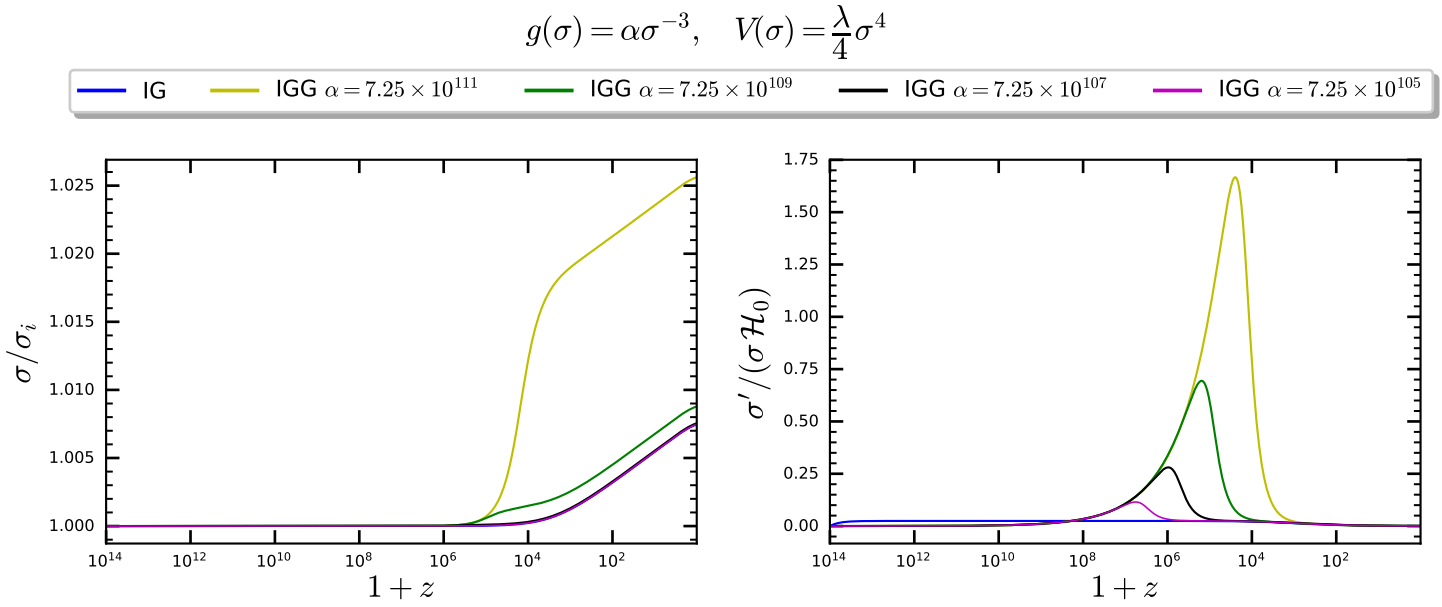

Figure 4.1: Evolution of the scalar field σ and its derivative σ' as a function of redshift z for IG and IGG with quartic potential with different choices of α and $\gamma = 5 \times 10^{-4}$.

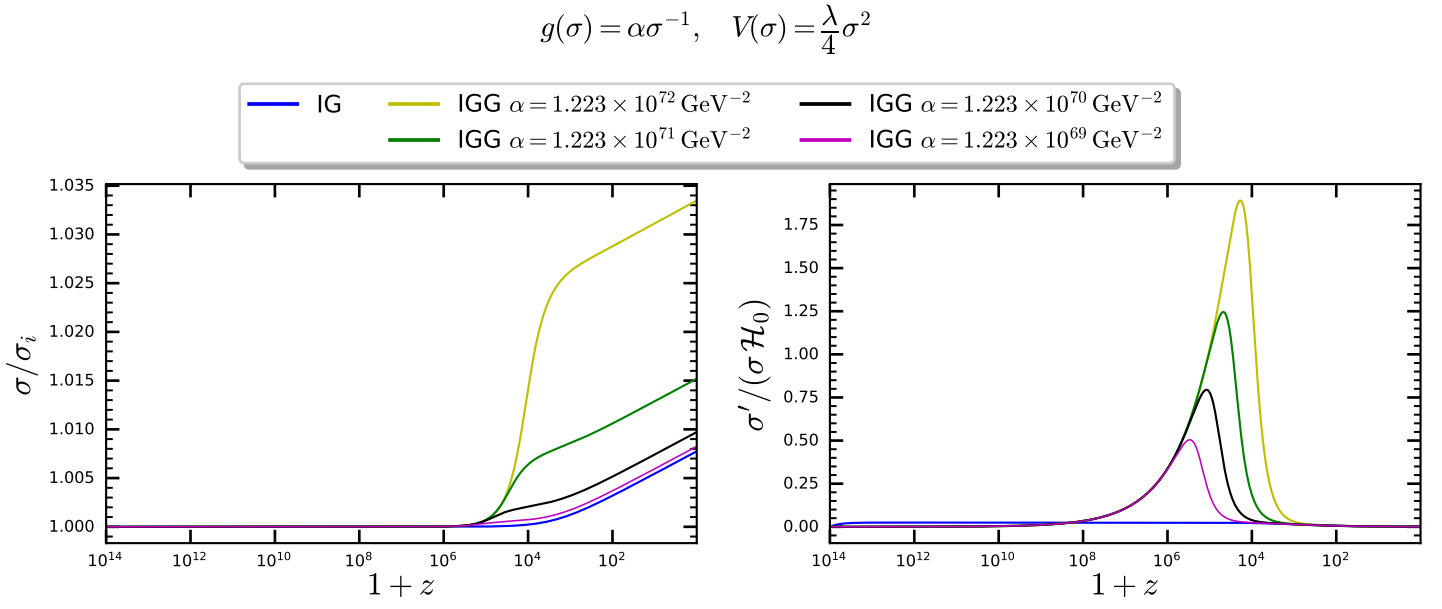

Figure 4.2: Evolution of the scalar field σ and its derivative σ' as a function of redshift z for IG and IGG with quadratic potential for different choices of α and $\gamma = 5 \times 10^{-4}$.

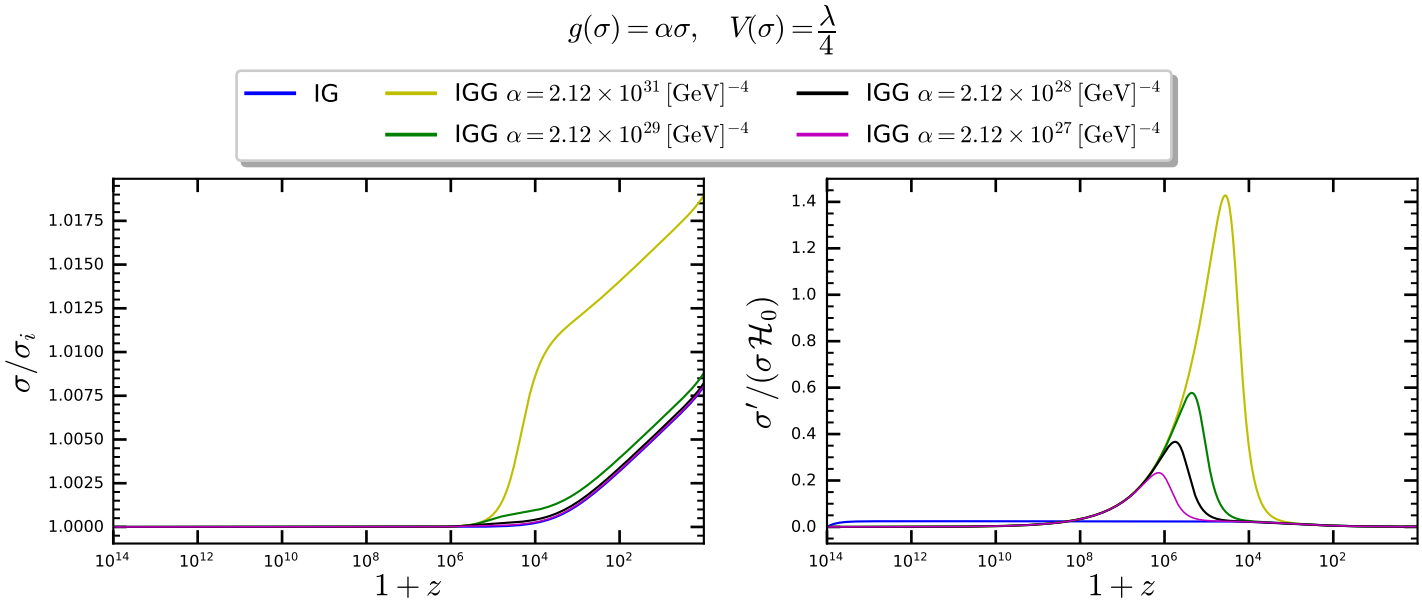

Figure 4.3: Evolution of the scalar field σ and its derivative σ' as a function of redshift z for IG and IGG with a constant potential, for different choices of α and $\gamma = 5\times10^{-4}$.

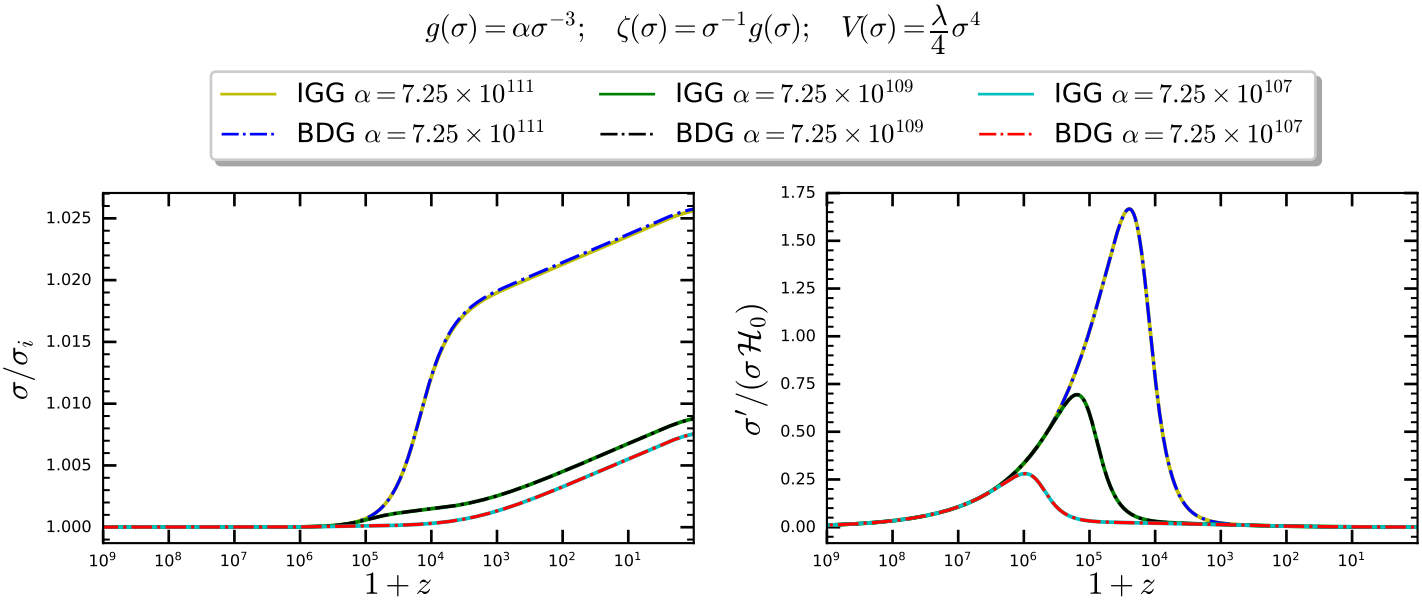

Figure 4.4: Evolution of the scalar field σ and its derivative σ' as a function of redshift z for IGG and BDG with a quartic potential for different choices of α and $\gamma = 5\times10^{-4}$.

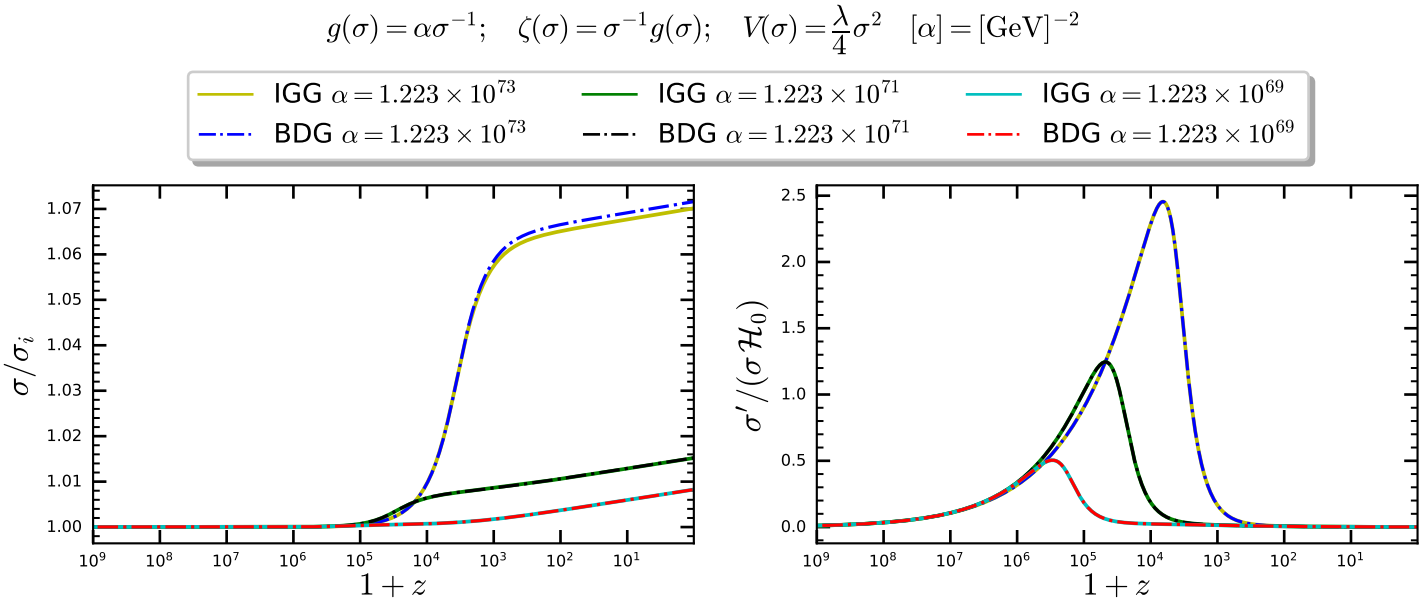

Figure 4.5: Evolution of the scalar field σ and its derivative σ' as a function of redshift z for IGG and BDG with a quadratic potential for different choices of α and $\gamma = 5\times10^{-4}$.

In order to study the evolution of the density parameters we define them as

$$\Omega_{rad} = \frac{\rho_{rad}}{3\,\gamma\,\sigma^2\,H}\,, \tag{4.39}$$

$$\Omega_{m} = \frac{\rho_{m}}{3\,\gamma\,\sigma^2\,H}\,, \tag{4.40}$$

$$\Omega_{\sigma} = \frac{\rho_{\sigma}}{3\,\gamma\,\sigma^2\,H}\,, \tag{4.41}$$

with

$$\rho_\sigma = \frac{\dot\sigma^2}{2} + V(\sigma) - 6\,H\,\gamma\,\sigma\,\dot\sigma + \dot\sigma^3\left[6\,g(\sigma)\,H - g_{,\sigma}\dot\sigma + 3\,\zeta(\sigma)\dot\sigma\right]. \tag{4.42}$$

Where, for $g=\zeta=0$ we have IG, for $\zeta=0$ IGG and for $\zeta=g\sigma^{-1}$ BDG.

In figure 4.6 the density parameters for IGG are compared with IG for $\gamma=5\times10^{-4}$: on the left the case of a quartic potential it's displayed, while on the right we show the quadratic potential. Both on the left and on the right panel we can see that for the largest value of α plotted there's a different evolution of Ω_{rad} and Ω_σ in the early Universe. In fact while the Universe is still in the radiation era, there's a non negligible scalar field density that can become larger than the matter one. For smaller values of α the differences between IG and IGG are not visible from the plots in the quartic case, while a slight difference can still be observed in the instance of the quadratic potential. Since IG with $\gamma=5\times10^{-4}$ has an evolution of the density parameters almost

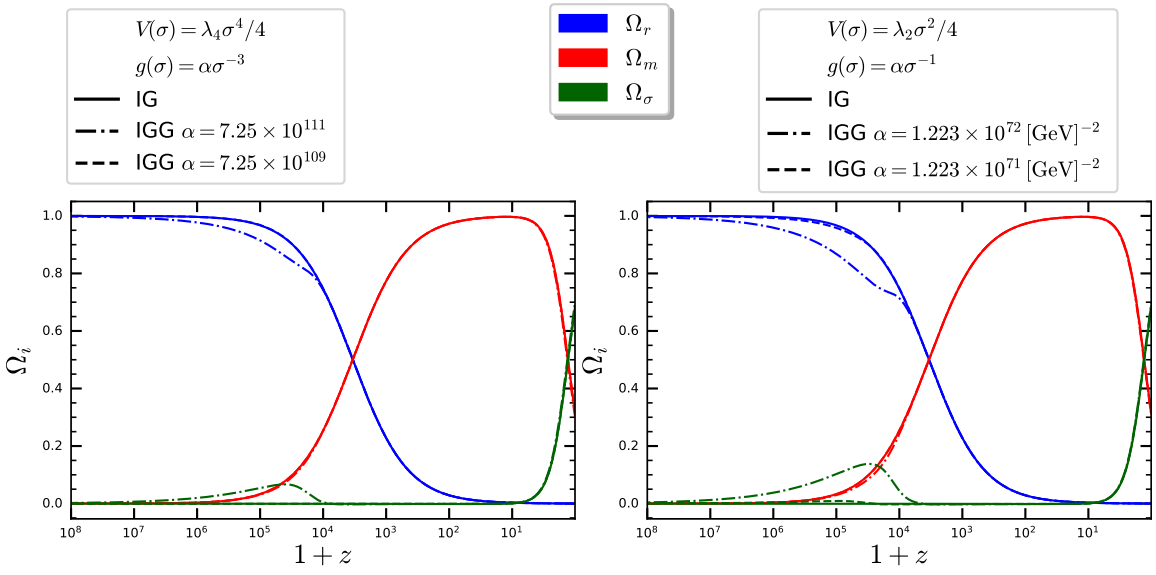

Figure 4.6: On the left it's displayed the evolution of the density parameters in IG and IGG, for $\gamma = 5 \times 10^{-4}$ and different choices of α. The quartic potential case is shown on the left while on the right the results for the quadratic potentials are displayed

indistinguishable from ΛCDM, we expect to obtain similar results when comparing IGG to ΛCDM. This is confirmed by the plots in figure 4.7.

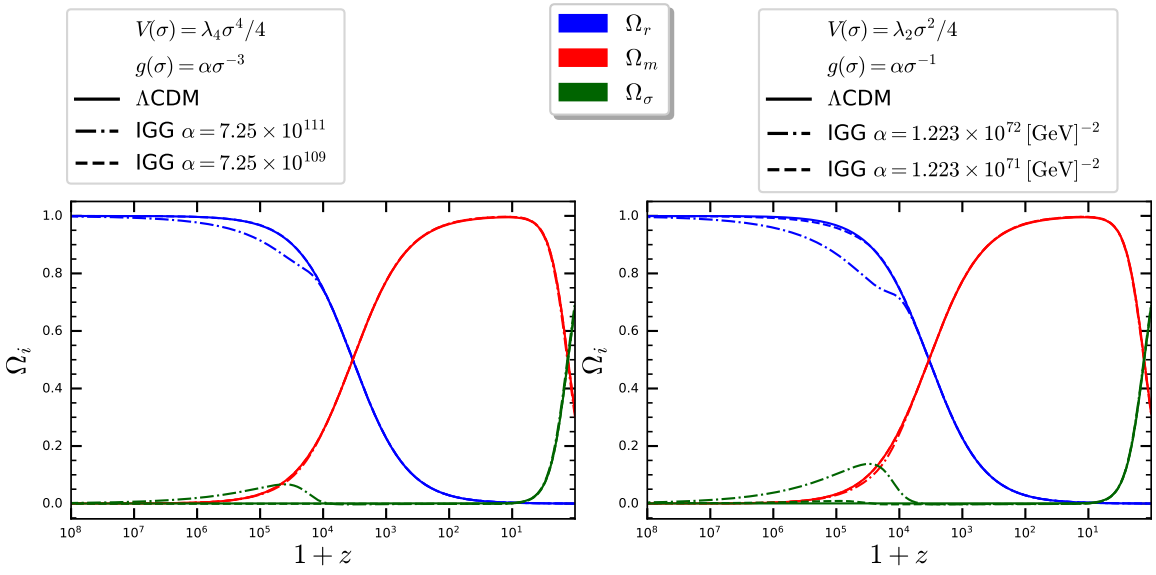

Figure 4.7: On the left it's displayed the evolution of the density parameters in ΛCDM and IGG, for $\gamma = 5 \times 10^{-4}$ and different choices of α. The quartic potential case is shown on the left while on the right the results for the quadratic potentials are displayed

4.3.3 Effective equation of state for dark energy

A key quantity describing dark energy is the equation of state (EOS) $w_{\rm DE} = P_{\rm DE}/\rho_{\rm DE}$, where $\rho_{\rm DE}$ and $P_{\rm DE}$ are, respectively, the dark energy density and pressure. The simplest model accounting for non constant EOS assumes the parametrization $w_{\rm DE} = w_0 - (1-a)w_a$, where a is the scale factor, normalized to 1 today, and $w_0\,, w_a$ are constants; the data analysis of Planck 2018 combined with the SN Ia and BAO data constrained these parameters to $w_0 = -0.961 \pm 0.077$ and $w_a = -0.28^{+0.31}_{-0.27}$ at 68% confidence level [3]. The data constraints are compatible with a cosmological constant but do not exclude possible time variation. We must note that the constraints from CMB data to the dark energy EOS are affected by parameter degeneracy and require the combination, and for the future missions also cross-correlation, with LSS data to break this degeneracies.

In order to define properly the equation of state for the IGG and BDG model we use a procedure similar to the one carried out in chapter 3 for the EOS of the entire Horndeski theory: we rewrite the Friedmann equations (4.14) and (4.15) as

$$3F_0H^2 = \rho_{\rm m} + \rho_{\rm DE} \tag{4.43}$$

$$2F_0\dot{H} = -\rho_{\rm m} - P_{\rm m} - \rho_{\rm DE} - P_{\rm DE} \tag{4.44}$$

where the density and pressure of dark energy are given by

$$\rho_{\rm DE} = 3H^2\big(F_0 - F\big) + \frac{\dot\sigma^2}{2} + V(\sigma) - 3H\dot F + \dot\sigma^3\Big(6\,g\,H - g_{,\sigma}\,\dot\sigma\, + 3\zeta\,\dot\sigma\Big)\,, \tag{4.45}$$

$$P_{\rm DE} = 2\dot H\big(F - F_0\big) + \dot\sigma^2 + \ddot F - H\,\dot F + \dot\sigma^2\Big[2\big(3\,g\,H - g_{,\sigma}\,\dot\sigma\big)\dot\sigma\, + 4\zeta\,\dot\sigma^2 - 2\,g\,\ddot\sigma\Big] - \rho_{\rm DE}\,. \tag{4.46}$$

If we now specialize it to the BDG/IGG models: $F(\sigma) = \gamma\sigma^2$ we have

$$\rho_{\rm DE} = 3\gamma H^2\big(\sigma_0^2 - \sigma^2\big) + \frac{\dot\sigma^2}{2} + V(\sigma) - 6H\,\sigma\dot\sigma + \dot\sigma^3\Big(6\,g\,H - g_{,\sigma}\,\dot\sigma\, + 3\zeta\,\dot\sigma\Big)\,, \tag{4.47}$$

$$P_{\rm DE} = 2\gamma\dot H\big(\sigma^2 - \sigma_0^2\big) + 2\gamma\big(\dot\sigma^2 + \sigma\ddot\sigma\big) + \dot\sigma^2\Big[2\big(3\,g\,H - g_{,\sigma}\,\dot\sigma\big)\dot\sigma\, + 4\zeta\,\dot\sigma^2 - 2\,g\,\ddot\sigma\Big] - \rho_{\rm DE}\,. \tag{4.48}$$

As usual, for $g = \zeta = 0$ we have IG, for $\zeta = 0$ IGG and for $\zeta = g\sigma^{-1}$ BDG. The effective parameter of state for dark energy can then be defined, as it is customary, as

$$w_{\rm DE} \equiv \frac{P_{\rm DE}}{\rho_{\rm DE}}\,; \tag{4.49}$$

its evolution for IG and IGG with quartic potential and for different values of α is shown In Fig. 4.9: we can see how the parameter $w_{\rm DE}$ follows the dominant component: during the radiation epoch it has a value of $\sim 1/3$, then in the matter era it decreases towards zero; finally, at present epoch, it becomes negative, $w_{\rm DE} = -1$, mimicking a dominant cosmological constant. We can see from the figure that the evolution of the effective parameter of state has an anomalous behaviour for larger values of alpha with a bump in the radiation era, while it tends to IG as α gets smaller, becoming almost indistinguishable from the IG evolution already at $\alpha = 5 \times 10^{-6}$. Similar considerations can be applied to figure 4.10 where the evolution of the EOS in the case of quadratic potential is presented.

To discuss the bump in the EOS, we refer to figure 4.8, where the second derivative of the scalar field is plotted. As we can see, from eq. (4.48) the pressure is dependent by this quantity, and since it multiplies $-g(\sigma)$ we can conclude that the effect of this term is more important the larger the parameter α. We can see from the aforementioned equation and figure, that as the second derivative of the field decreases the pressure increases and we observe the bumps in the EOS in correspondence of the minima of σ''. We can see how this minima are deeper and shifted towards earlier times as α gets

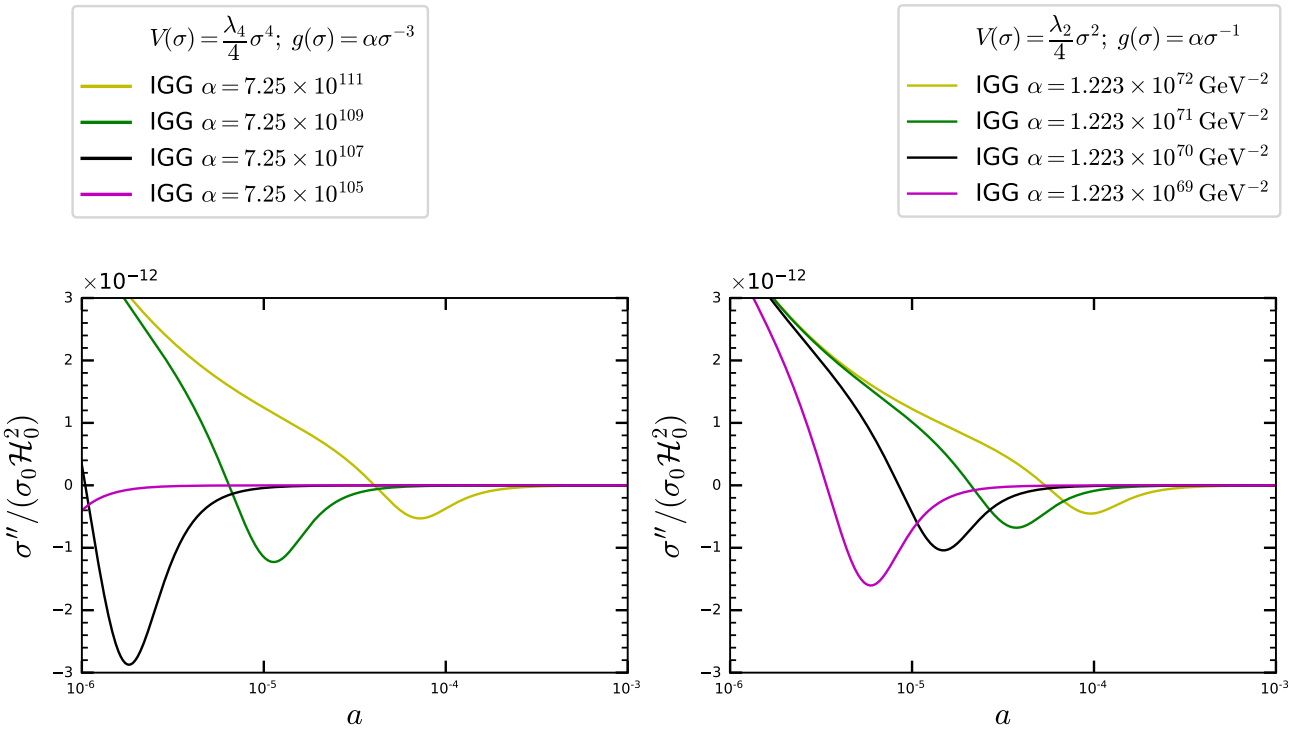

Figure 4.8: Evolution of the second derivative of the scalar field in IGG with a quartic potential (left) and with a quadratic one (right), for various value of the Galileon parameter α.

smaller, for this reason the bump in the EOS is shifted towards earlier times for smaller values of α. This effect is more prominent for larger value of α, in spite of the fact that the decline of the second derivative of σ is less steep and the minima less deep in these cases. As time passes $\sigma'' \to 0$ and the effects of this term become negligible, thus allowing the IGG equation of state to approach the IG behaviour.

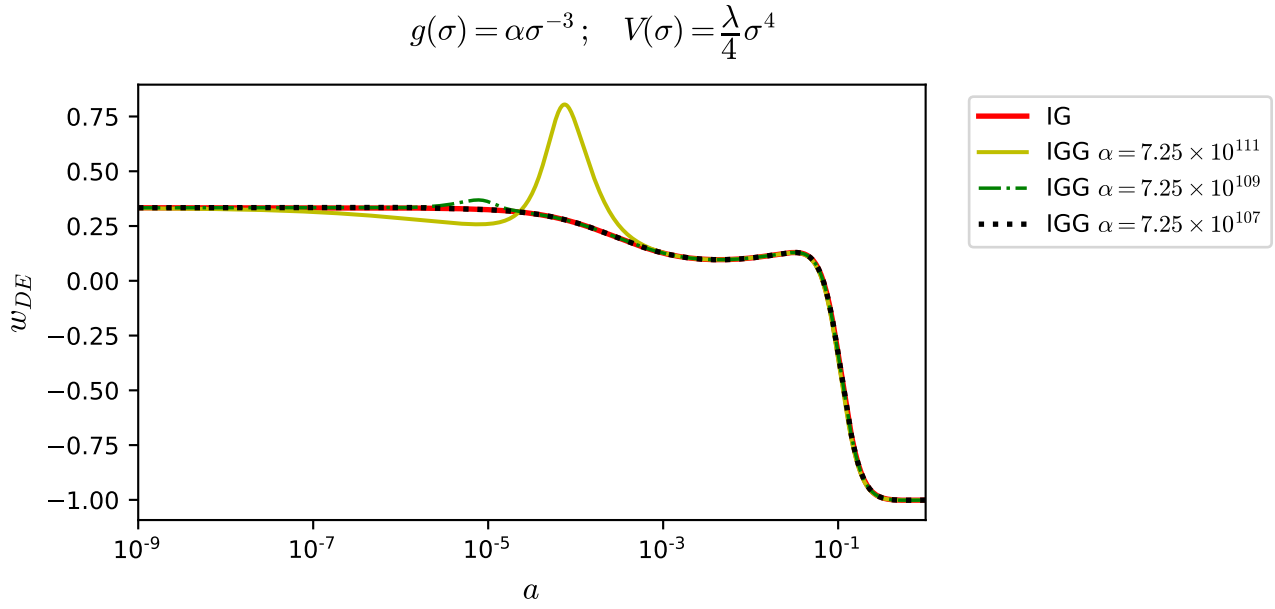

Figure 4.9: Evolution of the parameter w_{DE} in Induced Gravity and Induced Gravity Galileon, with a quartic potential for $\gamma = 5 \times 10^{-4}$ and various values of α.

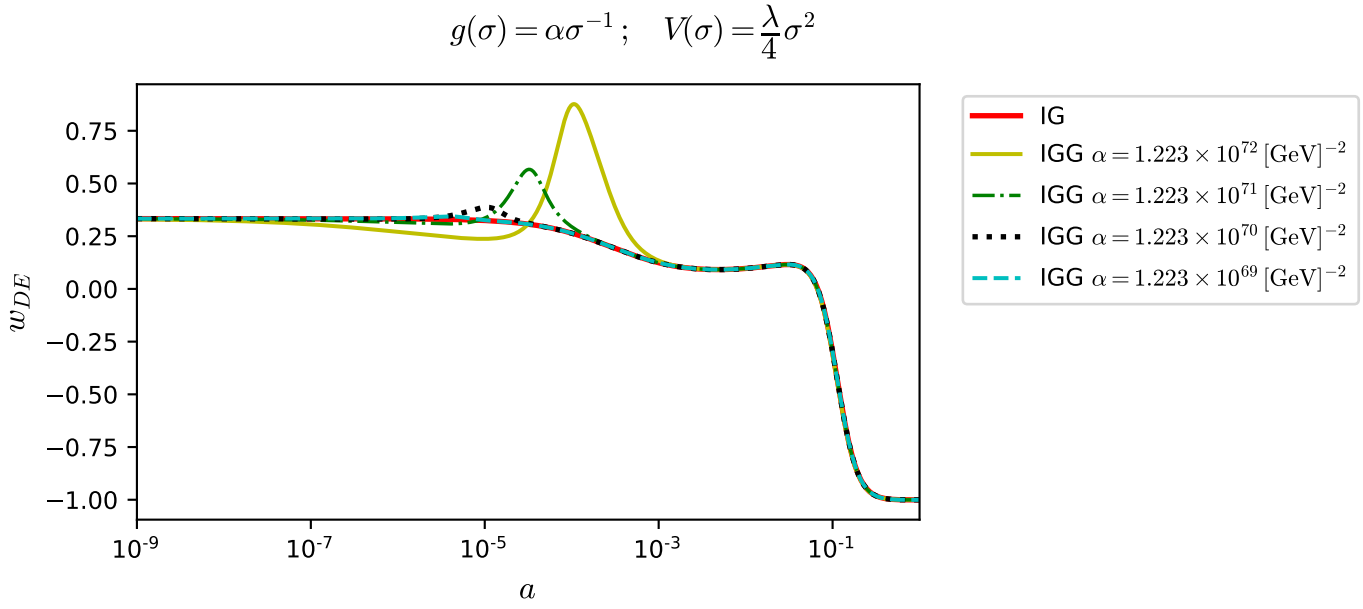

Figure 4.10: Evolution of the parameter w_{DE} in Induced Gravity and Induced Gravity Galileon, with a quadratic potential for $\gamma = 5 \times 10^{-4}$ and different choices of α.

Chapter 5

Cosmological effects of the Galileon-like interaction term

In this chapter we present the equations for the linear cosmological perturbations in the synchronous gauge for the Induced Gravity Galileon and the Brans-Dicke Galileon. Then, we discuss the effects of the Galileon term on CMB anisotropies and matter power spectrum. We derive the predictions for CMB anisotropies and the matter power spectrum by further extending the CLASSig code [13, 14, 135] with the modified perturbed Einstein and scalar field equations for both IGG and BDG models, in a similar manner of what we already did for the background in the previous chapter. With the tool we developed we follow the Galileon term impact jointly in the background and cosmological perturbations.

5.1 Equations for cosmological perturbations in the IGG and BDG models

In this section we derive the expressions for the perturbed field equations in both the Induced Gravity Galileon (IGG) (4.4) and Brans-Dicke Galileon (BDG) (4.3) models. For convenience we write them in the synchronous gauge which is the one used in the numerical implementation. Just like in the case of the background equations of motion, we will give the equation for the BDG, which already contain the equations for the IGG model and they can be formally recovered by setting $\zeta = 0$.

The procedure to derive the equations is the same that we outlined in Section (2.2). In the Jordan frame the energy-momentum tensors of all the species in the Universe are separately conserved, this implies that the equations for the density contrasts, the velocities and the anisotropic stresses of baryonic matter, CDM, radiation and neutrinos

are the same as in general relativity and we can use the Boltzmann equations of Sec. (2.3) and the tight-coupling approximation (2.63). This means we only need to derive the modified perturbed field equations for the metric and for the scalar field σ. We split the scalar field into the sum of a background space-independent part and a perturbation

$$\sigma(\tau, \mathbf{x}) = \bar{\sigma}(\tau) + \delta\sigma(\tau, \mathbf{x}). \tag{5.1}$$

In the following, to lighten the notation we will use just σ in place of $\bar{\sigma}$. We work as usual in the Fourier space where the scalar field perturbation reads:

$$\delta\sigma = \int d^3k\, \delta\sigma(\tau, \mathbf{k})\, e^{i\mathbf{k}\cdot\mathbf{x}}\,. \tag{5.2}$$

We recast the equations for the metric perturbations in a similar way to their counterparts in Einstein Gravity (2.30)-(2.33):

$$k^2\eta - \frac{1}{2}\mathcal{H}h' = -\frac{a^2}{2}\left(\delta\tilde{\rho} - \delta\tilde{\rho}^{(g)}\right), \tag{5.3}$$

$$k^2\eta' = \frac{a^2}{2}\left[\left(\tilde{\rho} + \tilde{P}\right)\tilde{\theta} + \left(\tilde{\rho}^{(g)} + \tilde{P}^{(g)}\right)\tilde{\theta}^{(g)}\right], \tag{5.4}$$

$$h'' + 2\mathcal{H}h' - 2k^2\eta = -3a^2\left(\delta\tilde{P} + \delta\tilde{P}^{(g)}\right), \tag{5.5}$$

$$h'' + 6\eta'' + 2\mathcal{H}(h' + 6\eta') - 2k^2\eta = -3a^2\left(\tilde{\rho} + \tilde{P}\right)\tilde{\sigma}\,. \tag{5.6}$$

Where a tilde denotes the effective perturbations defined as:

$$\begin{aligned}\delta\tilde{\rho} \equiv \frac{\delta\rho_m}{\gamma\sigma^2} + \frac{h'\sigma'}{a^2\sigma} - \frac{2}{a^2}\Bigg\{\frac{\delta\sigma}{\sigma}\left[\frac{a^2\rho_m}{\gamma\sigma^2} + \frac{\sigma'^2}{2\gamma\sigma^2} + \frac{a^2}{\gamma\sigma}\left(\frac{V}{\sigma} - \frac{V_{,\sigma}}{2}\right) - \frac{3\mathcal{H}\sigma'}{\sigma} + k^2\right] \\ + \frac{\delta\sigma'}{\sigma}\left(\mathcal{H} - \frac{\sigma'}{2\gamma\sigma}\right)\Bigg\},\end{aligned} \tag{5.7}$$

$$\begin{aligned}\delta\tilde{\rho}^{(g)} \equiv \frac{2}{\gamma a^4}\frac{\sigma'^2}{\sigma^2}\Bigg\{\frac{\delta\sigma}{\sigma}\left[3\mathcal{H}\sigma'\left(\sigma g_{,\sigma} - 2\,g\right) - \frac{\sigma'^2}{2}\left(\sigma g_{,\sigma,\sigma} - 2g_{,\sigma}\right) + k^2\sigma g + \frac{3\sigma'^2}{2}\left(\zeta_{,\sigma}\sigma - 2\zeta\right)\right] \\ + \delta\sigma'\left(9\mathcal{H}g - 2g_{,\sigma}\sigma' - 6\zeta\sigma'\right) + \frac{1}{2}h'\sigma' g\Bigg\},\end{aligned} \tag{5.8}$$

$$\big(\tilde{\rho}+\tilde{P}\big)\tilde{\theta}\equiv\frac{(\rho_m+P_m)}{\gamma\sigma^2}+\frac{2k^2}{a^2}\left\{\frac{\delta\sigma}{\sigma}\left[\frac{\sigma'}{2\gamma\sigma}(1+2\gamma)-\mathcal{H}\right]+\frac{\delta\sigma'}{\sigma}\right\}, \tag{5.9}$$

$$\big(\tilde{\rho}^{(g)}+\tilde{P}^{(g)}\big)\tilde{\theta}^{(g)}\equiv\frac{2k^2}{\gamma a^4}\frac{\sigma'^2}{\sigma^2}\Big[\delta\sigma(\,4\mathcal{H}g-g_{,\sigma}\sigma'+2\zeta\sigma'\,)-\delta\sigma' g\Big], \tag{5.10}$$

$$\begin{aligned}\delta\tilde{P}\equiv\frac{\delta P_m}{\gamma\sigma^2}+\frac{1}{a^2}\Bigg\{&-\frac{\delta\sigma}{\sigma}\left[\frac{a^2}{\gamma\sigma}\left(V_{,\sigma}-\frac{2V}{\sigma}\right)+\frac{2a^2P_m}{\gamma\sigma^2}+\frac{\sigma'^2}{\gamma\sigma^2}+\frac{4\sigma'^2}{\sigma^2}+\frac{2\sigma''}{\sigma}+\frac{2\mathcal{H}\sigma'}{\sigma}-\frac{4k^2}{3}\right]\\&+\delta\sigma'\left(\frac{\sigma'}{\gamma\sigma^2}(1+4\gamma)+\frac{2\mathcal{H}}{\sigma}\right)+\frac{2\,\delta\sigma''}{\sigma}+\frac{2\sigma'}{3\sigma}h'\Bigg\},\end{aligned} \tag{5.11}$$

$$\begin{aligned}\delta\tilde{P}^{(g)}\equiv\frac{1}{\gamma a^4}\frac{\sigma'^2}{\sigma^2}\Bigg\{&\frac{\delta\sigma}{\sigma}\Big[4\,g\,\sigma''-4\mathcal{H}\,g\,\sigma'+\sigma'^2\big(2\,g_{,\sigma}\,-g_{,\sigma,\sigma}\,\sigma\big)+\sigma'^2\big(\,2\zeta\,-\zeta_{,\sigma}\,\sigma\big)\Big]\\&-\delta\sigma'\Big(\,2g_{,\sigma}\sigma'-4\mathcal{H}\,g+2\,g\frac{\sigma''}{\sigma'}+4\,\zeta\,\sigma'\,\Big)-2\,g\,\delta\sigma''\Bigg\},\end{aligned} \tag{5.12}$$

$$(\tilde{\rho}+\tilde{P})\tilde{\sigma}\equiv\frac{(\rho_m+P_m)\sigma_u}{\gamma\sigma^2}+\frac{1}{3a^2}\left[\frac{4k^2\delta\sigma}{\sigma}+2(h'+6\eta')\frac{\sigma'}{\sigma}\right]. \tag{5.13}$$

The quantities $\tilde{\sigma}$ and σ_u should not be confused with the scalar field, in fact they are respectively the modified and the usual general relativistic anisotropic shear perturbation defined in (2.29).

We distinguish explicitly between the quantities coming from IG and the ones arising from the Galileon term to make as manifest as possible the reduction of IGG and BDG models to IG when $g(\sigma)=\zeta(\sigma)=0$.

Perturbing the Klein-Gordon equation (4.12) we obtain the equation for the evolution of the fluctuations of the scalar field:

$$\delta\sigma''=\left\{1-\frac{2\sigma'^2}{a^2}\left[3\,g\left(\frac{1}{\sigma}-\frac{2\mathcal{H}}{\sigma'}+2\,g_{,\sigma}\right)-6\,\zeta\right]\right\}^{-1}\frac{2}{a^2}\delta\tilde{\mathcal{G}}\,, \tag{5.14}$$

where $\delta\tilde{\mathcal{G}}$ is defined as

$$
\begin{aligned}
\delta\tilde{\mathcal{G}} \equiv \delta\sigma\Bigg\{ & -\frac{a^2}{2}\left[\frac{a^2}{(1+6\,\gamma)}\left(\frac{\rho_m+P_m}{\sigma^2}+\frac{4\,V}{\sigma^2}-\frac{4\,V_{,\sigma}}{\sigma}+V_{,\sigma,\sigma}\right)+k^2-\frac{\sigma'^2}{\sigma^2}\right] \\
& + g\left[2k^2\left(\frac{\sigma'^2}{2\,\sigma}-\sigma''-\mathcal{H}\,\sigma'\right)-\frac{3\,\sigma'^2}{\sigma^2}\,\sigma''\right]-2\,\zeta\,\sigma'^2k^2 \\
& + g_{,\sigma}\,\sigma'^2\left(\frac{3\,\sigma''}{\sigma}-\frac{\sigma'^2}{\sigma^2}-3\,\mathcal{H}'-\frac{6\,\mathcal{H}\,\sigma''}{\sigma'}\right)+2\,\zeta_{,\sigma}\big(4\,\mathcal{H}\,\sigma'-3\,\sigma''\big) \\
& + g_{,\sigma,\sigma}\sigma'^2\left(\frac{\sigma'^2}{\sigma}+2\,\sigma''-2\,\mathcal{H}\,\sigma'\right)-\frac{3\,\zeta_{,\sigma,\sigma}\sigma'^2}{2}+\frac{g_{,\sigma,\sigma,\sigma}\,\sigma'^4}{2}\Bigg\} \\
+\delta\sigma'\Bigg\{ & -a^2\left(\frac{\sigma'}{\sigma}+\mathcal{H}\right)+6\,g\left[\sigma''\left(\frac{\sigma'}{\sigma}-\mathcal{H}\right)-\mathcal{H}'\,\sigma'\right]+\zeta\big(10\,\mathcal{H}\,\sigma'^2-9\,\sigma'\,\sigma''\big) \\
& + 2g_{,\sigma}\,\sigma'^2\left(\frac{2\,\sigma'}{\sigma}-3\mathcal{H}+\frac{2\,\sigma''}{\sigma'}\right)-6\,\zeta_{,\sigma}\,\sigma'^3+2\,g_{,\sigma,\sigma}\sigma'^3\Bigg\} \\
+\frac{h'}{2}\Bigg[& -\frac{a^2\,\sigma'}{2}+g\,\sigma'^2\left(\frac{\sigma'}{\sigma}-3\,\mathcal{H}-\frac{2\,\sigma''}{\sigma'}\right)-8\,\zeta\sigma'^3\Bigg]-\frac{1}{2}h''\,g\,\sigma'^2 \\
+\frac{a^2}{2} & \frac{a^2(\delta\rho_m-3\,\delta P_m)}{(1+6\gamma)\sigma}\,.
\end{aligned}
\tag{5.15}
$$

While it's not as manifest as in the Einstein equations, the perturbed Klein-Gordon equation reduces to the one obtained in [137] for IG when $g(\sigma)=\zeta(\sigma)=0$. To solve this system of equations coupled with the Boltzmann equations introduced in section 2.3, we need to set initial conditions. If radiation remains dominant, the introduction of the Horndeski field doesn't change the initial conditions for the metric and energy-momentum tensor perturbations presented in section 2.4 [138]. For the scalar field, as a minimal starting case, we set the initial conditions $\delta\sigma=0$ and $\delta\sigma'=0$, reserving to increase the complexity in a future work.

5.2 Evolution of perturbed quantities

In this section we present the evolution of gauge invariant perturbations: the metric perturbation, the density contrast and the scalar field fluctuation. We then show their evolution in IGG for the case of the quartic potential.

5.2.1 Gauge invariant formalism

Metric perturbations

We first write the expressions for the the Bardeen potentials Ψ_{B} and Φ_{B} defined in (2.19) and (2.20), which are gauge invariant. These are related to the synchronous metric

perturbations by:

$$\Psi_{\text{B}} = \frac{1}{2k^2}\left[h'' + 6\eta'' + \mathcal{H}\left(h' + 6\eta'\right)\right], \tag{5.16}$$

$$\Phi_{\text{B}} = -\eta + \frac{1}{2k^2}\mathcal{H}\left(h' + 6\eta'\right). \tag{5.17}$$

Using these, the off-diagonal perturbed Einstein equation (5.6) becomes

$$\left(\Psi_{\text{B}} + \Phi_{\text{B}}\right) = -\frac{3a^2}{2k^2}\left(\tilde{\rho} + \tilde{P}\right)\tilde{\sigma}\,, \tag{5.18}$$

from which we can see that $\Psi_{\text{B}} + \Phi_{\text{B}}$ is a measure of the anisotropic stress.

Scalar field perturbation

The gauge-invariant scalar field perturbation $\delta\sigma$ is related to its correspondent in the synchronous gauge by [139, 140]:

$$\delta\sigma = \delta\sigma_{\text{S}} + \frac{\dot{\sigma}}{H}\eta = \delta\sigma_{\text{S}} + \frac{\sigma'}{\mathcal{H}}\eta\,, \tag{5.19}$$

where η is the metric perturbation introduced in section 2.1, and the subscript S denotes that variable is considered in the synchronous gauge.

Density perturbations

The gauge invariant density perturbation is given by [141]:

$$\delta \to \tilde{\delta} + 3(1+w)(\tilde{\theta} - \tilde{B})\frac{aH}{k^2}\,, \tag{5.20}$$

where, a tilde denotes a generic gauge, $\tilde{\theta}$ is the divergence of the peculiar velocity of the considered component, w is the equation of state parameter and $\tilde{B}$ is the metric perturbation defined in section 2.1. Since in the synchronous gauge $B_{\text{S}} = 0$, the gauge invariant density contrast δ is related to the synchronous one δ_{S} by

$$\delta = \delta_{\text{S}} + 3(1+w)\frac{aH}{k^2}\theta_{\text{S}}\,. \tag{5.21}$$

5.2.2 Perturbations evolution in IGG with a quartic potential

The evolution of the gauge invariant density contrasts for baryons photons and cold dark matter, shows negligible differences between IGG, IG and ΛCDM.

Figure 5.1 shows the relative gravitational slip $(\Psi_{\text{B}} + \Phi_{\text{B}})/\Psi_{\text{B}}$. Once again we see that the differences between the models are very minimal. It's worth noticing, though, an en-

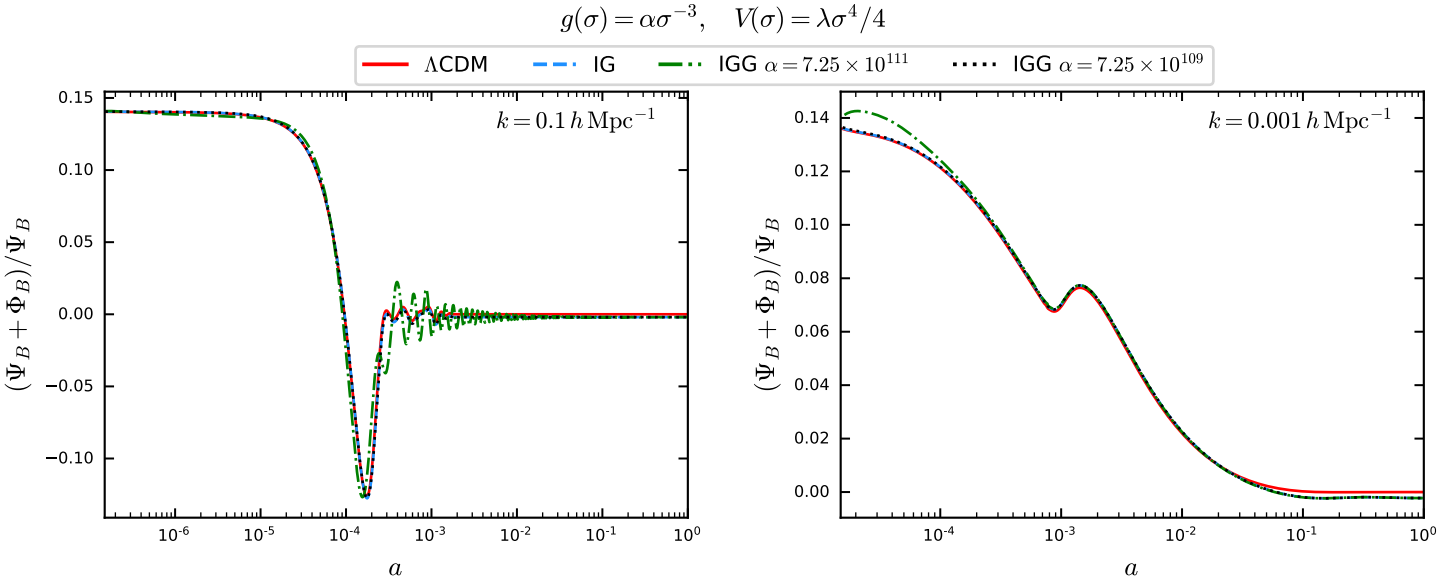

Figure 5.1: Relative gravitational slip at the scales $k = 0.1\,h\,\mathrm{Mpc}^{-1}$ (left) and $k = 0.001\,h\,\mathrm{Mpc}^{-1}$ (right). The red solid line is the ΛCDM while the other lines represent IG and IGG models, both with a quartic potential and $\gamma = 5 \times 10^{-4}$. Two values of α are plotted: 7.5×10^{111} and 7.5×10^{109}.

hancement of the anisotropic stress at early times at the largest scale ($k = 0.001\,h\,\mathrm{Mpc}^{-1}$) for the IGG model with $\alpha = 7.5 \times 10^{111}$.

The evolution of the relative fluctuations of the scalar field $\delta\sigma/\sigma$ are shown in figure 5.2, for the IG and the IGG models. It's clearly visible how such fluctuations oscillates more in IGG than IG, especially in the radiation era.

5.3 CMB anisotropies and matter power spectrum

In this section we present the results on the CMB power spectra and the matter power spectrum obtained from our extension of the CLASSig code to accomodate the IGG and BDG models. We start by comparing the various CMB spectra in the Galileon models and IG theory with the same potential, considering here only the case of the quartic and quadratic potentials. Then, we proceed with the analysis of the differences between IGG and BDG before comparing them with the ΛCDM predictions. Finally we consider the impact of Galileon terms on the matter power spectrum, showing how these scalar-tensor theories enhance it, producing also a larger peak with respect to the one predicted by ΛCDM.

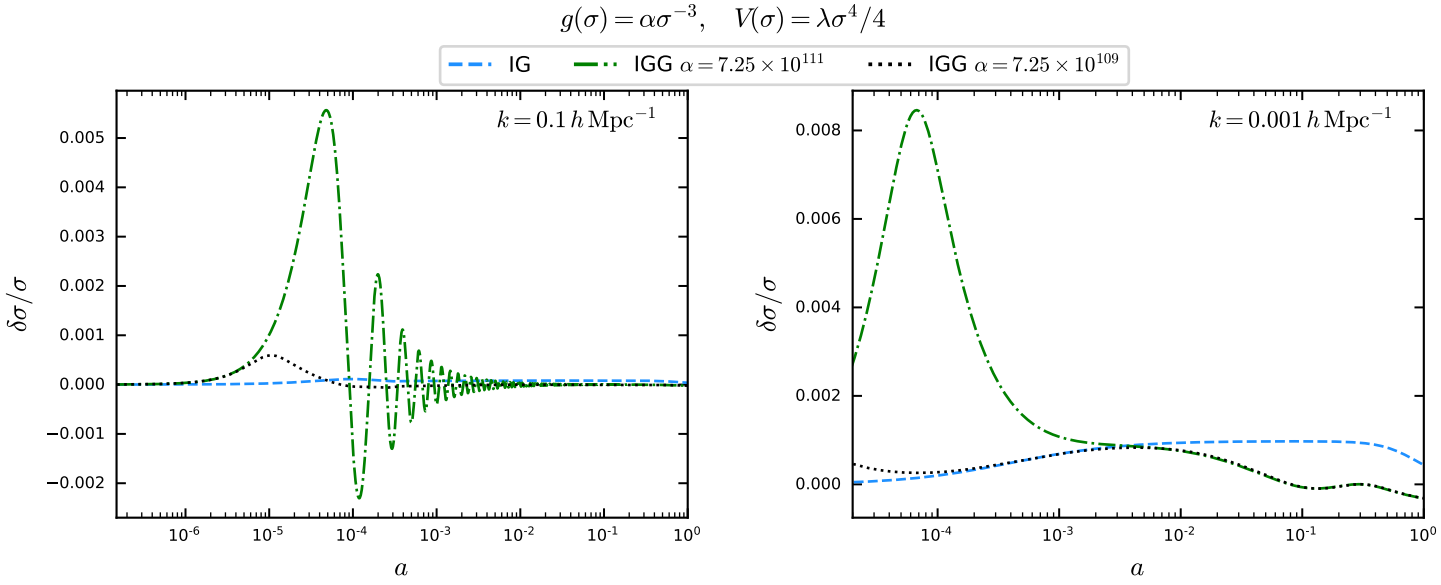

Figure 5.2: Relative scalar field perturbation $\delta\sigma/\sigma$ at the scales $k = 0.1\,h\,\mathrm{Mpc}^{-1}$ (left) and $k = 0.001\,h\,\mathrm{Mpc}^{-1}$ (right). The red solid line is the ΛCDM while the other lines represent IG and IGG models, both with a quartic potential and $\gamma = 5 \times 10^{-4}$. Two values of α are plotted: 7.5×10^{111} and 7.5×10^{109}.

CMB power spectra

In the left panels of figure 5.3 are shown the power spectra of the CMB temperature, E-mode polarization and their cross-correlation for the Induced gravity case with $\gamma = 5 \times 10^{-4}$ and the IGG model for the same value of γ and several values of the parameter α; in both theories we considered a quartic potential. On the right panels their relative differences are shown. In all cases, an enhancement of the peaks and the minima can be seen, and it's mostly visible for $\alpha = 7.5 \times 10^{111}$ where the relative difference with respect to IG reaches, at high multipoles, almost 10% for the C_ℓ^{TT} and the C_ℓ^{EE} spectra; in the latter a sensible difference (up to 7%) also arises at low multipoles. The relative differences in TE Cross correlations are more contained, around a maximum of 3% at high ℓ's. For smaller values of α, as we expected, the difference between the IG and the IGG model diminishes as a consequence that IGG converges to IG as α gets smaller.

In figure 5.5 we present, on the left, the power spectrum of the lensing potential ϕ and the lensing-temperature cross-correlation for IG and IGG for different values of α, while on the right the relative differences are shown. In the $C_\ell^{\phi\phi}$ power spectrum the differences with respect to IG are very small, reaching one part in a thousand across the entire spectrum only for $\alpha \sim 10^{109}$, and at high multipoles for $\alpha \sim 10^{107}$.

$$g(\sigma) = \alpha\sigma^{-3}, \quad V(\sigma) = \frac{\lambda}{4}\sigma^4$$

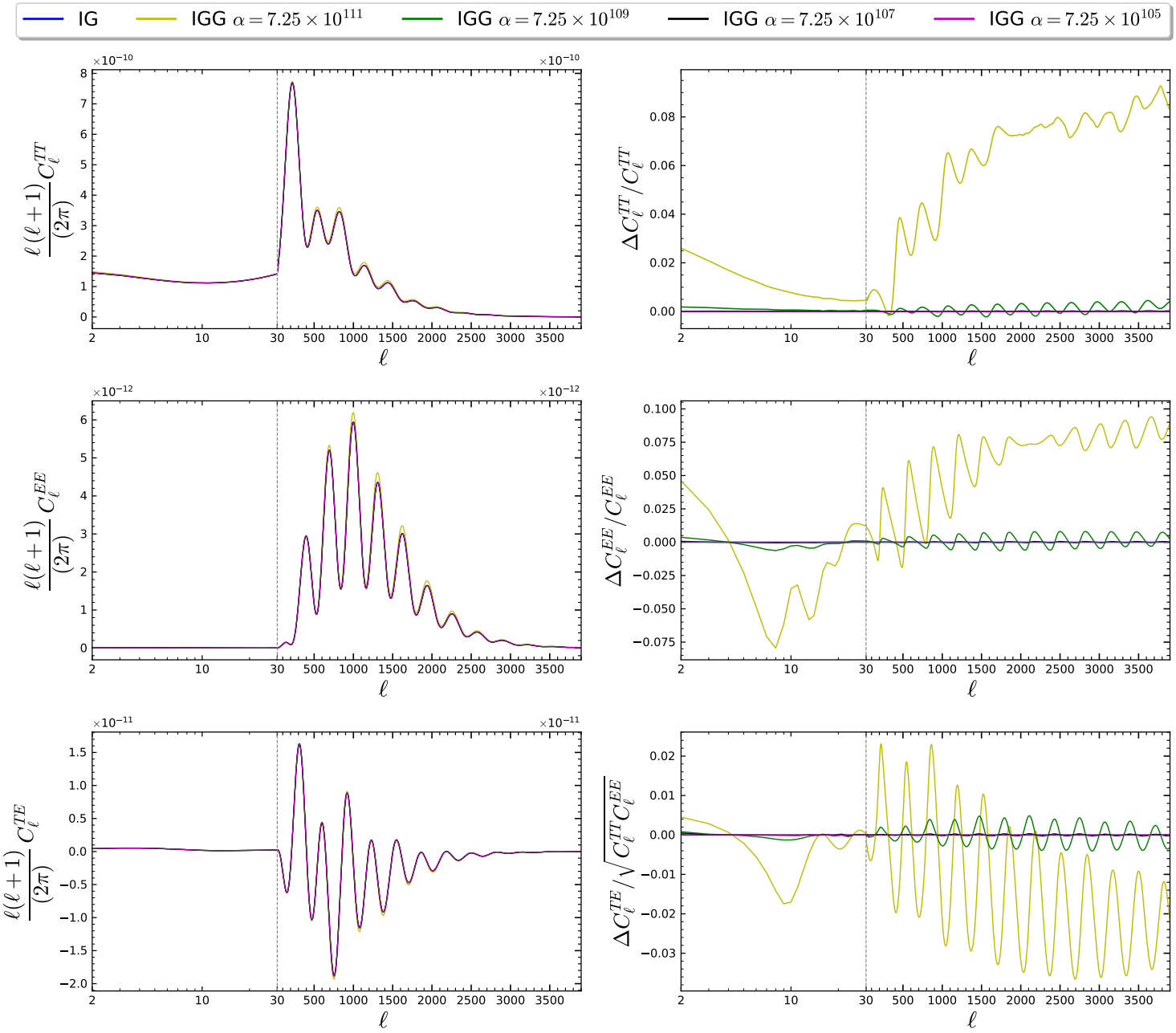

Figure 5.3: To the left, from the upper to the lower panel respectively, CMB TT, EE, TE power spectra for IG and IGG with a quartic potential, for $\gamma = 5 \times 10^{-4}$ and different values of α. In the right panels we show the relative differences between IGG and a reference IG model. We normalized ΔC_ℓ^{TE} to $\sqrt{C_\ell^{TT} C_\ell^{TE}}$.

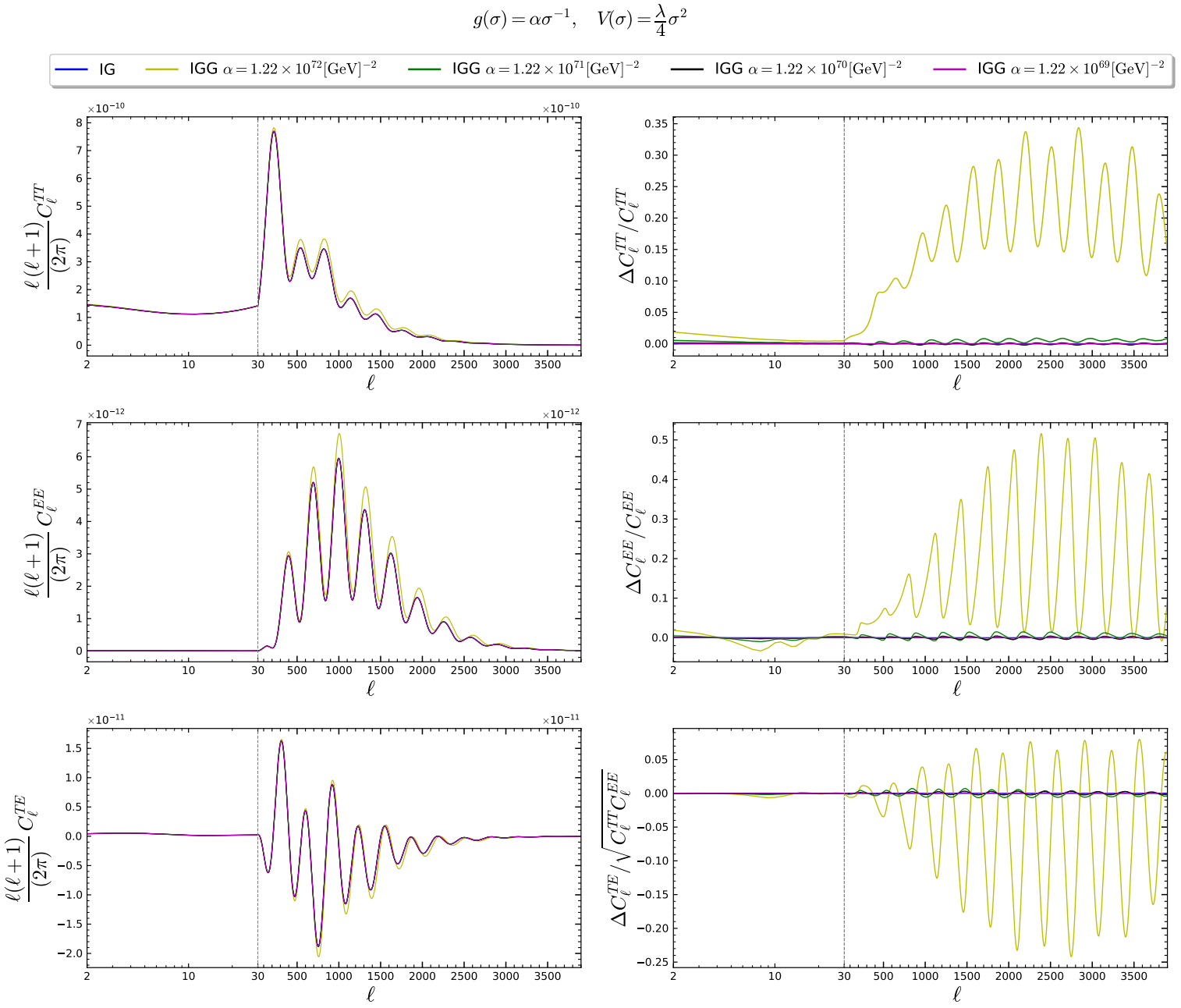

Figure 5.4: To the left, from the upper to the lower panel respectively, CMB TT, EE, TE power spectra for IG and IGG with a quadratic potential, for $\gamma = 5 \times 10^{-4}$ and different values of α. In the right panels we show the relative differences between IGG and a reference IG model. We normalized ΔC_ℓ^{TE} to $\sqrt{C_\ell^{TT} C_\ell^{TE}}$.

The lensing-temperature cross correlation in the same figure is more interesting since the differences between the models are already noticeable from the left panel, where it can be seen that the galileon term enhances and shifts the first peak at higher values of ℓ. While this is mostly visible for $\alpha = 7.5 \times 10^{109}$ a small effect is also noticeable for $\alpha = 7.5 \times 10^{107}$.

Figure 5.4 and 5.6 shows the TT, EE, TE, $\phi\phi$ and ϕT power spectra for IG and IGG with a quadratic potential. Qualitatively the analysis is similar to the quartic potential case but in this situation the relative differences between IG and IGG are less contained, especially for the largest value of the parameter $\alpha = 1.22 \times 10^{72}\,\mathrm{GeV}^{-2}$, where they reach 35% and 50% in the TT and EE power spectrum, respectively.

At this point we compare the two models extended with the Galileon-like interaction term, IGG and BDG. The result is that for all the values of α, BDG and IGG are almost equivalent in their predictions of the CMB power spectra and this is visible from figure (5.7) where the relative difference between the two models with a quartic potential is shown. Each BDG model is compared to a baseline IGG theory with the same value of α. The graph shows little to no difference in the TT, EE and TE spectra, in fact the most remarkable departure from the baseline is a relative difference in the C_ℓ^{EE}'s of around 0.001%, for $\alpha = 7.5 \times 10^{111}$. Also, the difference between the two models tends to zero as α gets smaller, that is to be expected because they both approach Induced Gravity in that limit.

Since BDG and IGG would be indistinguishable, in the next figures we only show IGG against a reference ΛCDM model.

In figure (5.8) the TT, EE and TE cross correlation spectra are shown for ΛCDM and IGG with a quartic potential, together with their relative differences. In the TT spectrum it can be seen that the power spectrum from the IGG model tends to stay above the ΛCDM one, especially for $\alpha = 7.5 \times 10^{111}$ where we observe relative differences up to 15% at high multipoles. While for smaller values of α these differences are reduced, we can still observe an enhancement of the TT spectrum in the IGG model at large ℓ's. In the EE power spectrum we see relative differences up to 20% for $\alpha = 7.5 \times 10^{111}$ and up to 10% for $\alpha = 7.5 \times 10^{109} - 7.5 \times 10^{107}$ at high multipoles. In the TE cross correlation spectrum differences are more contained reaching 10% for the largest value of α considered and 7% for the other two values of the parameter.

Figures 5.9 shows a comparison of the same power spectra between ΛCDM and IGG with a quadratic potential. Here, the analysis is qualitatively the same as the case of quartic potential: the spectra are overall enhanced and this is already visible from the left panels, especially for the case $\alpha = 1.22 \times 10^{72}[\mathrm{GeV}]^{-2}$ where the peaks are clearly more

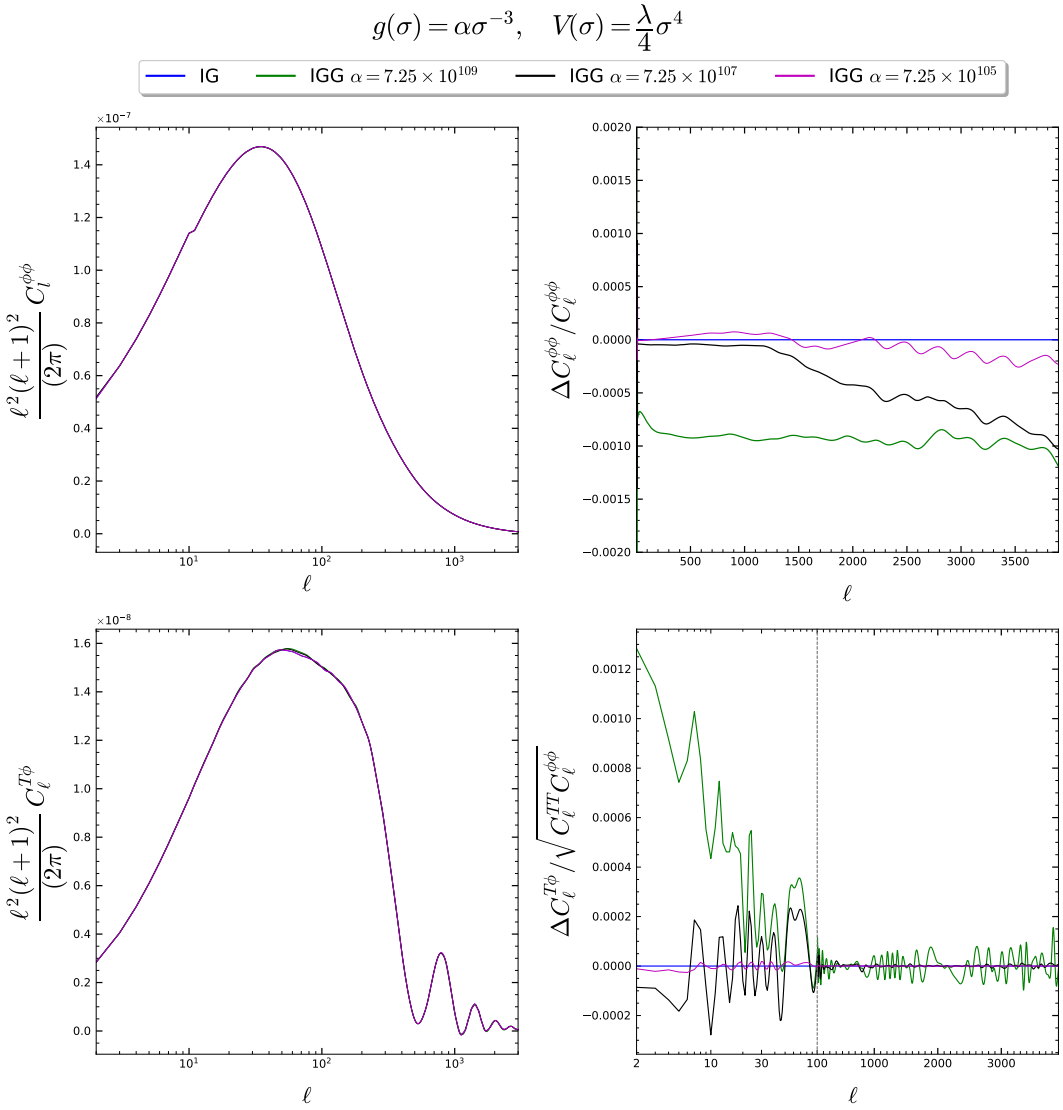

Figure 5.5: To the left, from the upper to the lower panel respectively, lensing potential and temperature-lensing cross-correlation power spectra for IG and IGG with a quartic potential for $\gamma = 5 \times 10^{-4}$ and different values of α. In the right panels we show the relative differences between IGG and a reference IG model. We normalized $\Delta C_\ell^{T\phi}$ to $\sqrt{C_\ell^{TT} C_\ell^{\phi\phi}}$.

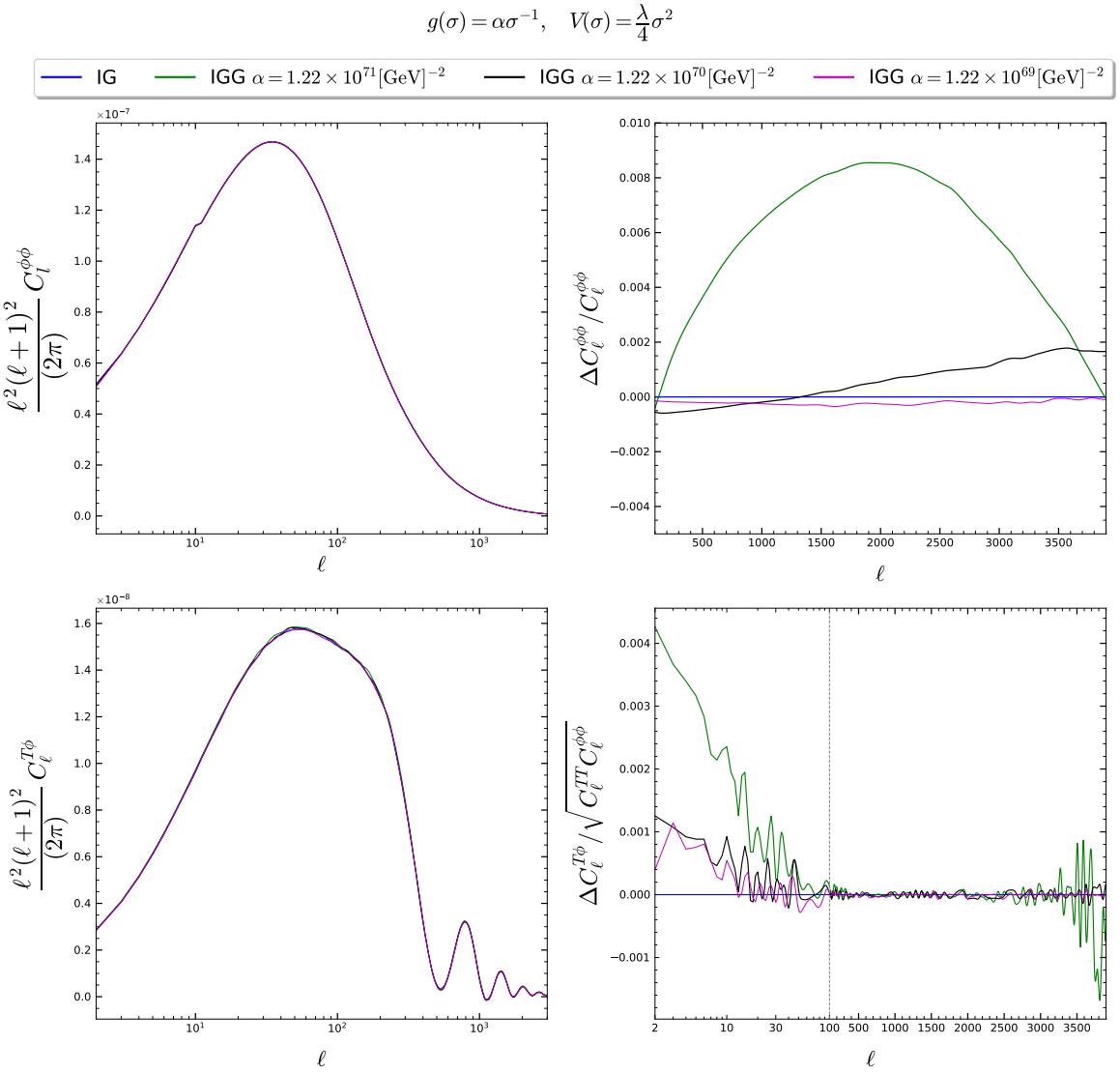

Figure 5.6: To the left, from the upper to the lower panel respectively, lensing potential and temperature-lensing cross-correlation power spectra for IG and IGG with a quadratic potential, for $\gamma = 5 \times 10^{-4}$ and different values of α. In the right panels we show the relative differences between IGG and a reference IG model. We normalized $\Delta C_\ell^{T\phi}$ to $\sqrt{C_\ell^{TT} C_\ell^{\phi\phi}}$.

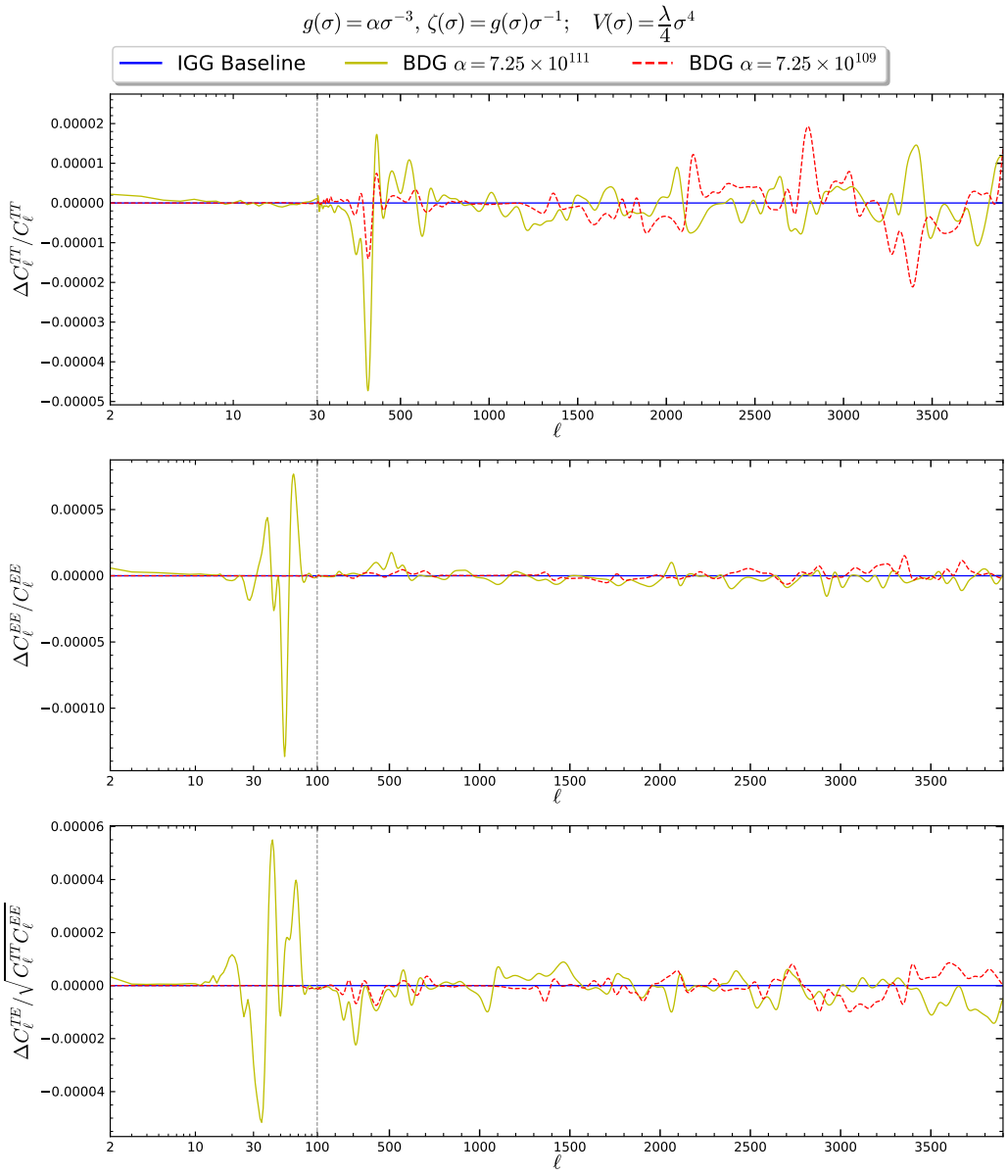

Figure 5.7: From top to bottom: relative differences in the TT, EE, TE CMB power spectra between BDG and reference IGG models with the same values of α. ΔC_ℓ^{TE} normalized to $\sqrt{C_\ell^{TT} C_\ell^{EE}}$.

pronounced than ΛCDM. Also, the relative differences are more significant compared to the quartic case, reaching 40% and 70% for this value of α, in the TT and EE spectrum, respectively.

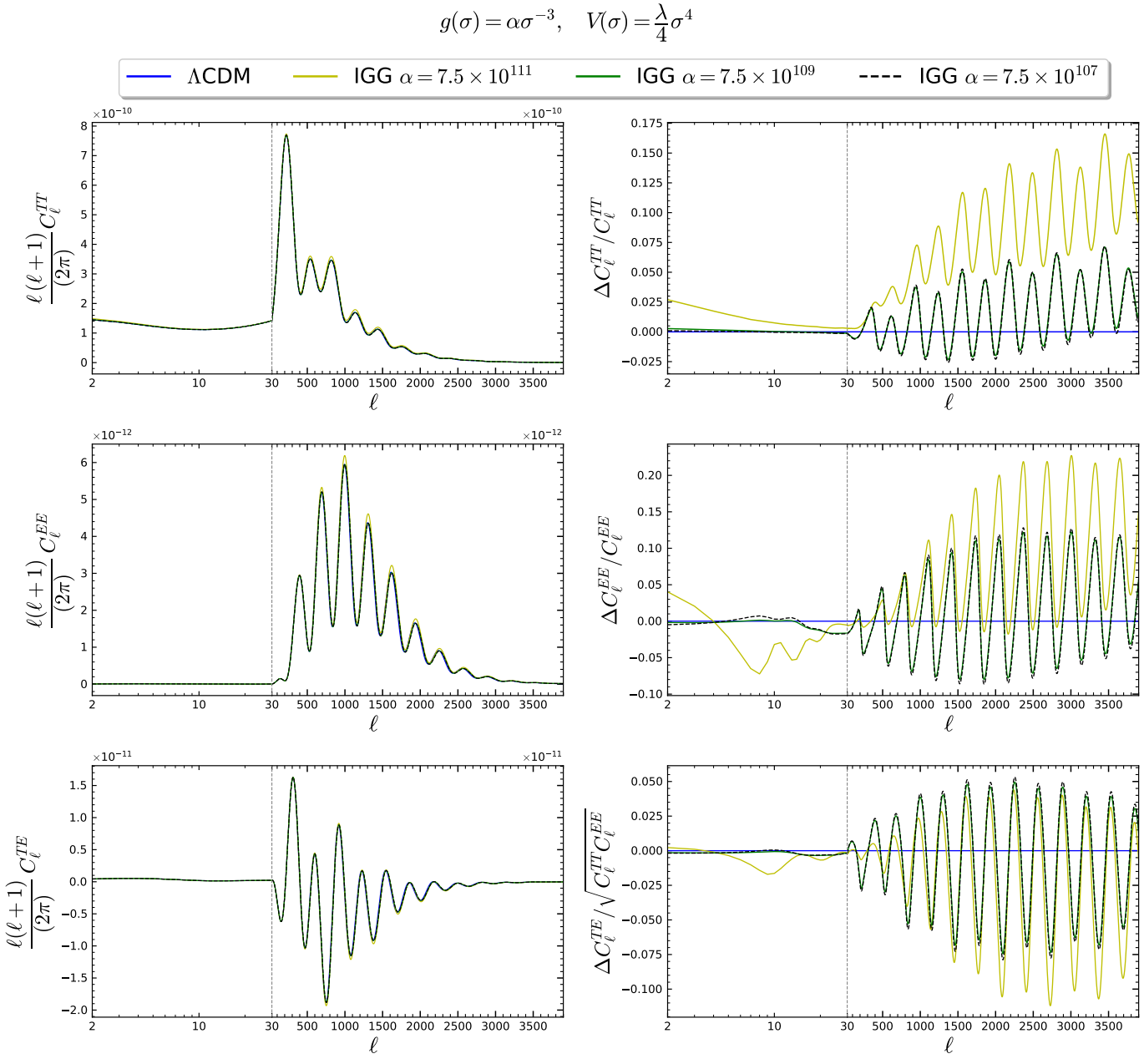

Figure 5.8: To the left, from the upper to the lower panel respectively, CMB TT, EE, TE power spectra for ΛCDM and IGG with a quartic potential for $\gamma = 5 \times 10^{-4}$ and different values of α. In the right panels we show the relative differences between IGG and a reference ΛCDM model. We normalized ΔC_ℓ^{TE} to $\sqrt{C_\ell^{TT} C_\ell^{TE}}$.

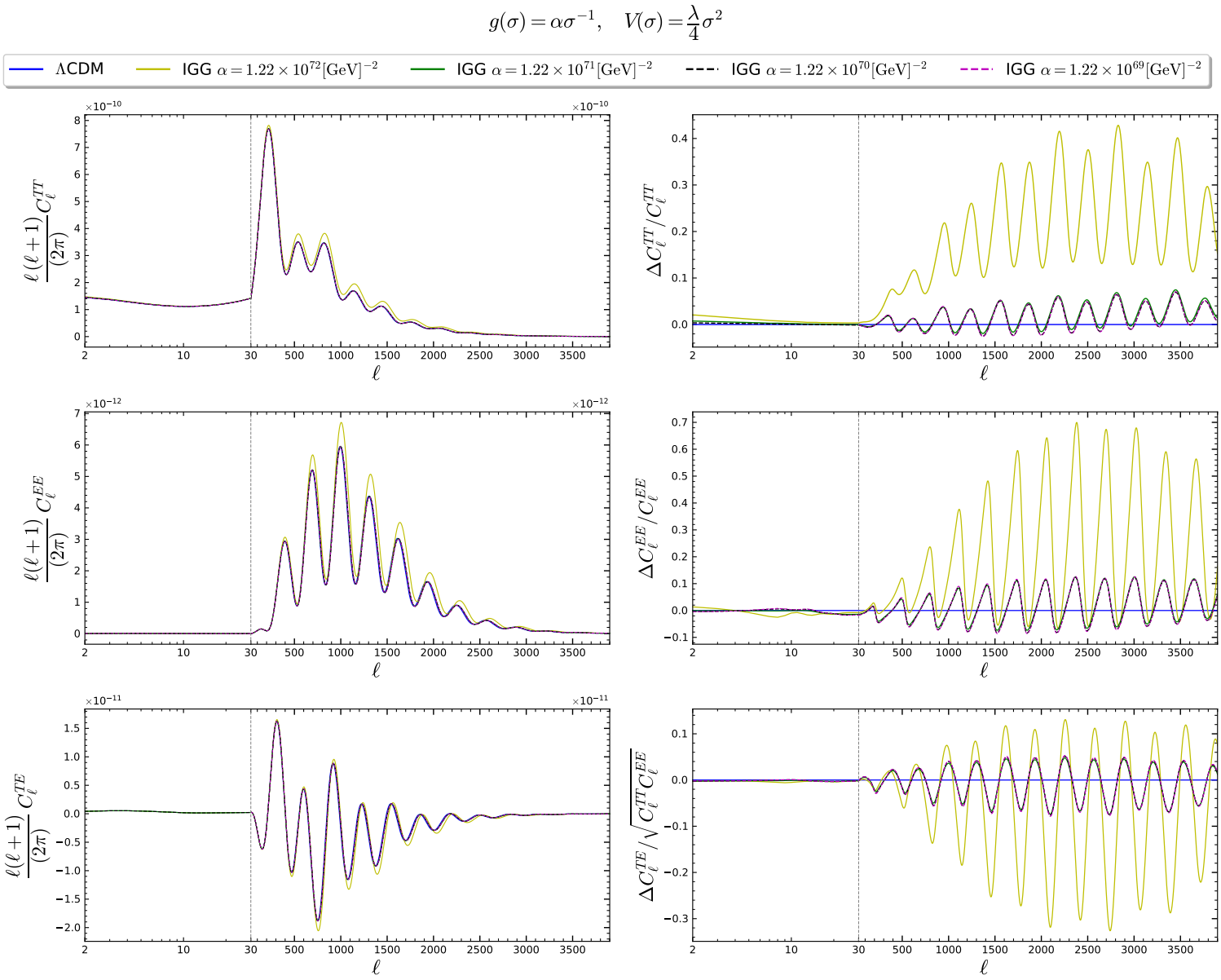

Figure 5.9: To the left, from the upper to the lower panel respectively, CMB TT, EE, TE power spectra for ΛCDM and IGG with a quadratic potential for $\gamma = 5 \times 10^{-4}$ and different values of α. In the right panels we show the relative differences between IGG and a reference ΛCDM model. We normalized ΔC_ℓ^{TE} to $\sqrt{C_\ell^{TT} C_\ell^{TE}}$.

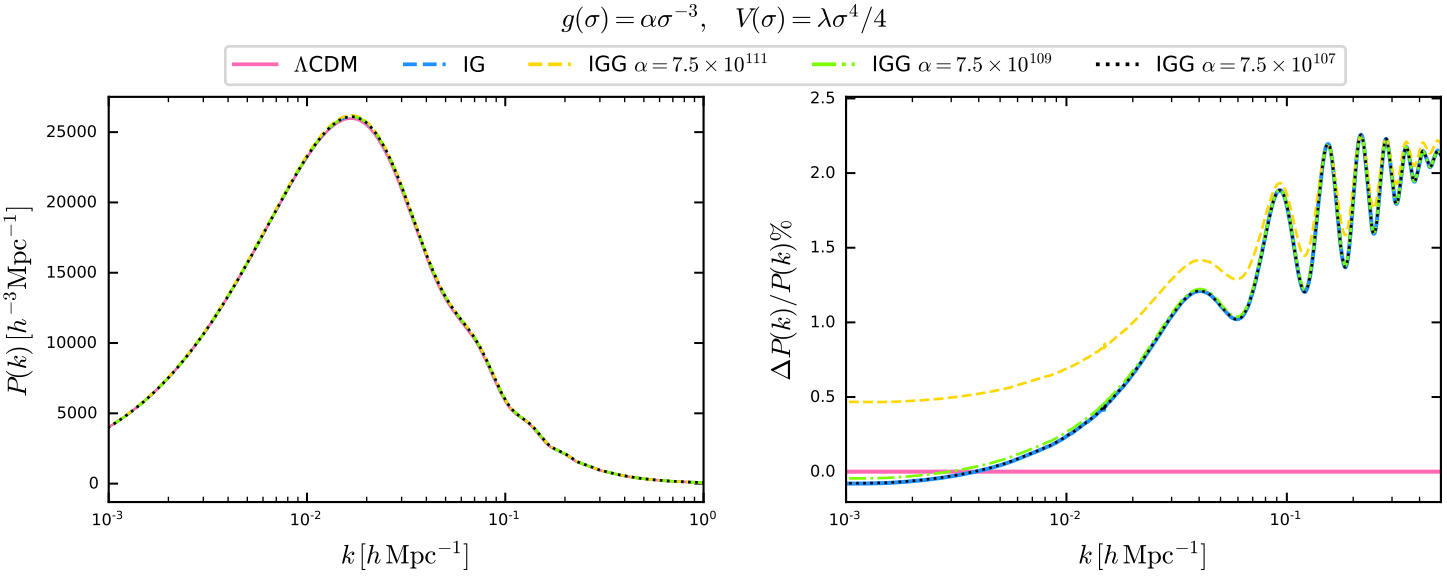

Figure 5.10: On the left the matter power spectra of ΛCDM (solid pink line), IG and IGG with $\gamma = 5 \times 10^{-4}$ and a quartic potential are plotted. On the right we show the relative differences between the modified gravity models and ΛCDM.

Matter power spectrum

The matter power spectrum is an important probe for cosmological parameters; its shape depends on the evolution of the perturbations, which in turn depend on gravity. We then expect some differences with respect to the ΛCDM model in theories of modified gravity, such as IG and IGG. Figure 5.10 and 5.11 show the linear matter power spectrum at $z = 0$ and the relative differences between the scalar-tensor models and ΛCDM. In fig. 5.10 IG and IGG models with a quartic potentials are plotted, while in fig.5.11 the same theories with a quadratic potential are shown against ΛCDM. We can see in both cases an enhancement of the peak in the modified gravity models, this enhancement is strongly dependent on the model, being the largest in the IGG models which depart more significantly from IG. The power spectrum at the smaller scales (higher values of k) is also enhanced in these models. The position of the peak is $\sim 1.65 \times 10^{-2}\,h\,\mathrm{Mpc}^{-1}$ for all considered cases. The Induced Gravity model produces a weak shift towards smaller scales while the IGG models with the same potential this shift is reduced.

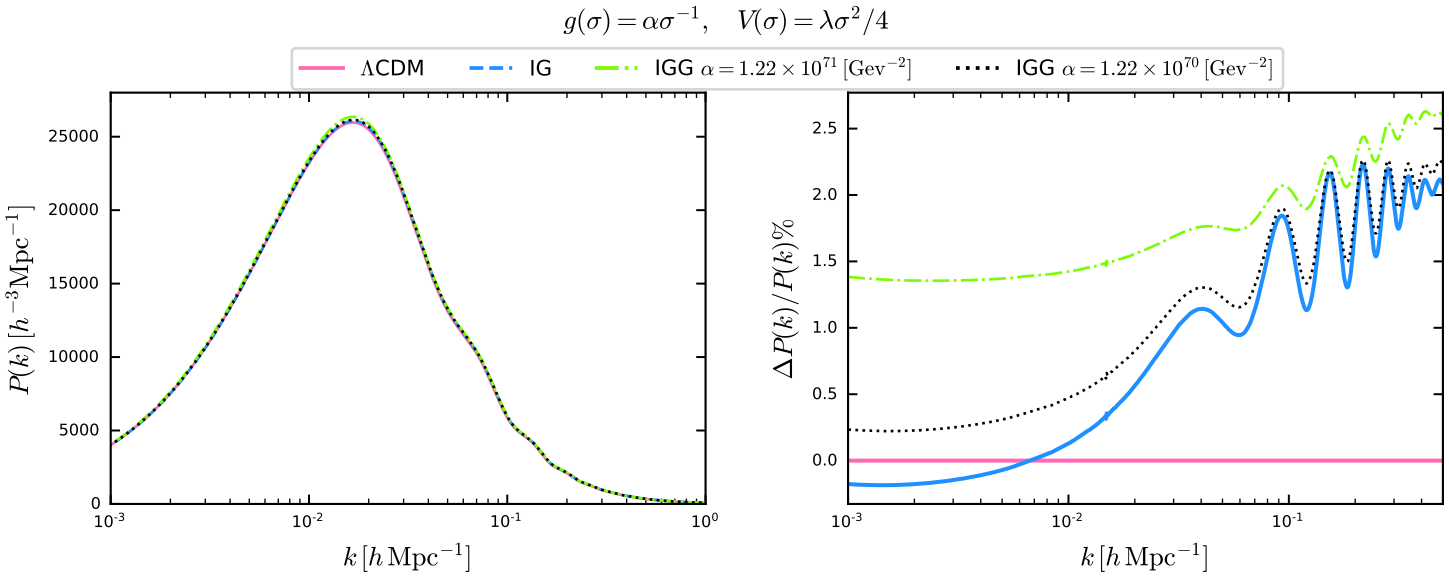

Figure 5.11: On the left the matter power spectra of ΛCDM (solid pink line), IG and IGG with $\gamma = 5 \times 10^{-4}$ and a quadratic potential are plotted. On the right we show the relative differences between the modified gravity models and ΛCDM.

Conclusions

The cosmic concordance ΛCDM model, which explains the accelerated expansion of our Universe by the cosmological constant, is a good fit to a host of cosmological observations. Nonetheless, the study of alternative cosmological models is blooming, driven also by some discordances arisen between different cosmological probes after the first Planck data release. Thanks to the increased precision of data in the coming years, these discordances might either be reconciled or confirm a cosmological model beyond ΛCDM.

Modified gravity, among which scalar tensor theories of gravity are one of the simplest examples, is an alternative to ΛCDM that has received a lot of attention. In these models the scalar field which mediates the gravitational interaction between matter and the metric can also be responsible for the late-time accelerated expansion of the Universe. The simplest scalar-tensor models of gravity are constrained by a host of cosmological and astrophysical measurements as well as by ground laboratory experiments. For example, for the extended Jordan-Brans-Dicke theory, the most recent cosmological constraints from Planck 2018 and a combination of baryonic Acoustic Oscillation (BAO) data from different galaxy surveys are $\gamma < 5.5 \times 10^{-4}$ [6] at 95 % confidence level (CL). These cosmological constraints depend weakly on the potential, but could be relaxed when the coupling to the Ricci scalar is extended from the quadratic form of the eJBD case to more complicated forms which also turn on the second post-Newtonian parameter $\beta_{\rm PN}$. When screening mechanism are absent, the tightest constraints come however within the Solar System: $\gamma_{\rm PN} - 1 = (2.1 \pm 2.3) \times 10^{-5}$ at 68% CL [7] and $\beta_{\rm PN} - 1 = (4.1 \pm 7.8) \times 10^{-5}$ at 68% CL [8].

Therefore, we studied an extension of these models that includes a cubic interaction term $(\partial\sigma)^2\Box\sigma$ in the Lagrangian of Induced Gravity or eJBD. This term is particularly interesting because it can give rise to the so called Vainsthein screening [9, 10], which, thanks to the presence of nonlinear second derivative terms in the equation of motion for the scalar field, allows to recover general relativity in the surrounding of local sources of matter. In fact these terms lead to the decoupling of the field from matter within a radius r_V commonly called the Vainshtein radius. Thus, this mechanism could help relaxing

the Solar System constraints and allow measurable deviations from GR at cosmological scales. Since it is sufficient to consider scalar fields with a non minimal coupling to the Ricci scalar by $F(\sigma) = N_{pl}^2 + \xi\sigma^2$ in order to have cosmological constraints at the level of those from the Solar System [11, 12], we restricted ourselves to the eJBD case $F(\sigma) = \gamma\sigma^2$ in an attempt to unlock cosmology from the Solar System.

We have implemented the cubic interaction term in both Induced gravity and eJBD because this term is not invariant under field redefinition. We have performed a full treatment of the model, from analytic derivation of the equations at the level of background and perturbations, an original derivation of a class of scaling solution in absence of matter (which should approximately describe the accelerated stage) and finally to the numerical implementation of the above equations in a dedicated Einstein Boltzmann code. This has required a dedicated extension of the Einstein-Boltzmann code CLASSig [13, 14].

We performed the numerical studies for various monomial forms of the potential $V(\sigma)$ and $g(\sigma)$, the function modulating the strenght of the Galileon-like cubic interaction, whose exponents are related as analitically found for the class of scaling solution. In particular we restricted ourselves to a quartic, quadratic and constant potential $V(\sigma)$ and to an initial zero velocity for the scalar field.

We used the extended Einstein-Boltzmann code to study the background cosmology and derive the predictions for the CMB anisotropies angular power spectra, both in temperature and in polarization and for the matter power spectrum. We also presented the evolution of the field's fluctuations as well as the evolution of the Bardeen potentials.

The main results in the study of the background cosmology are:

- An original derivation of a class of scaling solution in absence of matter that should approximately describe the accelerated stage of the Universe at late times.
- Numerical evolution of important background quantities such as the density parameters, where we show how the contribution of the field to the energy density becomes important at recent times although in some cases a non-negligible contribution was observed in the radiation era.
- The study of the behaviour of the effective parameter of state for dark energy, which, varying in time and following the dominant component during the evolution of the Universe, becomes negative in the recent epoch, approaching $w_{\rm DE} = -1$ and mimicking a dominant cosmological constant.

We shall now briefly describe the results obtained for the CMB anisotropies angular power spectra, and for the matter power spectrum. We compare these results with the corresponding ones in Induced Gravity without the Galileon term and ΛCDM.

The comparison with IG in the CMB power spectra showed some interesting features: an amplification of the peaks, both for the quartic and quadratic potential, in the TT, EE and TE power spectra. The TT and EE spectra were overall enhanced in the IGG model with respect to IG, especially at small scales, and alterations to these spectra were of the same order of magnitude.

We have also shown how the presence of the cubic interaction enhances the matter power spectrum, especially at the largest scales (small values of k). In IGG the peak of the matter power spectrum was more prominent with respect to IG.

The comparison between our Galileon models and ΛCDM showed an enhancement of the TT and EE power spectra in all the considered cases. We observe that the largest value of α analysed ($\alpha \simeq 7.25 \times 10^{111}$ and $\alpha \sim 10^{72}\,\mathrm{GeV}^{-2}$ for the quartic and quadratic case respectively) can produce deviations in C_ℓ's larger than 5% from ΛCDM bestfit, which are tipically larger than Planck 2018 errors. Better quantitative results will be obtained by a more complete MCMC exploration which allows to vary all the parameters of the model. The relative differences in the matter power spectrum were of $\sim 2\%$ at the smallest scales and in general the spectrum in the IGG model remained above the ΛCDM one. The peak of the spectrum, like in IG, was more prominent and slightly shifted towards higher values of k.

In general, the relative differences between IGG and ΛCDM tended to be larger than the ones between IG and ΛCDM across the entire spectrum.

Let us now discuss some future perspectives for this thesis, which already contains several original results leading at least to one publication.

The computation of the Vainsthein radius for the models we considered has not been carried out in this work, therefore it's still unclear whether or not the constraints given by cosmology on the parameters of the models are consistent with the ones necessary to obtain screening on the scales of the solar system. Thus we plan to compare the two in order to see if cosmologically allowed parameters guarantees effective screening around local sources. Moreover, it would be interesting to derive analytical initial conditions in the radiation era and an approximate analytic solution in the matter era for the background scalar field which can be verified against the numerical results found here. As a last remark, general and conservative constraints on the magnitude of the Galileon term, and the other parameters, could be obtained with the most recent data by a Markov chain Monte Carlo exploration as in [6, 14, 100] This methodology would allow to explore possible degeneracy of the additional Galileon term with other parameters and working assumptions of this thesis.

Riassunto in italiano

La costante cosmologica Λ non rappresenta l'unica possibilità per descrivere l'attuale espansione accelerata dell'Universo. Infatti, un'importante alternativa ad essa sono i modelli di gravità modificata: in molti di questi modelli l'energia oscura viene descritta modificando il settore gravitazionale della teoria. Una sottoclasse di queste teorie sono i modelli scalari tensoriali in cui, oltre alla metrica, è presente un campo scalare che modula l'interazione gravitazionale. I modelli scalari tensoriali più semplici, come per esempio la teoria di gravità indotta (IG), o equivalentemente un modello Jordan-Brans-Dicke esteso con un potenziale (eJBD), sono fortemente vincolati da osservazioni cosmologiche ed astrofisiche. Pertanto in questa tesi studiamo un' estensione di tali teorie con un termine di tipo Galileone $g(\sigma)(\, g^{\mu\nu}\partial_\mu\sigma\partial_\nu\sigma)\Box\sigma$ nella Lagrangiana. Questo termine è particolarmente interessante perché può dar luogo al cosidetto meccanismo di Vainsthein che permetterebbe alla teoria di ridursi alla Relatività Generale nelle vicinanze di sorgenti di materia, per distanze minori del cosiddetto raggio di Vainshtein, r_V. Le deviazioni dalla Relatività Generale rimarrebbero per distanze maggiori di r_V. Ci restringiamo a un termine di accoppiamento con lo scalare di Ricci del tipo $F(\sigma) = \gamma\sigma^2$, per il quale i vincoli derivanti dal Sistema Solare sono più stringenti di quelli cosmologici. Abbiamo dunque implementato il termine di interazione cubica sia in IG e nel modello eJBD, dato che tale termine non è invariante per ridefinizione del campo. Abbiamo studiato il modello sia dal punto di vista analitico che numerico, derivando le equazioni del moto omogenee e quelle per le perturbazioni lineari; per la cosmologia omogenea abbiamo ottenuto una classe di soluzioni analitiche in assenza di materia, ed infine implementato tutte le equazioni in un codice Einstein-Boltzmann dedicato. A tale scopo abbiamo esteso il codice Einstein-Boltzmann CLASSig [13, 14]. Lo studio numerico è stato svolto per le forme monomiali del potenziale $V(\sigma)$ e di $g(\sigma)$, l'ampiezza del termine di tipo Galileone, usate nello studio delle soluzioni analitiche del modello. In particolare ci siamo ristretti ad uno studio di un potenziale quartico, quadratico e costante. Nei capitoli 4 e 5 sono presentati i risultati ottenuti che qui riassumiamo brevemente. Abbiamo studiato il modello esteso col termine di Galileone sia a livello di cosmologia omogenea che di

perturbazioni lineari. Per quanto riguarda la cosmologia omogenea, oltre alla derivazione delle soluzioni analitiche sopracitate utili per l'espansione accelerata, abbiamo ottenuto l'evoluzione numerica del modello in cui si è visto come il contributo del campo alla densità di energia totale dell'Universo diventa importante solo in epoca recente, anche se in alcuni casi un contributo non trascurabile si osserva già nell'era della radiazione ed in prossimità dell'equivalenza tra materia e radiazione. In particolare abbiamo analizzato il parametro di stato $w_{\rm DE}$ che è definito come il rapporto tra pressione e densità effettive dell'energia oscura. L'evoluzione di tale parametro fa sì che questo approcci il valore di -1 in tempi recenti, mimando quindi una costante cosmologica.

L'implementazione del codice numerico per studiare la teoria a livello di perturbazioni lineari ha permesso di ottenere le previsioni del modello per quanto riguarda gli spettri di potenza angolare delle anisotropie del fondo cosmico a microonde (CMB), in temperatura, polarizzazione e *lensing*, e lo spettro di potenza tridimensionale della materia $P(k)$. Questo ci ha consentito di confrontare tali risultati con le analoghe predizioni in IG e nel modello cosmologico standard ΛCDM.

In generale, per quanto riguarda le anisotropie della CMB, il modello esteso col termine di Galileone (IGG) ha mostrato delle differenze rispetto sia ad IG che ΛCDM, soprattutto per quanto riguarda l'ampiezza dei picchi degli spettri di potenza angolare TT ed EE, che è maggiore nel modello esteso in tutti i casi considerati. Lo stesso discorso vale anche per lo spettro di potenza della materia il cui picco è più prominente in IGG rispetto a IG e ΛCDM, e la differenza relativa in tale spettro tra IGG e ΛCDM è, a piccole scale (grandi valori di k), simile a quella osservata tra IG e ΛCDM, mentre alle scale più grandi è maggior, soprattuto per valori di α che fanno discostare IGG maggiormente da IG. Tali valori del parametro ($\alpha \simeq 7.25 \times 10^{111}$ e $\alpha \sim 10^{72}\,\mathrm{GeV}^{-2}$ rispettivamente per il potenziale quartico e quadratico) possono produrre deviazioni nei C_ℓ maggiori del 5% rispetto al ΛCDM e quindi tipicamente maggiori degli errori sperimentali di Planck 2018[3]. Risultati più quantitativi a riguardo potrebbero essere ottenuti attraverso un' esplorazione MCMC che permette di variare i parametri del modello e che, insieme ai risultati originali ottenuti in questo lavoro dovrebbe portare ad almeno una pubblicazione.

Bibliography

[1] Planck Collaboration et al. "Planck 2018 results. I. Overview and the cosmological legacy of Planck". In: *arXiv e-prints*, arXiv:1807.06205 (July 2018), arXiv:1807.06205. arXiv: 1807.06205 [astro-ph.CO].

[2] J. G. de Swart, G. Bertone, and J. van Dongen. "How dark matter came to matter". In: *Nature Astronomy* 1, 0059 (Mar. 2017), p. 0059. DOI: 10.1038/s41550-017-0059. arXiv: 1703.00013 [astro-ph.CO].

[3] Planck Collaboration. "Planck 2018 results. VI. Cosmological parameters". In: *arXiv e-prints*, arXiv:1807.06209 (July 2018), arXiv:1807.06209. arXiv: 1807.06209 [astro-ph.CO].

[4] B. P. Abbott et al. "GW170817: Observation of Gravitational Waves from a Binary Neutron Star Inspiral". In: *Phys. Rev. Lett.* 119.16 (2017), p. 161101. DOI: 10.1103/PhysRevLett.119.161101. arXiv: 1710.05832 [gr-qc].

[5] B. P. Abbott et al. "Gravitational Waves and Gamma-rays from a Binary Neutron Star Merger: GW170817 and GRB 170817A". In: *Astrophys. J.* 848.2 (2017), p. L13. DOI: 10.3847/2041-8213/aa920c. arXiv: 1710.05834 [astro-ph.HE].

[6] M. Ballardini et al. "Scalar-tensor theories of gravity, neutrino physics, and the H_0 tension". In: *arXiv e-prints*, arXiv:2004.14349 (Apr. 2020), arXiv:2004.14349. arXiv: 2004.14349 [astro-ph.CO].

[7] B. Bertotti, L. Iess, and P. Tortora. "A test of general relativity using radio links with the Cassini spacecraft". In: Nature 425.6956 (Sept. 2003), pp. 374–376. DOI: 10.1038/nature01997.

[8] C. M. Will. "The Confrontation between General Relativity and Experiment". In: *Living Reviews in Relativity* 17.1 (June 2014). ISSN: 1433-8351. DOI: 10.12942/lrr-2014-4. URL: http://dx.doi.org/10.12942/lrr-2014-4.

[9] A. Vainshtein. "To the problem of nonvanishing gravitation mass". In: *Phys. Lett. B* 39 (1972), pp. 393–394. DOI: 10.1016/0370-2693(72)90147-5.

[10] N. Chow and J. Khoury. "Galileon cosmology". In: Phys. Rev. D 80.2, 024037 (July 2009), p. 024037. DOI: 10.1103/PhysRevD.80.024037. arXiv: 0905.1325 [hep-th].

[11] M. Rossi et al. "Cosmological constraints on post-Newtonian parameters in effectively massless scalar-tensor theories of gravity". In: *arXiv e-prints*, arXiv:1906.10218 (June 2019), arXiv:1906.10218. arXiv: 1906.10218 [astro-ph.CO].

[12] M. Braglia et al. "A larger value for H_0 by an evolving gravitational constant". In: *arXiv e-prints*, arXiv:2004.11161 (Apr. 2020), arXiv:2004.11161. arXiv: 2004.11161 [astro-ph.CO].

[13] C. Umiltà. "Cosmological predictions for a scalar tensor dark energy model by a dedicated Einstein-Boltzmann code". MA thesis. URL: http://amslaurea.unibo.it/6580/.

[14] C. Umiltà et al. "CMB and BAO constraints for an induced gravity dark energy model with a quartic potential". In: J. Cosmology Astropart. Phys. 2015.8, 017 (Aug. 2015), p. 017. DOI: 10.1088/1475-7516/2015/08/017. arXiv: 1507.00718 [astro-ph.CO].

[15] A. Friedmann. "Über die Krümmung des Raumes". In: *Zeitschrift für Physik A* 10 (1922), pp. 377–386.

[16] G. Lemaître. "Un Univers homogène de masse constante et de rayon croissant rendant compte de la vitesse radiale des nébuleuses extra-galactiques". In: *Annales de la Société; Scientifique de Bruxelles* 47 (Jan. 1927), pp. 49–59.

[17] H. P. Robertson. "Kinematics and World-Structure". In: ApJ 82 (Nov. 1935), p. 284. DOI: 10.1086/143681.

[18] H. P. Robertson. "Kinematics and World-Structure II." In: ApJ 83 (Apr. 1936), p. 187. DOI: 10.1086/143716.

[19] A. G. Walker. "On Milne's Theory of World-Structure". In: *Proceedings of the London Mathematical Society* 42 (Jan. 1937), pp. 90–127. DOI: 10.1112/plms/s2-42.1.90.

[20] E. Hubble. "A relation between distance and radial velocity among extra-galactic nebulae". In: *Proceedings of the National Academy of Sciences* 15.3 (1929), pp. 168–173. ISSN: 0027-8424. DOI: 10.1073/pnas.15.3.168. eprint: https://www.pnas.org/content/15/3/168.full.pdf. URL: https://www.pnas.org/content/15/3/168.

[21] R. H. Cyburt et al. "Big bang nucleosynthesis: Present status". In: *Rev. Mod. Phys.* 88 (1 2016), p. 015004. DOI: 10.1103/RevModPhys.88.015004. URL: https://link.aps.org/doi/10.1103/RevModPhys.88.015004.

[22] A. A. Penzias and R. W. Wilson. "A Measurement of Excess Antenna Temperature at 4080 Mc/s." In: ApJ 142 (July 1965), pp. 419–421. DOI: 10.1086/148307.

[23] G. Gamow. "Expanding Universe and the Origin of Elements". In: *Phys. Rev.* 70 (7-8 Oct. 1946), pp. 572–573. DOI: 10.1103/PhysRev.70.572.2. URL: https://link.aps.org/doi/10.1103/PhysRev.70.572.2.

[24] R. A. Alpher, H. Bethe, and G. Gamow. "The Origin of Chemical Elements". In: *Physical Review* 73.7 (Apr. 1948), pp. 803–804. DOI: 10.1103/PhysRev.73.803.

[25] G. Gamow. "The Origin of Elements and the Separation of Galaxies". In: *Physical Review* 74.4 (Aug. 1948), pp. 505–506. DOI: 10.1103/PhysRev.74.505.2.

[26] R. A. Alpher and R. Herman. "Evolution of the Universe". In: *Nature* 162.4124 (1948), pp. 774–775. ISSN: 14764687. DOI: 10.1038/162774b0. URL: https://doi.org/10.1038/162774b0.

[27] R. A. Alpher, R. Herman, and G. A. Gamow. "Thermonuclear Reactions in the Expanding Universe". In: *Phys. Rev.* 74 (9 Nov. 1948), pp. 1198–1199. DOI: 10.1103/PhysRev.74.1198.2. URL: https://link.aps.org/doi/10.1103/PhysRev.74.1198.2.

[28] G. Gamow. "On Relativistic Cosmogony". In: *Rev. Mod. Phys.* 21 (3 July 1949), pp. 367–373. DOI: 10.1103/RevModPhys.21.367. URL: https://link.aps.org/doi/10.1103/RevModPhys.21.367.

[29] R. A. Alpher. "A Neutron-Capture Theory of the Formation and Relative Abundance of the Elements". In: *Phys. Rev.* 74 (11 Dec. 1948), pp. 1577–1589. DOI: 10.1103/PhysRev.74.1577. URL: https://link.aps.org/doi/10.1103/PhysRev.74.1577.

[30] R. A. Alpher and R. C. Herman. "Remarks on the Evolution of the Expanding Universe". In: *Phys. Rev.* 75 (7 Apr. 1949), pp. 1089–1095. DOI: 10.1103/PhysRev.75.1089. URL: https://link.aps.org/doi/10.1103/PhysRev.75.1089.

[31] S. Perlmutter et al. "Measurements of Ω and Λ from 42 High-Redshift Supernovae". In: ApJ 517.2 (June 1999), pp. 565–586. DOI: 10.1086/307221. arXiv: astro-ph/9812133 [astro-ph].

[32] A. G. Riess et al. "Observational Evidence from Supernovae for an Accelerating Universe and a Cosmological Constant". In: *The Astronomical Journal* 116.3 (Sept. 1998), pp. 1009–1038. DOI: 10.1086/300499. URL: https://doi.org/10.1086%2F300499.

[33] A. Einstein. "The Foundation of the General Theory of Relativity". In: *Annalen Phys.* 49.7 (1916). [Annalen Phys.354,no.7,769(1916)], pp. 769–822. DOI: 10.1002/andp.200590044,10.1002/andp.19163540702.

[34] R. H. Cyburt et al. "Big bang nucleosynthesis: Present status". In: *Rev. Mod. Phys.* 88 (1 2016), p. 015004. DOI: 10.1103/RevModPhys.88.015004. URL: https://link.aps.org/doi/10.1103/RevModPhys.88.015004.

[35] S. Weinberg. *Gravitation and cosmology: principles and applications of the general theory of relativity*. Wiley, 1972. ISBN: 9780471925675. URL: https://books.google.fr/books?id=XLbvAAAAMAAJ.

[36] J. A. Wheeler and K. Ford. "Geons, Black Holes and Quantum Foam: A Life in Physics". In: *American Journal of Physics* 68.6 (2000), pp. 584–585. DOI: 10.1119/1.19497. eprint: https://doi.org/10.1119/1.19497. URL: https://doi.org/10.1119/1.19497.

[37] T. Padmanabhan. *Gravitation: Foundations and Frontiers*. Cambridge University Press, 2010. DOI: 10.1017/CBO9780511807787.

[38] R. D'Inverno and L. D'Inverno. *Introducing Einstein's Relativity*. Comparative Pathobiology - Studies in the Postmodern Theory of Education. Clarendon Press, 1992. ISBN: 9780198596868. URL: https://books.google.it/books?id=isdsCAAAQBAJ.

[39] A. G. Riess et al. "Large Magellanic Cloud Cepheid Standards Provide a 1% Foundation for the Determination of the Hubble Constant and Stronger Evidence for Physics beyond ΛCDM". In: *Astrophys. J.* 876.1 (2019), p. 85. DOI: 10.3847/1538-4357/ab1422. arXiv: 1903.07603 [astro-ph.CO].

[40] D. Baumann. *Cosmology*. 2012. URL: http://physics.bu.edu/~schmaltz/PY555/baumann_notes.pdf.

[41] A. M. Boesgaard and G. Steigman. "Big Bang Nucleosynthesis: Theories and Observations". In: *Annual Review of Astronomy and Astrophysics* 23.1 (1985), pp. 319–378. DOI: 10.1146/annurev.aa.23.090185.001535. eprint: https://doi.org/10.1146/annurev.aa.23.090185.001535. URL: https://doi.org/10.1146/annurev.aa.23.090185.001535.

[42] Planck Collaboration et al. "Planck 2018 results. X. Constraints on inflation". In: *arXiv e-prints*, arXiv:1807.06211 (July 2018), arXiv:1807.06211. arXiv: 1807.06211 [astro-ph.CO].

[43] S. Weinberg. *Cosmology*. Cosmology. OUP Oxford, 2008. ISBN: 9780191523601. URL: https://books.google.it/books?id=nqQZdg020fsC.

[44] A. Riotto. "Inflation and the Theory of Cosmological Perturbations". In: 2018. URL: https://inspirehep.net/record/1658978/files/riotto.pdf.

[45] V. Mukhanov. *Physical Foundations of Cosmology*. 2005. DOI: 10.2277/0521563984.

[46] A. A. Starobinsky. "Spectrum of relict gravitational radiation and the early state of the universe". In: *JETP Lett.* 30 (1979). [,767(1979)], pp. 682–685.

[47] A. A. Starobinsky. "A New Type of Isotropic Cosmological Models Without Singularity". In: *Phys. Lett.* 91B (1980). [,771(1980)], pp. 99–102. DOI: 10.1016/0370-2693(80)90670-X.

[48] D. Kazanas. "Dynamics of the universe and spontaneous symmetry breaking". In: ApJ 241 (Oct. 1980), pp. L59–L63. DOI: 10.1086/183361.

[49] K. Sato. "First-order phase transition of a vacuum and the expansion of the Universe". In: MNRAS 195 (May 1981), pp. 467–479. DOI: 10.1093/mnras/195.3.467.

[50] A. H. Guth. "Inflationary universe: A possible solution to the horizon and flatness problems". In: Phys. Rev. D 23.2 (Jan. 1981), pp. 347–356. DOI: 10.1103/PhysRevD.23.347.

[51] A. D. Linde. "A new inflationary universe scenario: A possible solution of the horizon, flatness, homogeneity, isotropy and primordial monopole problems". In: *Physics Letters B* 108.6 (Feb. 1982), pp. 389–393. DOI: 10.1016/0370-2693(82)91219-9.

[52] A. Linde. "Coleman-Weinberg theory and the new inflationary universe scenario". In: *Physics Letters B* 114.6 (1982), pp. 431 –435. ISSN: 0370-2693. DOI: https://doi.org/10.1016/0370-2693(82)90086-7. URL: http://www.sciencedirect.com/science/article/pii/0370269382900867.

[53] A. Albrecht and P. J. Steinhardt. "Cosmology for Grand Unified Theories with Radiatively Induced Symmetry Breaking". In: *Phys. Rev. Lett.* 48 (17 Apr. 1982), pp. 1220–1223. DOI: 10.1103/PhysRevLett.48.1220. URL: https://link.aps.org/doi/10.1103/PhysRevLett.48.1220.

[54] V. Mukhanov and S. Winitzki. *Introduction to Quantum Effects in Gravity*. Cambridge University Press, 2007. DOI: 10.1017/CBO9780511809149.

[55] F. Zwicky. "Die Rotverschiebung von extragalaktischen Nebeln". In: *Helvetica Physica Acta* 6 (Jan. 1933), pp. 110–127.

[56] G. Bertone and D. Hooper. "History of dark matter". In: *Rev. Mod. Phys.* 90.4 (2018), p. 045002. DOI: 10.1103/RevModPhys.90.045002. arXiv: 1605.04909 [astro-ph.CO].

[57] P. A. Oesch et al. "A Remarkably Luminous Galaxy at z=11.1 Measured with Hubble Space Telescope Grism Spectroscopy". In: ApJ 819.2, 129 (Mar. 2016), p. 129. DOI: 10.3847/0004-637X/819/2/129. arXiv: 1603.00461 [astro-ph.GA].

[58] S. Hawking. "Gravitationally collapsed objects of very low mass". In: MNRAS 152 (Jan. 1971), p. 75. DOI: 10.1093/mnras/152.1.75.

[59] P. Schneider. *Extragalactic Astronomy and Cosmology*. Berlin, Heidelberg: Springer Berlin Heidelberg, 2006. ISBN: 978-3-540-33174-2. DOI: 10.1007/978-3-540-33175-9. URL: http://dx.doi.org/10.1007/978-3-540-33175-9.

[60] R. D. Peccei and H. R. Quinn. "CP Conservation in the Presence of Pseudoparticles". In: *Phys. Rev. Lett.* 38 (25 June 1977), pp. 1440–1443. DOI: 10.1103/PhysRevLett.38.1440. URL: https://link.aps.org/doi/10.1103/PhysRevLett.38.1440.

[61] A. Einstein. "Kosmologische Betrachtungen zur allgemeinen Relativitätstheorie". In: *Sitzungsberichte der Königlich Preußischen Akademie der Wissenschaften (Berlin* (Jan. 1917), pp. 142–152.

[62] G. Lemaitre. "Evolution of the Expanding Universe". In: *Proceedings of the National Academy of Sciences* 20.1 (1934), pp. 12–17. ISSN: 0027-8424. DOI: 10.1073/pnas.20.1.12. eprint: https://www.pnas.org/content/20/1/12.full.pdf. URL: https://www.pnas.org/content/20/1/12.

[63] E. A. S. "The cosmological controversy". In: *Science Progress* 34 (1939), pp. 225–236.

[64] Y. B. Zeldovich. "Cosmological Constant and Elementary Particles". In: *JETP Lett.* 6 (1967). [Pisma Zh. Eksp. Teor. Fiz.6,883(1967)], p. 316.

[65] P. J. E. Peebles and B. Ratra. "Cosmology with a Time-Variable Cosmological "Constant"". In: ApJ 325 (Feb. 1988), p. L17. DOI: 10.1086/185100.

[66] P. J. Peebles and B. Ratra. "The cosmological constant and dark energy". In: *Reviews of Modern Physics* 75.2 (Apr. 2003), pp. 559–606. DOI: 10.1103/RevModPhys.75.559. arXiv: astro-ph/0207347 [astro-ph].

[67] S. Tsujikawa. "Quintessence: a review". In: *Classical and Quantum Gravity* 30.21 (Oct. 2013), p. 214003. DOI: 10.1088/0264-9381/30/21/214003. URL: https://doi.org/10.1088%2F0264-9381%2F30%2F21%2F214003.

[68] I. Zlatev, L. Wang, and P. J. Steinhardt. "Quintessence, Cosmic Coincidence, and the Cosmological Constant". In: *Phys. Rev. Lett.* 82 (5 Feb. 1999), pp. 896–899. DOI: 10.1103/PhysRevLett.82.896. URL: https://link.aps.org/doi/10.1103/PhysRevLett.82.896.

[69] C.-P. Ma and E. Bertschinger. "Cosmological Perturbation Theory in the Synchronous and Conformal Newtonian Gauges". In: ApJ 455 (Dec. 1995), p. 7. DOI: 10.1086/176550. arXiv: astro-ph/9506072 [astro-ph].

[70] S. Dodelson. *Modern Cosmology*. Amsterdam: Academic Press, 2003. ISBN: 9780122191411. URL: http://www.slac.stanford.edu/spires/find/books/www?cl=QB981:D62:2003.

[71] J. M. Bardeen. "Gauge-invariant cosmological perturbations". In: Phys. Rev. D 22.8 (Oct. 1980), pp. 1882–1905. DOI: 10.1103/PhysRevD.22.1882.

[72] J. R. Bond and A. S. Szalay. "The collisionless damping of density fluctuations in an expanding universe". In: ApJ 274 (Nov. 1983), pp. 443–468. DOI: 10.1086/161460.

[73] M. Bucher, K. Moodley, and N. Turok. "General primordial cosmic perturbation". In: Phys. Rev. D 62.8, 083508 (Oct. 2000), p. 083508. DOI: 10.1103/PhysRevD.62.083508. arXiv: astro-ph/9904231 [astro-ph].

[74] A. R. Liddle and D. H. Lyth. *Cosmological Inflation and Large-Scale Structure*. Cambridge University Press, 2000. DOI: 10.1017/CBO9781139175180.

[75] H. Kurki-Suonio. *Cosmological Perturbation Theory, part 1*. Lecture notes for a course on cosmological perturbation theory given at the University of Helsinki. 2015.

[76] D. J. Fixsen. "The Temperature of the Cosmic Microwave Background". In: ApJ 707.2 (Dec. 2009), pp. 916–920. DOI: 10.1088/0004-637X/707/2/916. arXiv: 0911.1955 [astro-ph.CO].

[77] R. K. Sachs and A. M. Wolfe. "Perturbations of a Cosmological Model and Angular Variations of the Microwave Background". In: ApJ 147 (Jan. 1967), p. 73. DOI: 10.1086/148982.

[78] G. Nordström. "Zur Theorie der Gravitation vom Standpunkt des Relativitätsprinzips". In: *Annalen der Physik* 347.13 (1913), pp. 533–554. DOI: 10.1002/andp.19133471303. eprint: https://onlinelibrary.wiley.com/doi/pdf/10.1002/andp.19133471303. URL: https://onlinelibrary.wiley.com/doi/abs/10.1002/andp.19133471303.

[79] Y. Fujii and K. Maeda. *The scalar-tensor theory of gravitation*. Cambridge Monographs on Mathematical Physics. Cambridge University Press, 2007. ISBN: 9780521037525, 9780521811590, 9780511029882. DOI: 10.1017/CBO9780511535093. URL: http://www.cambridge.org/uk/catalogue/catalogue.asp?isbn=0521811597.

[80] P. Jordan. "Schwerkraft und Weltall: Grundlagen der theoretischen Kos- mologie". In: *Die Wissenschaft. F. Vieweg* (1955).

[81] C. Brans and R. H. Dicke. "Mach's Principle and a Relativistic Theory of Gravitation". In: *Phys. Rev.* 124 (3 Nov. 1961), pp. 925–935. DOI: 10.1103/PhysRev.124.925. URL: https://link.aps.org/doi/10.1103/PhysRev.124.925.

[82] P. A. M. Dirac. "A New Basis for Cosmology". In: *Proceedings of the Royal Society of London Series A* 165.921 (Apr. 1938), pp. 199–208. DOI: 10.1098/rspa.1938.0053.

[83] G. W. Horndeski. "Second-order scalar-tensor field equations in a four-dimensional space". In: *Int. J. Theor. Phys.* 10 (1974), pp. 363–384. DOI: 10.1007/BF01807638.

[84] R. P. Woodard. "The Theorem of Ostrogradsky". In: *arXiv e-prints*, arXiv:1506.02210 (June 2015), arXiv:1506.02210. arXiv: 1506.02210 [hep-th].

[85] T. Kobayashi, M. Yamaguchi, and J. Yokoyama. "Generalized G-Inflation — Inflation with the Most General Second-Order Field Equations —". In: *Progress of Theoretical Physics* 126.3 (Sept. 2011), pp. 511–529. DOI: 10.1143/PTP.126.511. arXiv: 1105.5723 [hep-th].

[86] C. Armendáriz-Picón, T. Damour, and V. Mukhanov. "k-Inflation". In: *Physics Letters B* 458.2-3 (July 1999), 209–218. ISSN: 0370-2693. DOI: 10.1016/s0370-2693(99)00603-6. URL: http://dx.doi.org/10.1016/S0370-2693(99)00603-6.

[87] T. Chiba, T. Okabe, and M. Yamaguchi. "Kinetically driven quintessence". In: *Physical Review D* 62.2 (June 2000). ISSN: 1089-4918. DOI: 10.1103/physrevd.62.023511. URL: http://dx.doi.org/10.1103/PhysRevD.62.023511.

[88] C. Armendariz-Picon, V. Mukhanov, and P. J. Steinhardt. "Dynamical Solution to the Problem of a Small Cosmological Constant and Late-Time Cosmic Acceleration". In: Phys. Rev. Lett. 85.21 (Nov. 2000), pp. 4438–4441. DOI: 10.1103/PhysRevLett.85.4438. arXiv: astro-ph/0004134 [astro-ph].

[89] C. Armendariz-Picon, V. Mukhanov, and P. J. Steinhardt. "Essentials of k-essence". In: Phys. Rev. D 63.10, 103510 (May 2001), p. 103510. DOI: 10.1103/PhysRevD.63.103510. arXiv: astro-ph/0006373 [astro-ph].

[90] M. Gasperini and G. Veneziano. "Pre-big-bang in string cosmology". In: *Astroparticle Physics* 1.3 (July 1993), pp. 317–339. DOI: 10.1016/0927-6505(93)90017-8. arXiv: hep-th/9211021 [hep-th].

[91] T. Damour and K. Nordtvedt. "Tensor - scalar cosmological models and their relaxation toward general relativity". In: *Phys. Rev. D* 48 (1993), pp. 3436–3450. DOI: 10.1103/PhysRevD.48.3436.

[92] T. Damour and A. M. Polyakov. "The string dilation and a least coupling principle". In: *Nuclear Physics B* 423.2-3 (July 1994), pp. 532–558. DOI: 10.1016/0550-3213(94)90143-0. arXiv: hep-th/9401069 [hep-th].

[93] L. Amendola. "Scaling solutions in general nonminimal coupling theories". In: Phys. Rev. D 60.4, 043501 (Aug. 1999), p. 043501. DOI: 10.1103/PhysRevD.60.043501. arXiv: astro-ph/9904120 [astro-ph].

[94] T. Chiba. "Quintessence, the gravitational constant, and gravity". In: Phys. Rev. D 60.8, 083508 (Oct. 1999), p. 083508. DOI: 10.1103/PhysRevD.60.083508. arXiv: gr-qc/9903094 [gr-qc].

[95] F. Perrotta, C. Baccigalupi, and S. Matarrese. "Extended quintessence". In: Phys. Rev. D 61.2, 023507 (Jan. 2000), p. 023507. DOI: 10.1103/PhysRevD.61.023507. arXiv: astro-ph/9906066 [astro-ph].

[96] B. Boisseau et al. "Reconstruction of a Scalar-Tensor Theory of Gravity in an Accelerating Universe". In: Phys. Rev. Lett. 85.11 (Sept. 2000), pp. 2236–2239. DOI: 10.1103/PhysRevLett.85.2236. arXiv: gr-qc/0001066 [gr-qc].

[97] A. D. Sakharov. "Vacuum quantum fluctuations in curved space and the theory of gravitation". In: *Sov. Phys. Dokl.* 12 (1968). [Dokl. Akad. Nauk Ser. Fiz.177,70(1967); Sov. Phys. Usp.34,no.5,394(1991); Gen. Rel. Grav.32,365(2000); Usp. Fiz. Nauk161,no.5,64(1991),51(1967)], pp. 1040–1041.

[98] A. Zee. "Broken-Symmetric Theory of Gravity". In: *Phys. Rev. Lett.* 42 (7 Feb. 1979), pp. 417–421. DOI: 10.1103/PhysRevLett.42.417. URL: https://link.aps.org/doi/10.1103/PhysRevLett.42.417.

[99] S. L. Adler. "Einstein gravity as a symmetry-breaking effect in quantum field theory". In: *Rev. Mod. Phys.* 54 (3 July 1982), pp. 729–766. DOI: 10.1103/RevModPhys.54.729. URL: https://link.aps.org/doi/10.1103/RevModPhys.54.729.

[100] M. Ballardini et al. "Cosmological constraints on induced gravity dark energy models". In: *Journal of Cosmology and Astroparticle Physics* 2016.5, 067 (May 2016), p. 067. DOI: 10.1088/1475-7516/2016/05/067. arXiv: 1601.03387 [astro-ph.CO].

[101] F. Finelli, A. Tronconi, and G. Venturi. "Dark energy, induced gravity and broken scale invariance". In: *Physics Letters B* 659.3 (Jan. 2008), pp. 466–470. DOI: 10.1016/j.physletb.2007.11.053. arXiv: 0710.2741 [astro-ph].

[102] A. Cerioni et al. "Inflation and reheating in induced gravity". In: *Physics Letters B* 681.5 (Nov. 2009), pp. 383–386. DOI: 10.1016/j.physletb.2009.10.066. arXiv: 0906.1902 [astro-ph.CO].

[103] D. Paoletti et al. "Isocurvature fluctuations in the effective Newton's constant". In: *Physics of the Dark Universe* 25, 100307 (Sept. 2019), p. 100307. DOI: 10.1016/j.dark.2019.100307. arXiv: 1809.03201 [astro-ph.CO].

[104] A. Nicolis, R. Rattazzi, and E. Trincherini. "Galileon as a local modification of gravity". In: *Physical Review D* 79.6 (Mar. 2009). ISSN: 1550-2368. DOI: 10.1103/physrevd.79.064036. URL: http://dx.doi.org/10.1103/PhysRevD.79.064036.

[105] C. Deffayet, G. Esposito-Farèse, and A. Vikman. "Covariant Galileon". In: Phys. Rev. D 79.8, 084003 (Apr. 2009), p. 084003. DOI: 10.1103/PhysRevD.79.084003. arXiv: 0901.1314 [hep-th].

[106] A. de Felice and S. Tsujikawa. "Cosmology of a Covariant Galileon Field". In: Phys. Rev. Lett. 105.11, 111301 (Sept. 2010), p. 111301. DOI: 10.1103/PhysRevLett.105.111301. arXiv: 1007.2700 [astro-ph.CO].

[107] A. de Felice and S. Tsujikawa. "Generalized Galileon cosmology". In: Phys. Rev. D 84.12, 124029 (Dec. 2011), p. 124029. DOI: 10.1103/PhysRevD.84.124029. arXiv: 1008.4236 [hep-th].

[108] C. Deffayet et al. "Imperfect dark energy from kinetic gravity braiding". In: *Journal of Cosmology and Astroparticle Physics* 2010.10 (Oct. 2010), 026–026. ISSN: 1475-7516. DOI: 10.1088/1475-7516/2010/10/026. URL: http://dx.doi.org/10.1088/1475-7516/2010/10/026.

[109] O. Pujolàs, I. Sawicki, and A. Vikman. "The imperfect fluid behind kinetic gravity braiding". In: *Journal of High Energy Physics* 2011.11 (Nov. 2011). ISSN: 1029-8479. DOI: 10.1007/jhep11(2011)156. URL: http://dx.doi.org/10.1007/JHEP11(2011)156.

[110] F. P. Silva and K. Koyama. "Self-accelerating universe in Galileon cosmology". In: Phys. Rev. D 80.12, 121301 (Dec. 2009), p. 121301. DOI: 10.1103/PhysRevD.80.121301. arXiv: 0909.4538 [astro-ph.CO].

[111] I. Quiros. "Selected topics in scalar-tensor theories and beyond". In: *International Journal of Modern Physics D* 28.7, 1930012-156 (Jan. 2019), pp. 1930012–156. DOI: 10.1142/S021827181930012X. arXiv: 1901.08690 [gr-qc].

[112] R. Kase and S. Tsujikawa. "Dark energy in Horndeski theories after GW170817: A review". In: *International Journal of Modern Physics D* 28.5, 1942005 (Jan. 2019), p. 1942005. DOI: 10.1142/S0218271819420057. arXiv: 1809.08735 [gr-qc].

[113] A. Goldstein et al. "An Ordinary Short Gamma-Ray Burst with Extraordinary Implications: Fermi-GBM Detection of GRB 170817A". In: *Astrophys. J.* 848.2 (2017), p. L14. DOI: 10.3847/2041-8213/aa8f41. arXiv: 1710.05446 [astro-ph.HE].

[114] T. Kobayashi, M. Yamaguchi, and J. Yokoyama. "Inflation Driven by the Galileon Field". In: Phys. Rev. Lett. 105.23, 231302 (Dec. 2010), p. 231302. DOI: 10.1103/PhysRevLett.105.231302. arXiv: 1008.0603 [hep-th].

[115] S. Capozziello, R. de Ritis, and A. A. Marino. "Some aspects of the cosmological conformal equivalence between the 'Jordan frame' and the 'Einstein frame'". In: *Classical and Quantum Gravity* 14.12 (Dec. 1997), pp. 3243–3258. DOI: 10.1088/0264-9381/14/12/010. arXiv: gr-qc/9612053 [gr-qc].

[116] V. Faraoni and E. Gunzig. "Einstein frame or Jordan frame ?" In: *arXiv e-prints*, astro-ph/9910176 (Oct. 1999), astro–ph/9910176. arXiv: astro-ph/9910176 [astro-ph].

[117] J. Khoury and A. Weltman. "Chameleon Fields: Awaiting Surprises for Tests of Gravity in Space". In: Phys. Rev. Lett. 93.17, 171104 (Oct. 2004), p. 171104. DOI: 10.1103/PhysRevLett.93.171104. arXiv: astro-ph/0309300 [astro-ph].

[118] J. Khoury and A. Weltman. "Chameleon cosmology". In: Phys. Rev. D 69.4, 044026 (Feb. 2004), p. 044026. DOI: 10.1103/PhysRevD.69.044026. arXiv: astro-ph/0309411 [astro-ph].

[119] K. Hinterbichler and J. Khoury. "Screening Long-Range Forces through Local Symmetry Restoration". In: Phys. Rev. Lett. 104.23, 231301 (June 2010), p. 231301. DOI: 10.1103/PhysRevLett.104.231301. arXiv: 1001.4525 [hep-th].

[120] K. Hinterbichler et al. "Symmetron cosmology". In: Phys. Rev. D 84.10, 103521 (Nov. 2011), p. 103521. DOI: 10.1103/PhysRevD.84.103521. arXiv: 1107.2112 [astro-ph.CO].

[121] E. Babichev, C. Deffayet, and R. Ziour. "k-MOUFLAGE Gravity". In: *International Journal of Modern Physics D* 18.14 (Jan. 2009), pp. 2147–2154. DOI: 10.1142/S0218271809016107. arXiv: 0905.2943 [hep-th].

[122] H. Wei and R.-G. Cai. "K-chameleon and the coincidence problem". In: *Phys. Rev. D* 71 (2005), p. 043504. DOI: 10.1103/PhysRevD.71.043504. arXiv: hep-th/0412045.

[123] V. Faraoni. "Scalar field mass in generalized gravity". In: *Classical and Quantum Gravity* 26.14, 145014 (July 2009), p. 145014. DOI: 10.1088/0264-9381/26/14/145014. arXiv: 0906.1901 [gr-qc].

[124] S. S. Gubser and J. Khoury. "Scalar self-interactions loosen constraints from fifth force searches". In: *Phys. Rev. D* 70 (2004), p. 104001. DOI: 10.1103/PhysRevD.70.104001. arXiv: hep-ph/0405231.

[125] I. Quiros et al. "Chameleon effect in the Jordan frame of the Brans-Dicke theory". In: Phys. Rev. D 92.4, 044055 (Aug. 2015), p. 044055. DOI: 10.1103/PhysRevD.92.044055. arXiv: 1506.05420 [gr-qc].

[126] T. Kobayashi. "Horndeski theory and beyond: a review". In: *Reports on Progress in Physics* 82.8, 086901 (Aug. 2019), p. 086901. DOI: 10.1088/1361-6633/ab2429. arXiv: 1901.07183 [gr-qc].

[127] K. Koyama, G. Niz, and G. Tasinato. "Effective theory for the Vainshtein mechanism from the Horndeski action". In: Phys. Rev. D 88.2, 021502 (July 2013), p. 021502. DOI: 10.1103/PhysRevD.88.021502. arXiv: 1305.0279 [hep-th].

[128] A. Dima and F. Vernizzi. "Vainshtein screening in scalar-tensor theories before and after GW170817: Constraints on theories beyond Horndeski". In: Phys. Rev. D 97.10, 101302 (May 2018), p. 101302. DOI: 10.1103/PhysRevD.97.101302. arXiv: 1712.04731 [gr-qc].

[129] R. Kimura, T. Kobayashi, and K. Yamamoto. "Vainshtein screening in a cosmological background in the most general second-order scalar-tensor theory". In: Phys. Rev. D 85.2, 024023 (Jan. 2012), p. 024023. DOI: 10.1103/PhysRevD.85.024023. arXiv: 1111.6749 [astro-ph.CO].

[130] I. Quiros et al. "Brans-Dicke Galileon and the variational principle". In: *European Journal of Physics* 37.5 (Sept. 2016), p. 055605. DOI: 10.1088/0143-0807/37/5/055605. arXiv: 1605.00326 [gr-qc].

[131] A. De Felice and S. Tsujikawa. "Generalized Brans-Dicke theories". In: J. Cosmology Astropart. Phys. 2010.7, 024 (July 2010), p. 024. DOI: 10.1088/1475-7516/2010/07/024. arXiv: 1005.0868 [astro-ph.CO].

[132] T. Kobayashi. "Cosmic expansion and growth histories in Galileon scalar-tensor models of dark energy". In: Phys. Rev. D 81.10, 103533 (May 2010), p. 103533. DOI: 10.1103/PhysRevD.81.103533. arXiv: 1003.3281 [astro-ph.CO].

[133] A. Cerioni. "Cosmological perturbations in generalized theories of gravity". PhD thesis. alma, Apr. 2011. URL: http://amsdottorato.unibo.it/3562/.

[134] E. Bellini et al. "Comparison of Einstein-Boltzmann solvers for testing general relativity". In: Phys. Rev. D 97.2, 023520 (Jan. 2018), p. 023520. DOI: 10.1103/PhysRevD.97.023520. arXiv: 1709.09135 [astro-ph.CO].

[135] J. Lesgourgues. "The Cosmic Linear Anisotropy Solving System (CLASS) I: Overview". In: *arXiv e-prints*, arXiv:1104.2932 (Apr. 2011), arXiv:1104.2932. arXiv: 1104.2932 [astro-ph.IM].

[136] J. Bueno Sanchez and L. Perivolaropoulos. "Dark energy and matter perturbations in scalar-tensor theories of gravity". In: *J. Phys. Conf. Ser.* 283 (2011), p. 012006. DOI: 10.1088/1742-6596/283/1/012006.

[137] M. Braglia. "Initial conditions for cosmological perturbations in scalar-tensor dark-energy models". PhD thesis. URL: http://amslaurea.unibo.it/13860/.

[138] E. Bellini, I. Sawicki, and M. Zumalacárregui. "hi_class background evolution, initial conditions and approximation schemes". In: J. Cosmology Astropart. Phys. 2020.2, 008 (Feb. 2020), p. 008. DOI: 10.1088/1475-7516/2020/02/008. arXiv: 1909.01828 [astro-ph.CO].

[139] J.-C. Hwang and H. Noh. "Gauge-ready formulation of the cosmological kinetic theory in generalized gravity theories". In: Phys. Rev. D 65.2, 023512 (Jan. 2002), p. 023512. DOI: 10.1103/PhysRevD.65.023512. arXiv: astro-ph/0102005 [astro-ph].

[140] J.-C. Hwang and H. Noh. "Classical evolution and quantum generation in generalized gravity theories including string corrections and tachyons: Unified analyses". In: Phys. Rev. D 71.6, 063536 (Mar. 2005), p. 063536. DOI: 10.1103/PhysRevD.71.063536. arXiv: gr-qc/0412126 [gr-qc].

[141] H. Kodama and M. Sasaki. "Cosmological Perturbation Theory". In: *Prog. Theor. Phys. Suppl.* 78 (1984), pp. 1–166. DOI: 10.1143/PTPS.78.1.